**Title**
STUDIES OF THE ELECTROCHEMICAL BEHAVIOR OF POTASSIUM IN PROPYLENE CARBONATE

**Author**
Law, Henry Hon.

**Publication Date**
1979-05-01

LBL-9207 c.1

# Lawrence Berkeley Laboratory

UNIVERSITY OF CALIFORNIA, BERKELEY, CA

## Materials & Molecular Research Division

# STUDIES ON THE ELECTROCHEMICAL BEHAVIOR OF POTASSIUM IN PROPYLENE CARBONATE

Henry Hon Law
(Ph. D. thesis)

May 1979

Prepared for the U. S. Department of Energy
under Contract W-7405-ENG-48

LBL-9207

# STUDIES ON THE ELECTROCHEMICAL BEHAVIOR OF POTASSIUM IN PROPYLENE CARBONATE

Henry Hon Law
(Ph.D. Thesis)

May 1979

Prepared for the U. S. Department of Energy
under Contract W-7405-ENG-48

# Studies on the Electrochemical Behavior of Potassium in Propylene Carbonate

Henry Hon Law

Materials and Molecular Research Division, Lawrence Berkeley Laboratory
and Department of Chemical Engineering, University of California,
Berkeley, California 94720

## Abstract

The electrochemical behavior of potassium in propylene carbonate electrolytes has been investigated to establish the basic feasibility criteria of an ambient temperature process for the recovery of the metal from its simple salts.

The technical grade solvent is purified by passing it through a column of molecular sieves or activated alumina, or mixing it batch-wise with pre-treated charcoal, followed by vacuum distillation with a head temperature of 65°C. The solvent so treated contains less than 1 ppm water, less than 5 ppm propylene oxide, and negligible concentrations of glycols. When the $KACl_4$ solute is prepared by fusion at 500°C, the corrosion rate of potassium in the resulting electrolyte is negligible, in the order of $10^{-6}$ amp/cm$^2$. The current efficiency of potassium deposition from 0.5 M $KAlCl_4$ solutions is 97.5 $\pm$ 2.5%. The deposit contains less than 0.1% aluminum, probably in the form of occluded electrolyte.

The apparent exchange current density, as determined by galvanostatic measurements, is in the range of 1-5 × $10^{-5}$ amp/cm$^2$. The

morphology strongly depends on temperature: the metal deposits in loose powdery form at 30°C, fine needles at 50°C, and liquid globules at 70°C, above the melting point of potassium. At 70°C the presence of a cationic fluoro-surfactant at 0.1 - 1.0 gram/liter concentrations leads to the formation of larger, easily collectable metal globules.

The stability of potassium with respect to the electrolyte, and the near 100% current efficiency and relatively low cathodic overpotentials associated with the metal deposition process, may provide a basis for the development of a promising alternative to the present thermochemical method for the production of pure potassium metal.

dedicated

to

Jennie, Julius, James

and

my parents

# ACKNOWLEDGEMENTS

This dissertation would not have been possible without the cooperation and contributions of many people.

Helpful suggestions and cheerful moral support from all my friends in the research groups of Professor Tobias and Dr. Muller made my graduate work easier and more pleasant. My sincere thanks to Mr. Radoslav Atanasoski for his ideas and assistance. I would like to thank Mr. Oscar Chacon for his help in the early phase of my graduate work and Miss F. M. Kong for her assistance in the latter phase of my research. I am also grateful to Messrs. Geoffrey Prentice, Andrew Kindler, Peter Foller, and Mrs. Genevra Neumann for reading the manuscript. Discussions with Drs. Rolf Muller and Phillip Ross were stimulating and invaluable. Throughout this work, Mr. Larry Galovich has provided excellent support in design and construction of numerous apparatus with judgment, intuition, and common sense.

I wish to express my appreciation to Mrs. Linda McGuire for her care and diligence in typing portions of this dissertation, to Mrs. Gloria Pelatowski for her artistic illustrations, to Mr. Tom Morrison for performing the atomic absorption spectroscopic analyses, and to Ms.

Sherry Ogden for carrying out the mass spectroscopic analyses.

The Nafion membranes and Zonyl surfactants used in this work were kindly provided by Dupont Chemical Company.

Thanks are due to Professors Scott Lynn and James W. Evans for their review of this dissertation.

My overriding debt is to Professor Charles W. Tobias. His insight combined with his judicious guidance helped me to mature as a researcher. I have also benefitted greatly from him in the skill of communication, both oral and written. The debt I owe to him, I can never fully repay.

This work was supported by the Division of Materials Sciences, Office of Basic Energy Science, and the Division of Solar, Geothermal, Electric and Storage Systems, Office of the Assistant Secretary for Energy Technology, U. S. Department of Energy under contract No. W-7405-Eng-48.

## Table of Contents

## 1. Introduction

Alkali metals, because of their low electron affinity, cannot be recovered from their salts in aqueous solutions. Lithium and sodium are produced by electrolysis of their molten chlorides. However, the electroreduction of potassium in a similiar system is inefficient because the potassium metal and the molten choride are miscible. Such a process would be unattractive for industrial use.

The electrodeposition of alkali metals from aprotic organic solvents offers interesting, and potentially useful alternatives for the primary recovery and refining of alkali metals. Potassium was chosen as the subject of this investigation because of its abundance and the difficulty of obtaining it in pure form. Previous work in this laboratory has shown that potassium may be efficiently reduced from propylene carbonate (PC) solutions of certain potassium salts. This dissertation is aimed at the exploration of the feasibility of developing a practical process for the primary recovery and/or refining of potassium metal from PC electrolytes.

The current main industrial use of potassium is in the manufacture of potassium superoxide ($KO_2$), used as the source of oxygen for gas mask applications. The use of potassium in NaK alloy as a heat transfer fluid is also substantial. A potential use of potassium, taking the advantage of its low first ionization energy, is as the seeding material for magnetohydrodynamic (MHD) power plants for the conversion of heat directly to electricity. Although potassium possesses chemical similarities to the other members of the alkali metal family, it cannot compete with sodium for other industrial applications. Sodium is much cheaper than potassium because, unlike the latter, it may be produced relatively efficiently by molten salt electrolysis. In order to increase the industrial use of potassium, its price must be reduced to the same order of magnitude as that of sodium.

The common alkali metals were discovered by electrolysis in molten salt baths. This is also the current method for manufacturing lithium and sodium. However, because the electrolytic process used in the case of lithium and sodium cannot be implemented for potassium, the established method for potassium manufacture is a thermochemical one. Three reasons have been given[S1] for the failure of the molten salt electrolysis in potassium manufacture:

(1) Potassium has a high vapor pressure at possible cell-operating temperatures. The metal mist formed is undesirable.

(2) Corrosion is severe at the melting point of the potassium chloride (770°C). Eutectics allowing lower operating temperatures have not been developed.

(3) Potassium reacts with oxygen more readily than does sodium and cell designs (the Castner cell, for example) do not provide adequate protection from the air.

However, the most damaging inherent difficulty is the miscibility of potassium and the potassium chloride melt, which results in a low current efficiency. Complete miscibility occurs at temperatures above 790°C, a temperature only 18 degrees higher than the melting point of KCl.[J1]

The current industrial method for potassium manufacture (figure 1) involves a high temperature (800°C) thermochemical process, developed by the Callery Chemical Company.[J2] During operation, the raw materials, molten sodium and molten potassium chloride, are continuously introduced into the column. The sodium is vaporized in the boiler tubes and ascends the column, coming into contact with the descending liquid potassium chloride establishing the equilibrium $Na + KCl \rightarrow K + NaCl$, resulting in a mixture of sodium and potassium vapors. Potassium, separated by fractionation in the upper section

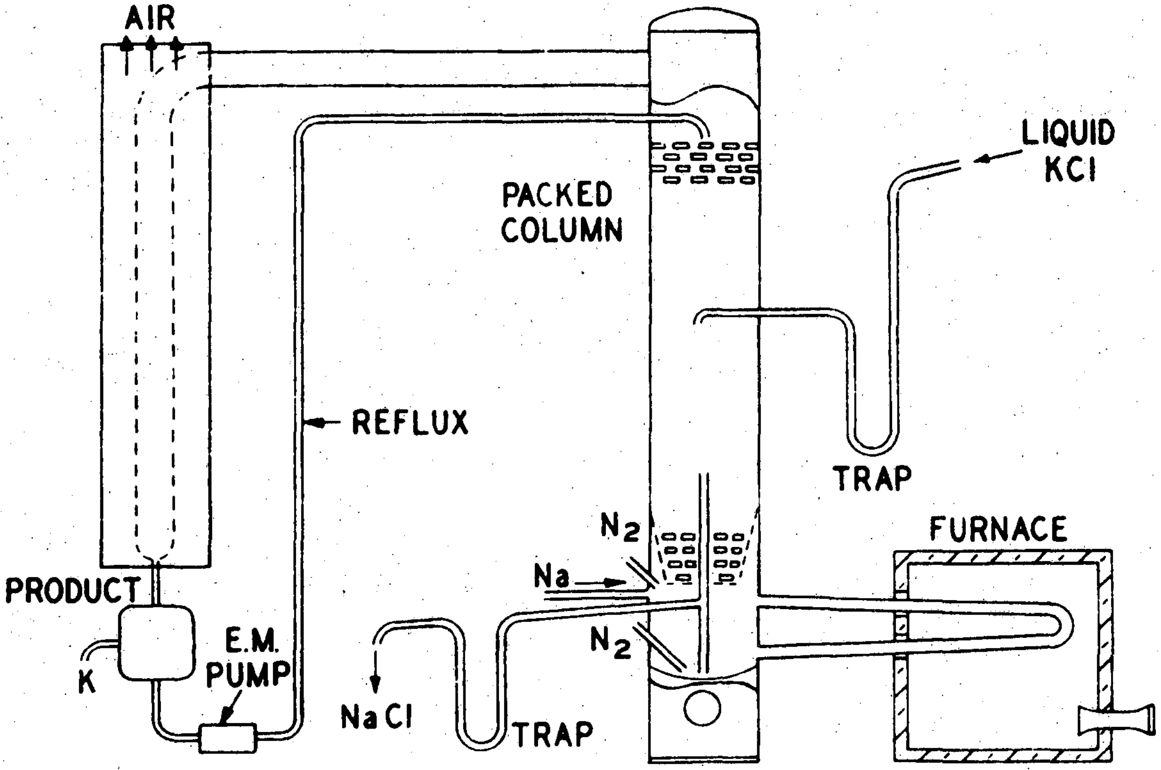

XBL 7812-13758

Figure 1-1. Continuous process for potassium production.[J2] of the column, is then condensed and collected. Since the process is operated at high temperature, energy and material costs are high. It is not certain to what degree the price could be lowered if the demand for potassium were to increase.

To replace the cumbersome Callery process, other thermal process schemes have been proposed. An Italian patent was granted for the preparation of metallic potassium from calcium carbide and potassium halide.[P1] Isbaev et al.[I1] reported the production of alkali metals and aluminum oxides by thermite reduction of aluminates. It is doubtful however that these efforts will result in new processes that can compete successfully with the Callery process.

The present selling price of potassium, by the Callery process, is five dollars per pound for technical grade (98.5% min.) in bulk quantity.[C1] Yet sodium, produced by electrolysis in the Downs cell, is only 60 cents per pound.[C7] This suggests that a process that could produce potassium at a significantly lower cost would be of interest.

Production of potassium by molten salt electrolysis is not attractive because of low efficiency, high operating temperature and hence high cost of energy and materials of containment. Desirable process alternatives therefore are likely to involve operations near ambient temperatures. Since potassium reacts with water, potential candidates for ionizing solvents will involve non-aqueous media.

The literature review of the deposition of alkali metals in non-aqueous solvents, given in section 2, shows that no particular solvent was found to have advantages over propylene carbonate. The initial exploratory study of PC started in 1955 by Harris and Tobias[H1], was followed by a large number of government sponsored exploratory projects for the development of high energy batteries with PC as the solvent. Results of most of these studies were included in Jasinski's review[J10] of the electrochemistry and applications of PC. More recently, the thermodynamic and kinetic behavior of alkali metals in PC was studied in depth by Jorne.[J3] The feasibility of potassium deposition in PC solutions was also established.[C2] These studies demonstrated that PC is an attractive solvent for producing potassium metal electrochemically at ambient temperature.

Propylene carbonate is an ionizing aprotic solvent capable of dissolving various inorganic salts. Its structure and physical properties are given in Table 1-1. PC has a broad liquidus range, from -49°C to 242°C. Its

Table 1-1. Physical properties of propylene carbonate.

| | |
|---|---|
| Structure | 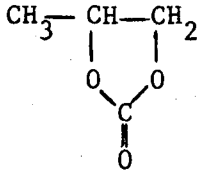 |
| Molecular Weight | 102.09 |
| Melting Point, °C | -49.2 |
| Boiling Point at 760 mm Hg, °C | 241.7 |
| Vapor Pressure at 25°C, mm Hg | 0.069 |
| at 60 °C, mm Hg | 0.80 |
| Density at 25°C, gm/cm$^3$ | 1.203 |
| at 60°C, gm/cm$^3$ | 1.161 |
| Viscosity at 25°C, millipoise | 24.8 |
| at 60°C, millipoise | 13.3 |
| Dielectric Constant at Room Temperature | 65.1 |
| Specific Conductance at 25°C, ohm$^{-1}$cm$^{-1}$ | 1.2 to 8.6 x $10^{-7}$ |
| at 60°C, ohm$^{-1}$cm$^{-1}$ | 1.5 to 10.0 x $10^{-7}$ |

electroactivity range (defined as the potential zone with which an electrochemical reaction can take place without being disturbed by massive oxidation or reduction of one of the medium components)[B3] can be as wide as 6.3 volts, depending on the electrolyte and the electrode material.[C4] Since it is neither toxic nor corrosive, PC is regarded as a good solvent for industrial use.

Based on these desirable characteristics of PC and the encouraging results by Jorne[J3] and Chacon[C2], this study was undertaken to assess the scientific criteria for the development of a practical process for the primary recovery and/or refining of potassium. After the literature survey and the experimental section, the feasibility of preparing large quantities of pure electrolytes in a straight-forward manner and the reproducibility of experimental results in these electrolytes are discussed. Emphasis is also placed on the determination of the stability of the electrolyte with respect to the metal, the current efficiency of the potassium deposition, the deposit morphology, and the cathodic overpotential dependence on operating parameters.

# 2. Literature Survey

## 2.1. Deposition of alkali metals from non-aqueous solvents

Interest in the electrodeposition of alkali metals from non-aqueous solvents has a long history. Early reviews on the subject were written first by Audrieth and Nelson,[A2] and later by Audrieth and Kleinberg.[A3] Brenner[B1] critically reviewed investigations of the deposition of metals from organic solvents up to 1967. Research efforts concentrating particularly on propylene carbonate are discussed separately in the next section.

In 1895, Laszczynski[L1] and Laszczynski and Gorski[L2] reported that they obtained potassium deposits from solutions of potassium thiocyanate in acetone and in pyridine. Levi and Voghera[L3] later showed that the deposits were compounds involving the metal and the solvent. Mandell and co-workers[M1] found that cathodic deposits obtained in the electrolysis of potassium salts in pyridine and in quinoline reacted vigorously with water. The composition of the deposit was not given. Fedot'ev and Kinkul'skaya[F1] operated an ethylenediamine bath containing salts of the alkali metals at 150°C; they obtained the metals at a very low current efficiency due to their reaction with the solvent. Putnam and Kobe[P3] obtained current efficiencies of about 90% for the deposition of potassium and sodium from a solution of their iodides in ethylenediamine at 100°C. Russian workers were interested in systems consisting of alkali halides and aluminum halides dissolved in an organic solvent. For the deposition of lithium and potassium, Mezhennii[M2] dissolved aluminum bromide along with lithium or potassium chloride in nitromethane. Current efficiencies around 30% were claimed. Pospekhov[P4] critically reviewed references on the extensive researches performed in Russia on the deposition of alkali metals from baths containing aluminum halides in nitrobenzene or nitromethane. He was pessimistic about the possibility of economically electrodepositing alkali metals from baths of nitro compounds. Cady and Taft[C8] mentioned the deposition of potassium by the electrolysis of potassium iodate dissolved in phosphorus oxychloride.

Recently, Pompe[P2] studied the electrodeposition of alkali metals from acetone, pyridine, and dimethylformamide in a horizontal mercury cell. He concluded that anions played an important role in the solvent decomposition reaction. The water content of the solvents was relatively high, ranging from 0.01% to 0.2%. He claimed to have obtained metallic deposits with high current efficiencies in pyridine and in dimethylformamide, but the range of the current passed was not given nor was the reference electrode specified. The duration of the electrolysis was limited to less than 30 minutes to avoid the absorption of moisture in the solutions. These results cannot be considered to be conclusive.

Most of these studies on the electrodeposition of alkali metals were qualitative and not systematic. No particular solvent was shown to possess superior advantages.

## 2.2. Electrodeposition of potassium in propylene carbonate

### 2.2.1. Electrochemistry of propylene carbonate solutions

Electrochemical studies in propylene carbonate were first carried out by Harris and Tobias[H1] in this laboratory over twenty years ago. They measured the solubilities and conductivities of various inorganic salts in propylene carbonate and in related solvents: ethylene carbonate, gamma-butyrolactone, and gamma-valerolactone. Qualitative deposition tests showed that alkali metals could be deposited in propylene carbonate solutions. However, potassium deposits were obtained only at current densities higher than 5 mA/cm$^2$.

A comprehensive study of the electrochemical behavior of alkali metals in propylene carbonate was reported by

Jorne and Tobias in a series of papers[J3-J9] starting in 1973. They established the feasibility of the electrodeposition of all alkali metals from propylene carbonate solutions. By using micropolarization measurements, the kinetic parameters of the deposition-dissolution process for solid alkali metals and their amalgams in alkali metal chloride-$AlCl_3$/PC solution were determined at 25°C. Exchange current densities were evaluated at different molalities of the alkali metal chlorides. The cathodic transfer coefficients were calculated from the concentration dependence of exchange current densities.[J4] From the EMF measurements, the activity coefficients, as well as the partial Gibbs free energies, entropies, and enthalpies of the cell reactions, were calculated.[J5] The free energies of solvation of the alkali metal chlorides in unit molality $AlCl_3$/PC solution were determined.[J6] Furthermore, they were able to interpret the conductance in terms of the solvation, the ionic equilibrium, and the structure making and breaking ability of alkali metals in $AlCl_3$/PC solution.[J7] A new process for the production and electrorefining of the alkali metals at ambient temperature was patented.[T1] Alkali metal amalgam from the commercial mercury-chlorine cell was to be transferred into an $AlCl_3$/PC electrorefining cell, where the alkali metal was to dissolve anodically from the amalgam, and deposited in a pure form at the cathode.[J9]

Jansta, Dousek and Riha reported their studies of electrochemical systems for galvanic cells in aprotic organic solvents in a series of papers .[D1-D5] Trace amount of water were eliminated in PC electrolytes by the use of sodium-potassium alloy. They found that propylene carbonate is inert to alkali metals even at elevated temperature in the absence of salts and in the absence of impurities containing active hydrogen.[D1] The electrochemical behavior of a highly dried $KPF_6$/PC system was studied and the pronounced effects of water present even in minute concentrations were demonstrated. Jansta et al. concluded that, from the carefully purified solvent, the current efficiency of potassium deposition was 100%.[D2] Quantitative evaluation of electrochemical effects of trace water in $KPF_6$/PC electrolyte was made by addition of known quantities of water. When the water concentration was above 10 ppm, the deposition of potassium on a stationary platinum electrode at a voltage sweep rate of 0.4 volt/min was greatly retarded or even blocked.[D3]

Chacon[C2] has studied the cathodic reduction of potassium from PC solutions of $KAlCl_4$ and $KPF_6$. He was able to obtain coherent metallic deposits only from electrolytes purified by a complex and tedious method .

Impurities were removed by passing the electrolyte through a chilled alumina column. Aluminum was not co-deposited with potassium. Overpotentials were measured. However, an inadvertent error made these overpotential data not meaningful-- the actual concentration of the potassium salt was much lower than the concentration given. This error resulted because the absorption capacity of the alumina column was under-estimated; when the electrolyte was passed through, much of the potassium salt was absorbed. Nevertheless, this work first demonstrated that obtaining a coherent potassium deposit was feasible.

The results described above leave little doubt about the feasibility of depositing potassium from PC electrolytes. No other solvent has been reported to provide conditions suitable for this reduction process.

### 2.2.2. Electrolyte stability

Investigations of the stability of PC electrolyte have been stimulated to a large degree by the recent interest in high specific energy batteries. While some authors claim to have demonstrated the stability of PC with respect to lithium and sodium-potassium alloy, others reported specific cases of solvent decomposition. So far the stability question has not been settled satisfactorily.

Boden[B4] tested a purified $LiClO_4$/PC solution for compatibility with lithium by measuring quantitatively the rate of gas evolution. After five days at 25°C, no evidence of gassing was observed. Jasinski et al.[J12] found no gross decomposition of the $LiClO_4$/PC electrolyte upon anodically discharging lithium metal at 71°C over a 900-hour test. Jansta, Dousek and Riha[D1] reported that highly dried propylene carbonate solvent, in the absence of salts and impurities containing active hydrogen, was inert to sodium-potassium alloy even at elevated temperature. No change was observed when pure propylene carbonate solvent contacted Na-K alloy, even after 200 hours, followed by a 5-hour heating to 80°C.

Dey and Sullivan[D7] first reported the electrochemical decomposition of PC on a graphite electrode to propylene gas and carbonate ion with almost 100% coulombic efficiency. Eichinger[E2] further claimed that at graphite electrode the decomposition reaction proceeded with "reasonably high" current densities because of the formation of alkali metal intercalation compounds. At active electrode surfaces, such as sintered nickel, copper- or steel-felt, the decomposition reaction occurred at "rather small" current densities by direct electrochemical reduction of PC.

In a later work, Jansta et al.[D4] reported that gas evolution was immediately observed when Li-Hg amalgam contacted highly dried PC. Na-Hg amalgam also decomposed PC, but at a rate an order of magnitude lower than in the case of Li-Hg. Potassium amalgam was found to be stable in a very dry 0.5 M $KPF_6$/PC solution. Thus the rate of PC decomposition by alkali metal amalgams decreased sharply in the order Li>Na>K. Jansta et al. believe that the rate is related to the atomic size of the alkali metals and hence to their tendency to form covalent bonds with carbon. The decomposition of PC by elemental lithium was also studied and found to be slower; no massive gas evolution was observed. It was proposed that a $Li_2CO_3$ layer on the lithium surface slows down the decomposition reaction.

In summary, pure PC solvent was shown to be inert upon prolonged contact with Na-K alloy, and no gassing was observed upon contacting lithium metal with $LiClO_4$/PC electrolyte. The electrodeposition of potassium on a graphite electrode was reported to lead to the decomposition of propylene carbonate to propylene and carbonate ion, and Li-Hg amalgam immediately decomposed PC upon contact. The stability of PC with respect to potassium will be further discussed in section 5.

### 2.2.3. Influence of the Impurities

Presence of impurities adds another dimension to the stability problem of PC electrolytes. The role of water and propylene glycol (propanediol) in PC electrochemistry is not well understood. Alkali metals are known to spontaneously react with water and glycol. The electrochemical behavior of active metals should be affected by the hydroxide layer formed on their surfaces. Furthermore, the decomposition of PC could possibly be catalyzed by impurities. For example, in $AlCl_3$/PC solutions, the hydrolysis of $AlCl_3$ would yield HCl and $Al(OH)_3$. Possible decomposition reactions by HCl have been suggested by Silvester and Tobias[S2] and are presented in Table 2-1.

The electrochemical behavior of water in PC electrolyte has been studied by various investigators. In Dey's work[D6], the concentration of water was in the range from 0.1 - 2.5 M. With $Et_4NClO_4$ as supporting electrolyte, Gosse and Denate[G1] found that the hydroxide ions resulting from water reduction reacted with PC to form bicarbonate ions and propylene glycol. The water concentration varied from $5 \times 10^{-3}$ - 1.25 M. Using chronopotentiometric and cyclic voltammetric techniques, Burrows and Kirkland[B2] studied the behavior of $LiClO_4$/ PC solutions containing 20 - 500 ppm of water ($10^{-3}$ -

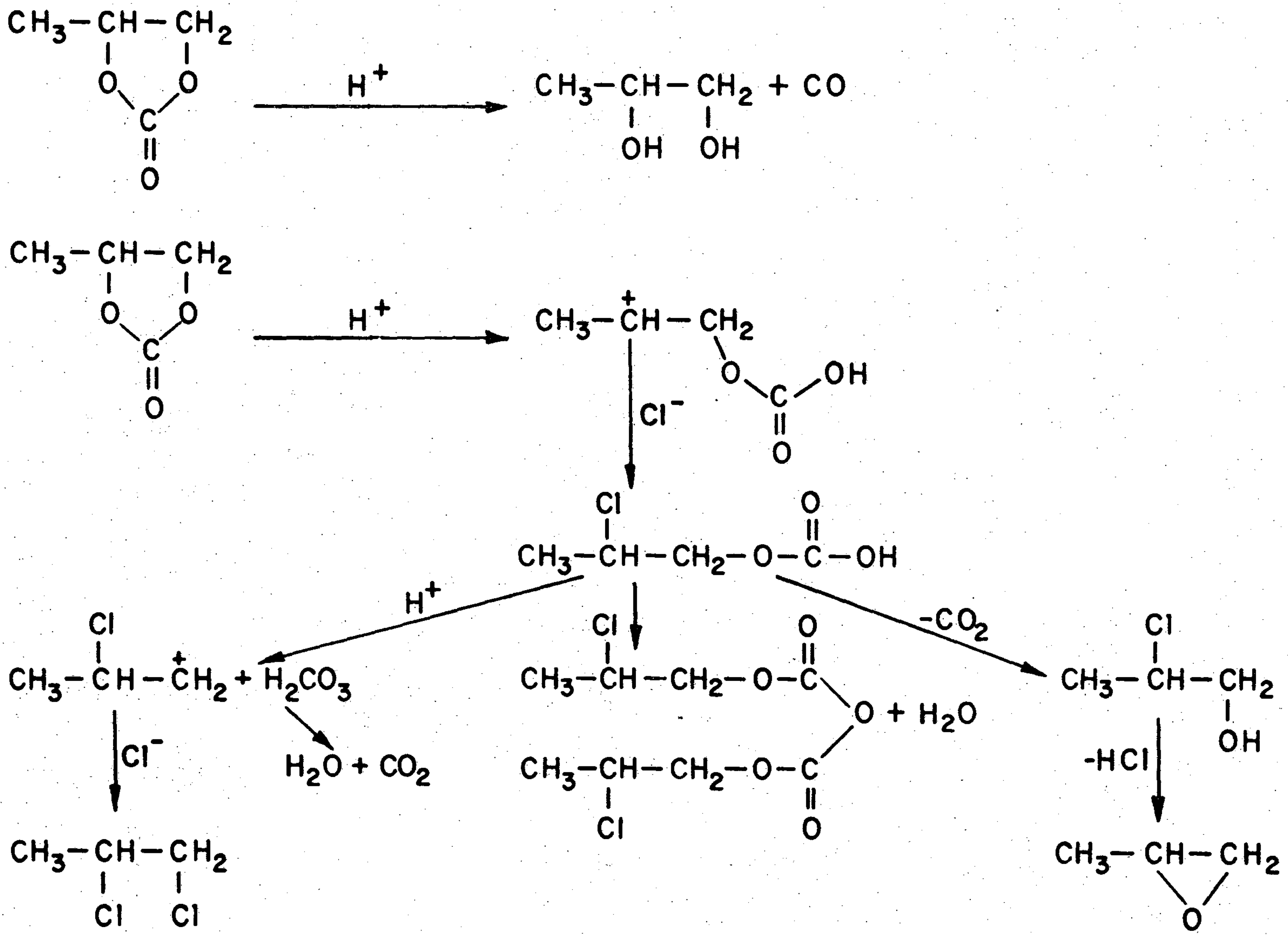

Table 2-1. Decomposition of PC in presence of acid (HCl) under anhydrous conditions.

XBL792-5731

$3x10^{-2}M$). Results were interpreted by assuming the blockage of the electrode surface by a porous, insoluble LiOH film. Jansta et al.[D3] reported the influence of water content on potential-current curves obtained at 100 mV/sec with Pt, Au, Ag, Ni and Cu electrodes in the concentration range 0 - 100 ppm in 0.5 M $KPF_6$/PC. Quantitative results on the effect of water were obtained for below 20 ppm of water. The deposition of potassium on a stationary electrode at a polarization rate of 0.4 volt/min was greatly retarded or blocked above 10 ppm. The effect of water on the electrochemical processes in PC electrolyte thus cannot be ignored. Comparison of different results can be meaningful only when comparing the effects of water at similar concentrations.

The determination of water at the ppm level is a difficult problem. The conventional Karl Fischer titration method is not adequate for water concentrations below 20 ppm. Cedergren[C5] developed a coulometric determination of water down to 0.5 ppm by using Karl Fischer reagent and a potentiometric end-point detection. Whether PC and its organic impurities would interfere with the Karl Fischer reagent is not known. Jasinski et al.[J11] employed gas-liquid chromatography to determine the water content of PC solvent to less than 2 ppm. However, this method is not suitable for PC electrolytes because of undesirable accumulation of salt in the g.c. column. In the work of Jansta et al.[D3] mentioned above, the potential-current curves measured by using a vibrating Pt electrode were correlated with the water concentration. Each E-i curve was obtained by sweeping linearly the potential on a fresh electrode. Water in the range between 0.01 and 50 ppm could be determined in aprotic solvents in the presence of alkali metal cations. The effect of water on the electrochemical behavior of potassium in propylene carbonate will be further discussed in section 4.3.

## 3. Experimental Procedure

Because of the exploratory nature of this project, many experiments have been performed to determine the best cell configurations for the desired measurements. The apparatus used for obtaining the results presented in sections that follow will be described below in detail.

Based on our experience gained during the initial phase of this investigation, experiments run outside of a controlled atmosphere always involve the danger of contamination. In an exploratory study, an uncertainty such as this would render the interpretation of results very difficult. For this reason working inside a dry glove box was considered essential. With the exception of runs involving aqueous solutions, all of the data presented here were obtained from experiments set up inside a dry glove box.

### 3.1. Glove Box Operation

Most of the experimental work was performed inside dry glove boxes with a helium atmosphere. Two glove boxes were employed. One was the vacuum type of Lawrence Livermore Laboratory design. It is the same one used by Jorne[J3], but the treatment of the inert gas atmosphere was substantially modified. The other one (Figure 3-17) was manufactured by Kewaunee and was extensively rebuilt to ensure effective isolation from the outside atmosphere. The pressure was maintained to within one inch of water of atmospheric pressure by a custom-made pressure controller using a sensitive sensor (Dwyer Series 3000 Photohelic switch/gage, ±5 in $H_2O$ full scale).

Great care was taken to ensure the quality of the helium in the glove box atmosphere. The helium gas was recirculated continuously at 3 cubic feet per minute through a periodically regenerated inert gas purifer (Kewaunee Scientific Equipment Model 2C1982 with automatic regeneration control) in which moisture and oxygen were continuously removed. The water content was maintained below 2 ppm (Moisture Monitor, type 26-303, Consolidated Electrodynamic Corp.). All of the materials used inside the glove box were transferred through an entrance chamber. The entrance chamber was pumped down to a vacuum lower than 10 millitorr before materials were transferred.

When the temperature was measured by a copper-constantan thermocouple, an electronic ice point (Omega Engineering, Model MCJ-T) was employed so that the thermoelectric voltage was independent of the room temperature and could be measured through the regular copper connectors by the recorder outside of the glove box. Each box was equipped with a vacuum source (60 mm Hg). Digital balances were placed inside the glove boxes (Sartorious Model 3705 or Scientech Model 220).

## 3.2. Solvent Purification and Analysis

Propylene carbonate (PC) (Jefferson Chemical Co., Houston, Texas) was purified in three separate steps. First, PC was passed through a column of molecular sieves and alumina or was mixed batchwise with purified activated charcoal. Second, volatile impurities were removed by bubbling helium through the solvent at vacuum for one day. The final step was vacuum distillation.

The first step was designed to remove most of the impurities. The alumina (aluminum oxide, Woelm basic, ICN, Cleveland, Ohio) and molecular sieves (Linde, 13X) were packed into a stainless steel column and were dried at 300°C under vacuum (1 micron Hg) for one day before use. The amounts used were 300 $cm^3$ molecular sieves and 300 $cm^3$ alumina for 3.5 liters PC. This procedure provided a simple and convenient method for laboratory work. We also found the use of activated charcoal satisfactory. This is a potentially inexpensive alternative to the use of molecular sieves and alumina. About 250 $cm^3$ purified activated charcoal was used for 3.5 liters PC. The charcoal was filtered out as PC was transferred to the distillation column. We prepared the charcoal (MC/B, Activated "DARCO", mesh 4-12) according to a standard procedure: the charcoal was (1) treated with a boiling azeotropic mixture of hydrochloric acid and water (6 M) in a Soxlett apparatus for three weeks, (2) washed with double distilled water until no further chloride ion could be detected and (3) dried under 60 mm Hg vacuum at 150°C for six days.

The helium bubbling set-up was part of the vacuum distillation column (Semi-CAL series 3650, Podbielniak, Dresser Industries). Helium served as a replacement for boiling chips, so that the solvent could boil "smoothly", and it also helped in the removal of light volatile impurities. The helium stream was started 24 hours before heat was supplied to the bottom pot, and was continued during the distillaton. PC was distilled at below 3.0 mm Hg with a head temperature of 65°C. The first 10% and the last 30% of the distillate were not used. The receiver system was modified with socket and ball joints and Teflon needle valves. Figure 3-1 depicts the complete distillation set-up and the column of alumina and molecular sieves with the drying oven.

The impurity content of the solvent was analyzed by a gas chromatograph (Varian Associates Model 3706) equipped with thermal conductivity and flame ionization detectors. The operating conditions, listed in table 3-1, were

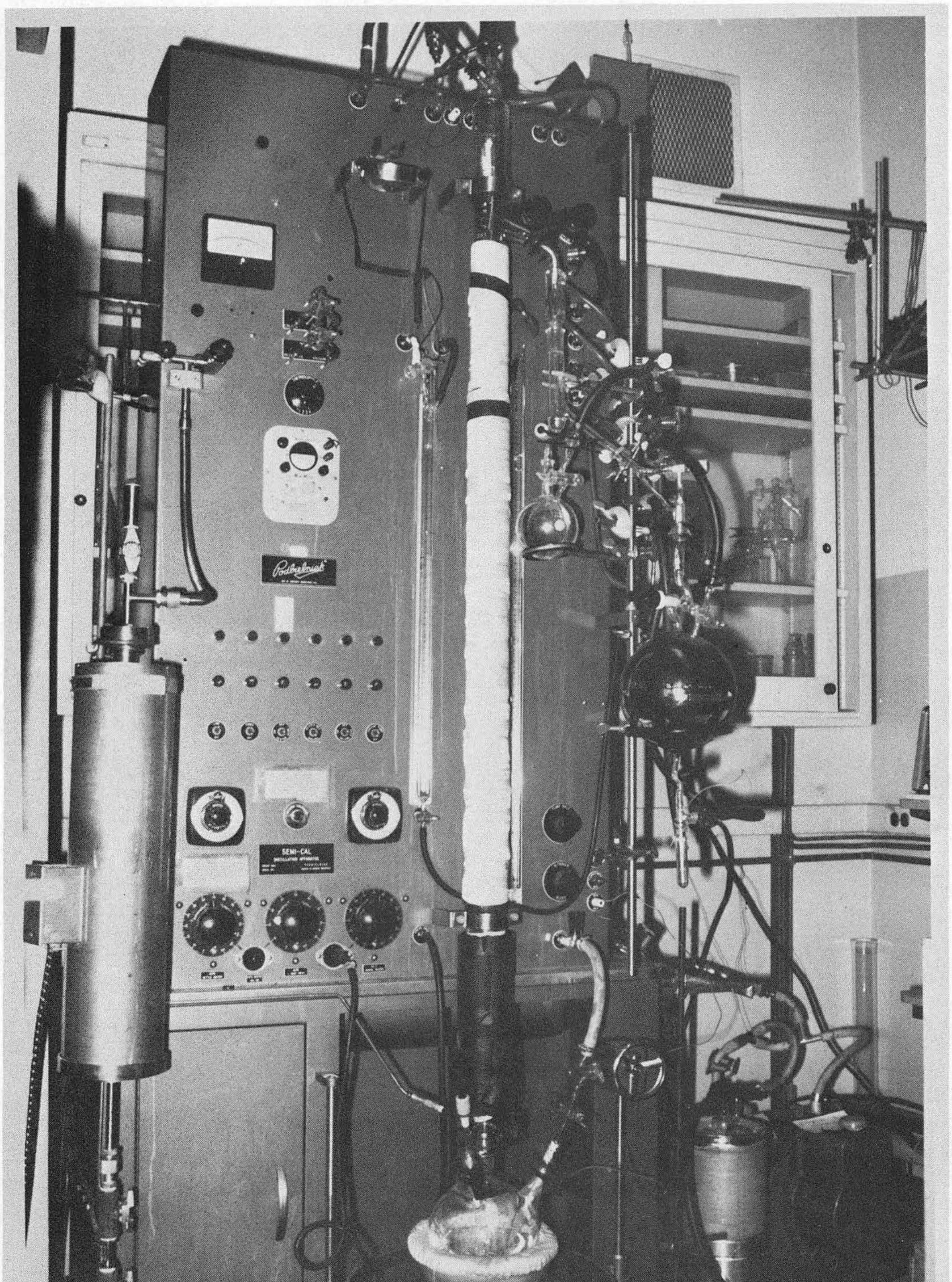

CBB 792-2601

Figure 3-1. Vacuum distillation apparatus.

Table 3-1

Operating Conditions of the Gas Chromatograph Detectors

| Detector | Flow Rate ml/min | | Temperature ,°C | |
|---|---|---|---|---|
| Flame Ionization | He | 30 | Injector | 130 |
| | Air | 300 | Column | 150 |
| | $H_2$ | 30 | Detector | 200 |
| Thermal Conductivity | He | 60 | Injector | 130 |
| | | | Column | 150 |
| | | | Detector | 200 |
| | | | Filament | 300 |

Carrier Gas: Helium

similar to those of Jasinski and Kirkland[J4]. Only water and propylene glycols were detected in the distillate. The concentrations were estimated by measuring the responses of 2 microliter samples of PC with and without known quantities of the impurities. The purified solvent contained less than 1 ppm water and less than 5 ppm propylene glycols.

### 3.3. Electrolyte Preparation

The potassium salts used in this study were KCl, $KPF_6$ and $KAlCl_4$. Analytical grade KCl and $KPF_6$ were finely ground and dried under vacuum (1 micron Hg) at an elevated temperature: KCl at 400°C and $KPF_6$ at 280°C. When necessary, the dried salt was ground again inside the glove box. The $KAlCl_4$ salt was not commercially available. Thus we had to develop a procedure to synthesize the double salt. Baud[B5] first prepared potassium tetrachloroaluminate in 1904 by heating a mixture of KCl and $AlCl_3$ at about 300°C. The formation of $KAlCl_4$ has been confirmed by Kendall and co-worker.[K4] From the temperature-composition curves, they determined the composition of the double salts formed.

The procedure developed for the preparation of $KAlCl_4$ is as follows. Equal molar amounts of $AlCl_3$ and KCl (analytical reagent grade) were placed into a Pyrex flask inside a polyethylene glove bag (Instruments for Research and Industry, Cheltenham, PA) under nitrogen atmosphere. The flask was then taken out of the glove bag and connected to the vacuum system (Figure 3-2). The salts were mixed by a vibrator while being pumped down to 1 micron Hg. The system was pressurized with helium before the mixture was melted at 250°C. The pressure was kept constant at slightly higher than one atm. by bleeding off

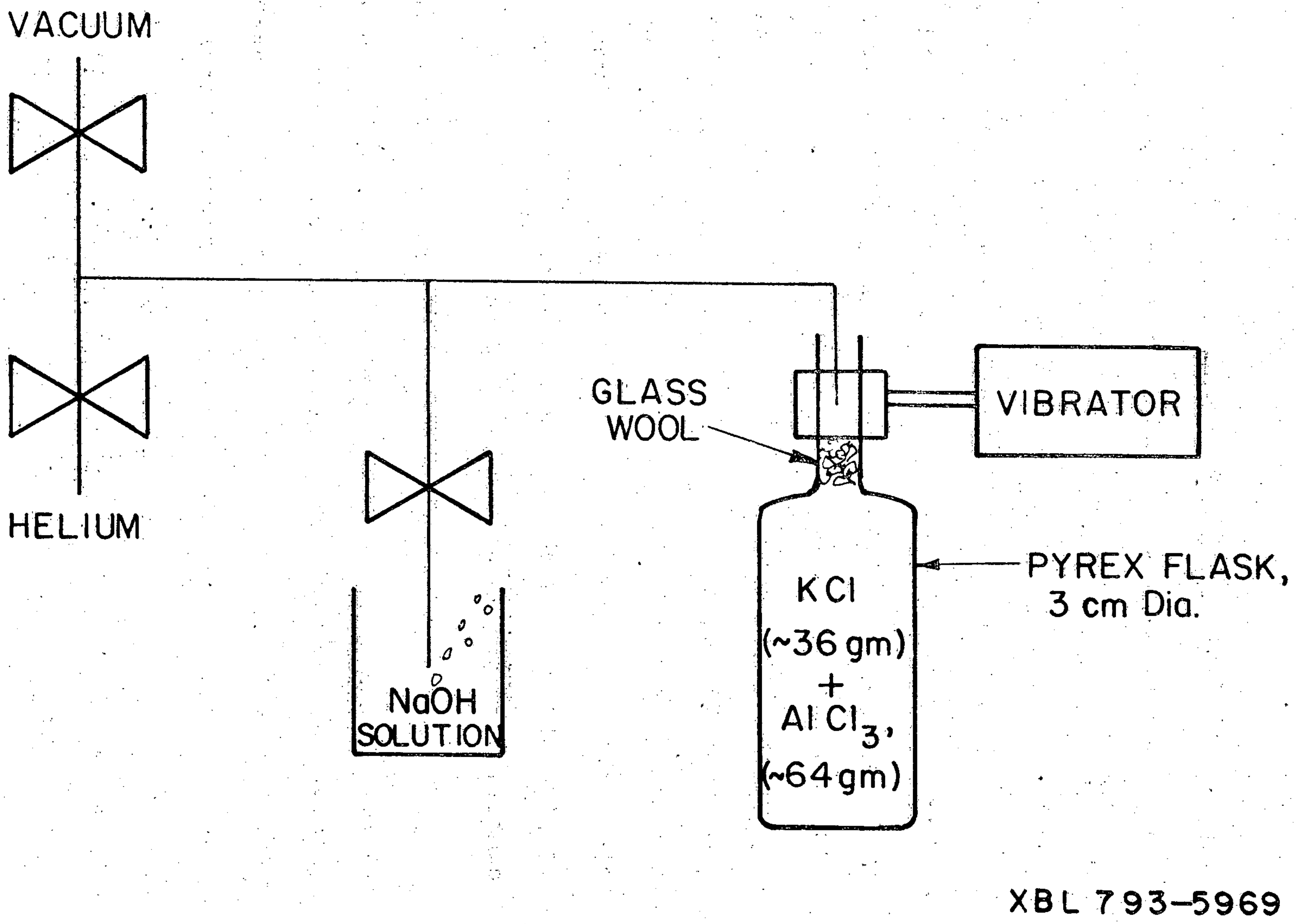

Figure 3-2. Schematic for the synthesis of $KAlCl_4$.

helium during the heating and the cooling of the Pyrex flask. The melt of KCl and $AlCl_3$ was light yellow, probably due to trace amount of ferric chloride in the aluminum chloride. We determined that by increasing the temperature to above 500°C, a reaction involving impurities occurred in which the melt became colorless and clear and a black precipitate formed. The Pyrex tube was shaken several times and kept at 550°C for 2 hours so that the black precipitate settled down to the bottom. The temperature was then decreased gradually to avoid any thermal current that would resuspend the black material. When the salt solidified, the system was pumped down to vacuum and the Pyrex tube was sealed off by melting the glass with a torch at a point above the glass wool. The salt was removed by breaking the Pyrex flask inside a glove box. It was ground finely before use.

The double salt so prepared contained less than 0.003% iron and 0.01 % silicon. The reaction that rendered the melt colorless was not investigated; however, it was found that the black precipitate contained carbon and at least one order of magnitude more iron and silicon than the white solid. By maintaining the temperature at 550°C, the $AlCl_3$ and KCl did not have to be purified before use, a significant advantage over other methods for preparing

$KAlCl_4$ solution. The heat of solution of $KAlCl_4$ in PC was not determined precisely. When 10.8 grams of double salt was added to 100 ml of PC in less than one half minute, the solution temperature rose from 25°C to only 32°C. No sign of solvent decomposition was observed even following such a rapid addition of the salt. However, as a precautionary measure, the salt was normally added to the solvent over 5 minutes. Due to a slight excess of KCl, the freshly prepared electrolyte was usually cloudy. After vacuum filtration (Whatman, GF/F fiber glass filter paper), the solution became clear and had only a very faint yellow color.

The concentration of potassium in the electrolyte was determined by using atomic absorption spectrocopy (Perkin-Elmer M360 spectrometer). By employing an automatic pipette (Centaur), a precise amount of electrolyte (10, 50 or 100 microliter) was easily removed from the electrolysis cell. The sample was then diluted with distilled water outside the glove box before analysis.

In experiments where a surfactant (Dupont Zonyl FSC) was used, the desired concentration was obtained by adding the appropriate amount of surfactant solution (10 gram/liter in PC) to the electrolyte. The standard PC solution was prepared by dissolving solid dried Zonyl surfactant in PC. Because the surfactant is available only in isopropanol/water solutions, the solid surfactant was obtained in this manner: the diluent was first evaporated; the residue was ground finely and was dried at 100°C under vacuum (1 micron Hg) for two days before transfer into the glove box.

## 3.4. Electrodes

### 3.4.1. Reference Electrode

The reference electrode used throughout this work was a potassium electrode immersed in the same solution. We found that a glass capillary tube containing potassium served very well. Such a design made it possible to place the reference electrode close to the working electrode with no difficulty. The reference electrode was renewed by simply cutting the capillary to expose a new surface. It could be prepared quite easily. Figure 3-3 depicts the types of reference electrodes employed. The Teflon holder had a side hole connected to the capillary (1.6 to 1.8 mm diameter); the reference electrode was prepared by using a syringe to draw the molten potassium into the capillary. Before use, the contact between the tungsten wire and the potassium was checked. An earlier version of this reference electrode was made from a disposable pipette with a capillary tip.

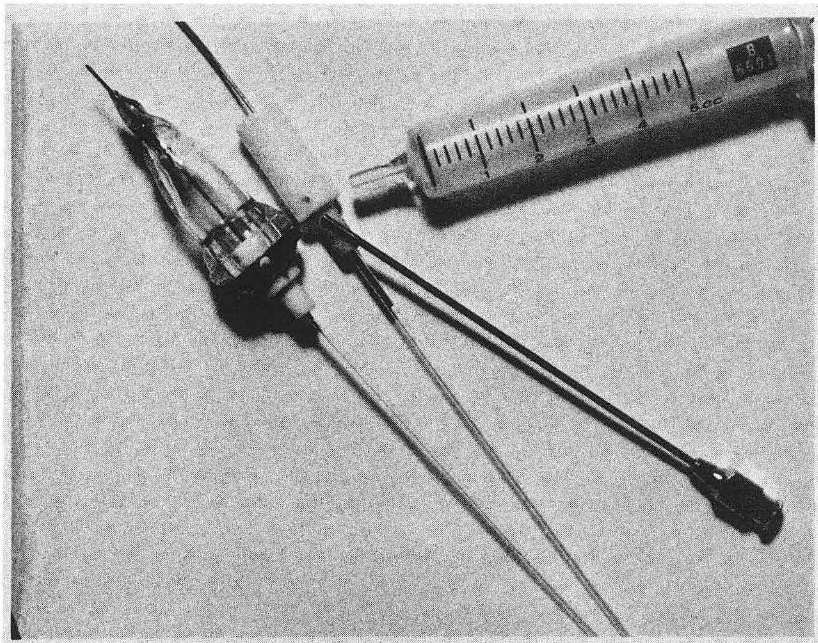

Figure 3-3. Teflon holders for the potassium reference electrode and the syringe for its preparation.

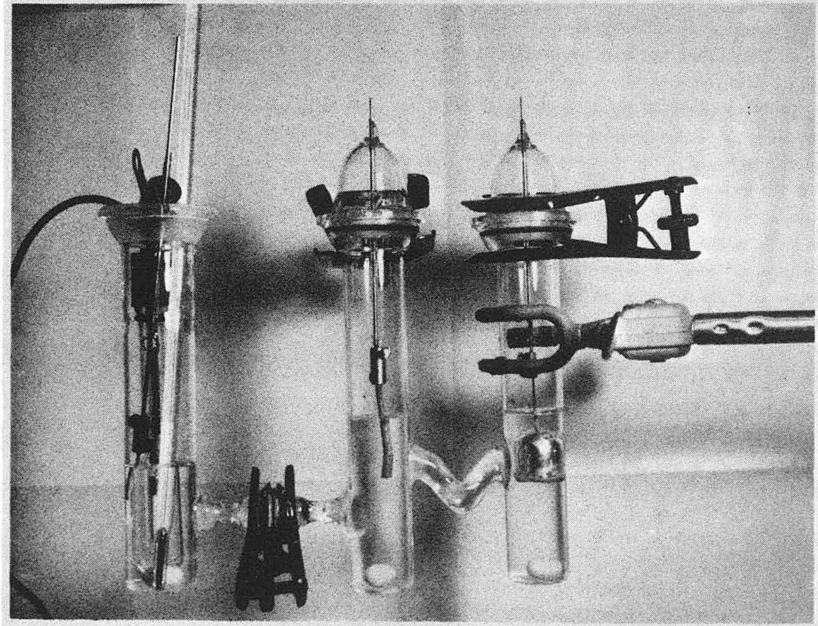

Figure 3-4. Electrochemical cell for the potential measurement of K and Tl in PC electrolyte versus a saturated calomel electrode in aqueous solution.

XBB 793-4108

The rest potential of a potassium electrode in 0.5 M $KAlCl_4$/PC solution relative to other reference electrodes was measured to allow comparison of certain results reported in the literature with those obtained in the present work. Figure 3-4 depicts the double H-cell used for this purpose. The non-aqueous chamber, on the right-hand side of the clamp, contained an anodized thallium wire and a large potassium cup electrode in 0.5 M $KAlCl_4$/PC electrolyte saturated in TlCl. The aqueous electrolyte, separated by a Dupont Nafion membrane from the non-aqueous section, contained 2.0 M KCl and 2.0 gram/liter KF. At 27.2°C, the potential of the saturated calomel electrode (Corning), with respect to the potassium electrode, was +3.020 volt. The potential of the anodized thallium wire relative to potassium was +2.302 volt. These potentials remained stable for several hours. The measurement was discontinued when a white precipitate was formed on the non-aqueous side of the Nafion membrane. This was an indication of water leaking through the membrane and hydrolyzing the aluminum chloride to form aluminum hydroxide.

### 3.4.2. Working and Counter Electrodes

Potassium has been deposited on various substrates: potassium, platinum, stainless steel, aluminum and an aluminum alloy (6061T6, >96% Al). The shape and size of the electrodes depended on the particular cell configuration. Representative samples along with the cells used are shown in section 3.5.

A special stainlss steel (304) electrode, shown in Figure 3-5, equipped with a heating filament deserves detailed description. Figure 3-6 depicts the internal construction which includes a heating element and a thermocouple built underneath the electrode surface, so that the temperature could be precisely measured and controlled. A small passage (with Teflon insulation) connects the electrode to the reference electrode chamber.

The anodic reaction coupled with the potassium deposition was either dissolution of aluminum or dissolution of potassium. Only very pure aluminum (from Orion, 99.9995%) was used for this purpose. The potassium used was from either Alfa Chemical (99.95%) or Mallinckrodt.

The platinum electrode was cleaned first by washing with distilled water and then by heating with a torch until red hot each time before use. The stainless steel electrode, after being cleaned with detergent, was thoroughly washed with distilled water and acetone. The aluminum electrodes were immersed in warm 1 M KOH for one minute to allow hydrogen evolution to assist in cleaning

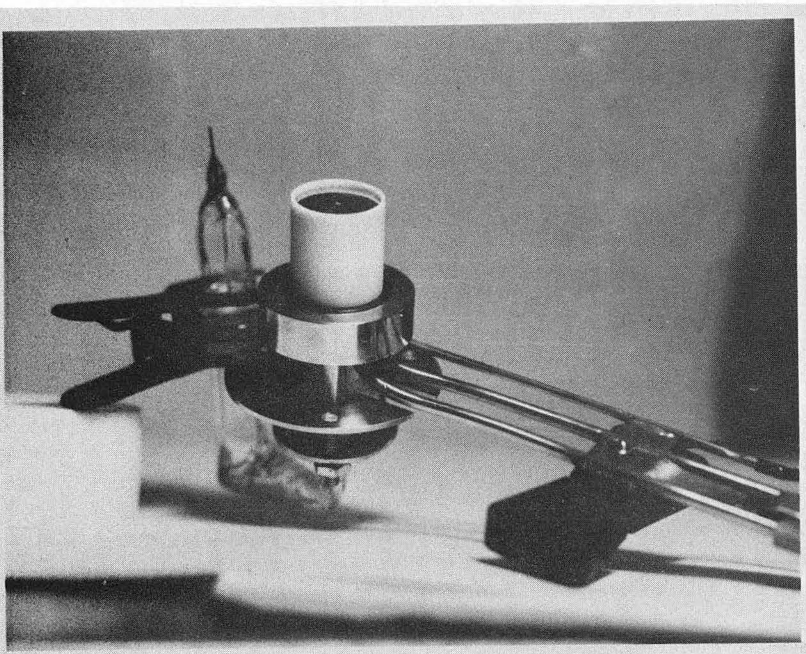

Figure 3-5. Stainless steel (304) electrode with built-in heater and thermocouple; the reference electrode chamber was connected to the electrode surface through a hole located at the axis of the electrode.

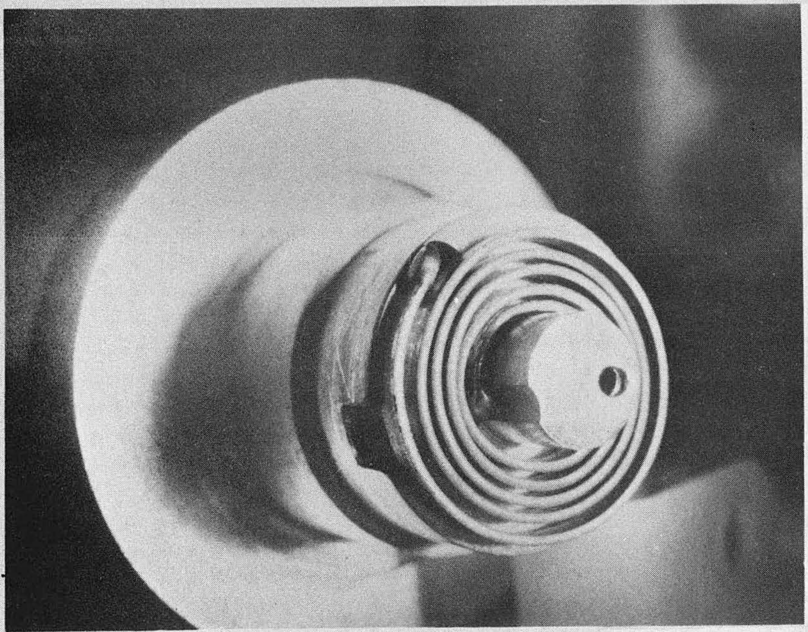

XBB 793-4105

Figure 3-6. Internal construction of the stainless steel electrode shown in figure 2-5.

the surface. The electrodes were carefully washed and dried before use.

## 3.5. Electrolysis Cells

Numerous cells of different design have been used in obtaining the results presented. Each configuration, usually evolved from several designs, had its own particular advantages. For the sake of brevity, the intermediate stages of the cell development are not presented. Because of the large number of cells used, it appears best to describe each one separately and to number them for reference.

#1 (Figure 3-7): The flask was a 25 ml (34/12) weighing bottle. Twenty ml of electrolyte were used. Electrodes were placed concentric to each other to assure uniform current distribution. Only in experiments where large surface area was needed was the Pt gauze cylinder employed as the working cathode (the anode was an aluminum cylinder). Otherwise, the working electrode was a solid cylinder as illustrated, made of either aluminum or stainless steel. Edge effects were minimized by using a Teflon cap and electrode holder.

In experiments designed to determine the amount of water in the electrolyte, a moving electrode was required.

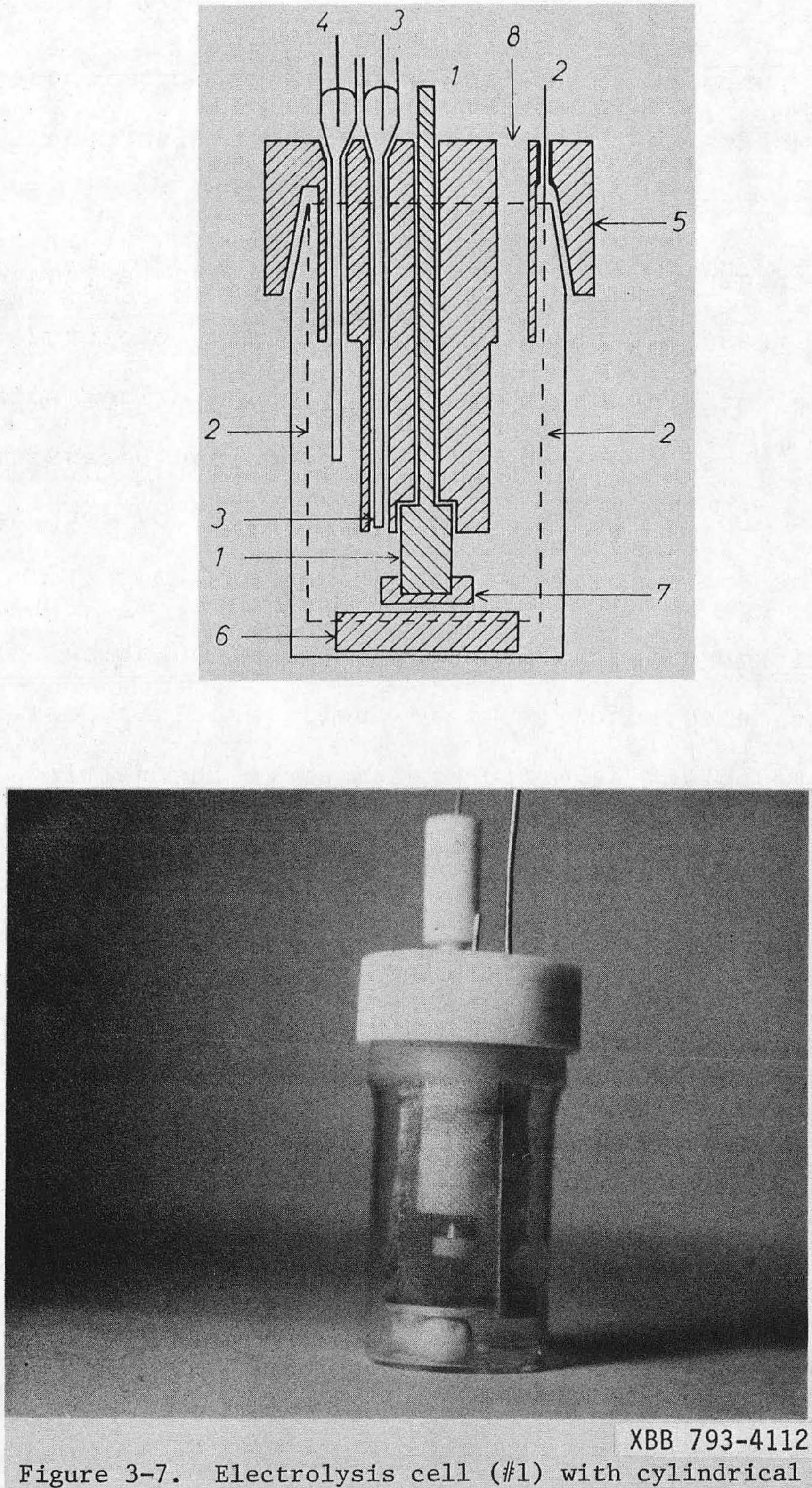

XBB 793-4112

Figure 3-7. Electrolysis cell (#1) with cylindrical geometry: (1) Center electrode; (2) Platinum screen electrode (2.5 cm diameter, 40 cm$^2$ surface area); (3) and (4) Potassium reference electrodes; (5) Teflon holder; (6) Teflon coated magnetic stirring bar; (7) Teflon cap for the center electrode; (8) Opening for thermometer or for taking samples of electrolyte.

For this purpose, a similar Teflon holder was constructed to accomodate a Pt wire as the center electrode. The Pt wire was vibrated by the stirring bar.

#2 (Figure 3-8): This set-up provided a convenient means to measure the behavior of potassium electrode below 63$^{o}$C (the melting point of potassium). The potassium electrode was prepared by pouring molten potassium into the glass cup. A flat surface was obtained by cutting off the excess potassium with a knife.

#3 (Figure 3-9): The vertical orientation of the potassium electrode in this cell made it possible to obtain overpotential measurements above the melting point of potassium. The counter electrode was a Pt electrode (the edges coated by soft glass) with a heavy potassium deposit on it. Before the measurement, an auxiliary potassium cup electrode was first used as an anode to deposit potassium on the counter electrode.

#4 (Figure 3-10): This H-cell with a reference electrode chamber was designed for electrolyses under vacuum. The anodic and cathodic chambers were connected to the laboratory vacuum source (60 mm Hg). After degassing for 30 minutes, the two chambers were isolated by turning off the valves to the laboratory vacuum. At the end of the electrolysis gas samples were collected by turning on the

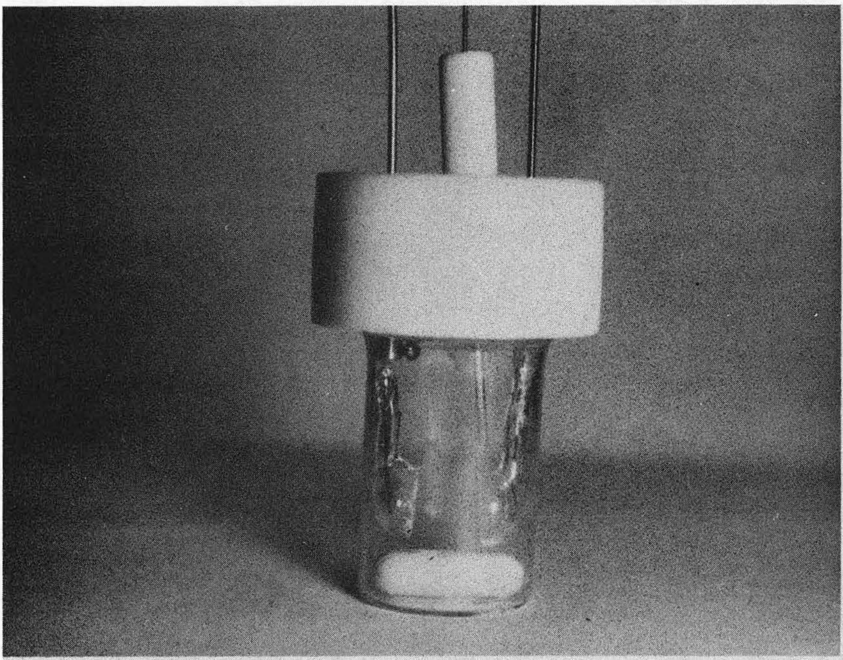

Figure 3-8. Electrolysis cell (#2) with two potassium cup electrodes for overpotential measurements below 63°C.

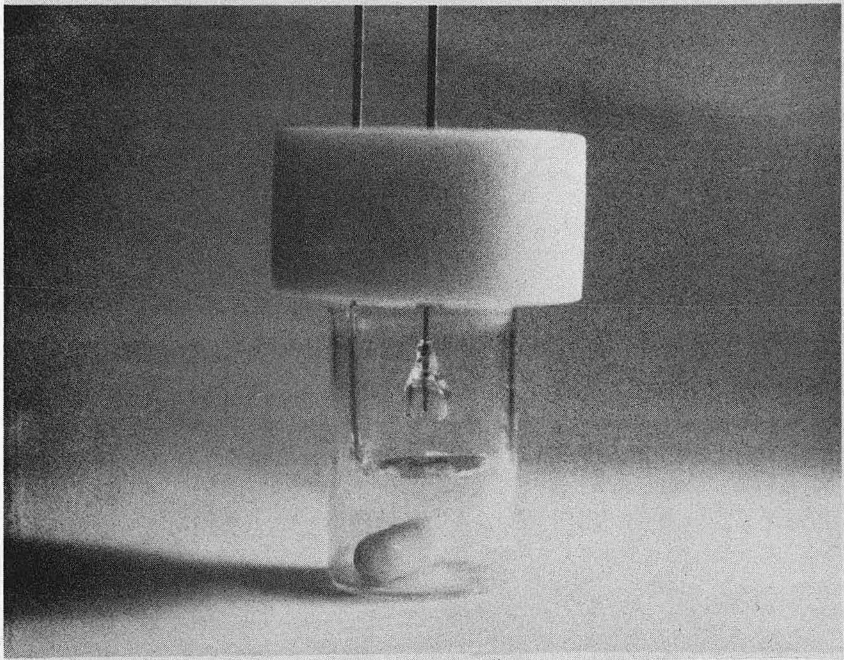

XBB 793-4105

Figure 3-9. Electrolysis cell (#3) with a potassium cup electrode for overpotential measurements at temperatures higher than the melting point of potassium.

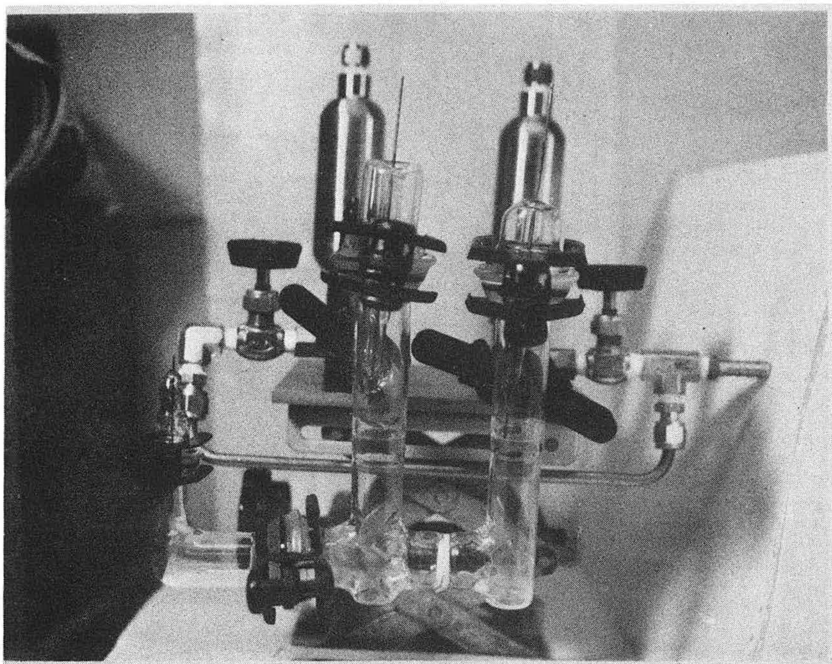

Figure 3-10. Electrolysis cell (#4) for electrolyses under vacuum with the gas samples collection apparatus.

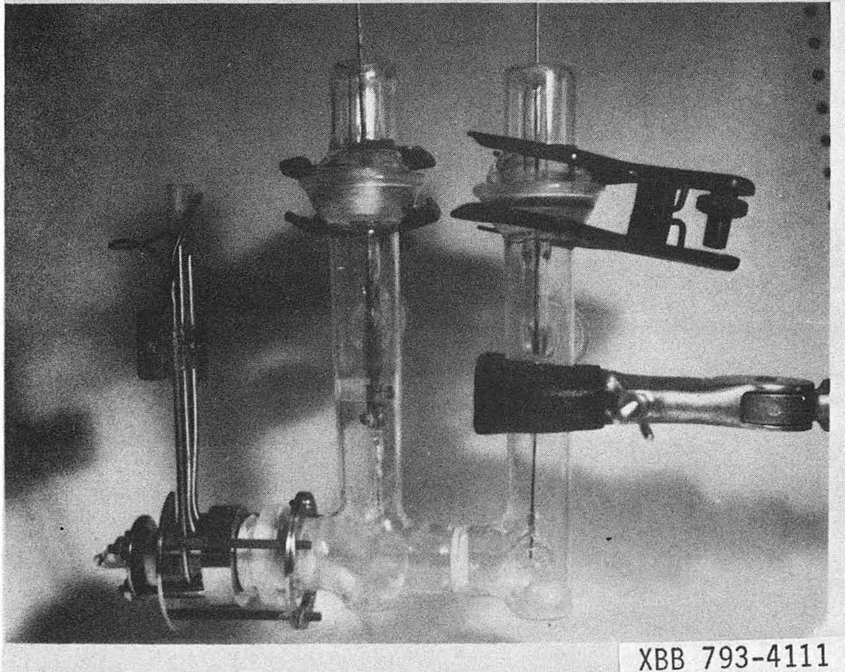

XBB 793-4111

Figure 3-11. Modified H-cell (#5) with a stainless steel heater electrode for potassium deposition studies.

quick action toggle switch high vacuum valves to the gas sample bottles (already at 1 micron Hg). The gas samples were analyzed by a low resolution mass spectrometer AEI MS-12.

#5 (Figure 3-11): Here the H-cell was equipped with a stainless steel heater electrode. Usually potassium cups served as counter electrodes. If necessary the potassium cup near the heater electrode could also serve as a reference electrode. Potassium deposited on stainless steel was used as an anode in other electrolysis experiments.

#6 (Figure 3-12): This rotating disk electrode (RDE) apparatus was essentially the same as the one used by Jorne[J3] and was modified so that it could be placed inside of the glove box. The electrolysis cell (Figure 3-13) was completely different. The RDE was a Pt electrode with a surface area 0.707 $cm^2$. The rotational speed range was 0 - 3600 rpm. The counter electrode was the stainless steel heater electrode with a potassium deposit obtained from another electrolysis. The electrolyte could also be heated and the temperature was controlled within $\pm 0.2^{\circ}C$.

#7 (Figure 3-13): This cell combined the advantages of the heater electrode and of cell #1. The cylindrical symmetry made it possible to use only 50 ml electrolyte in

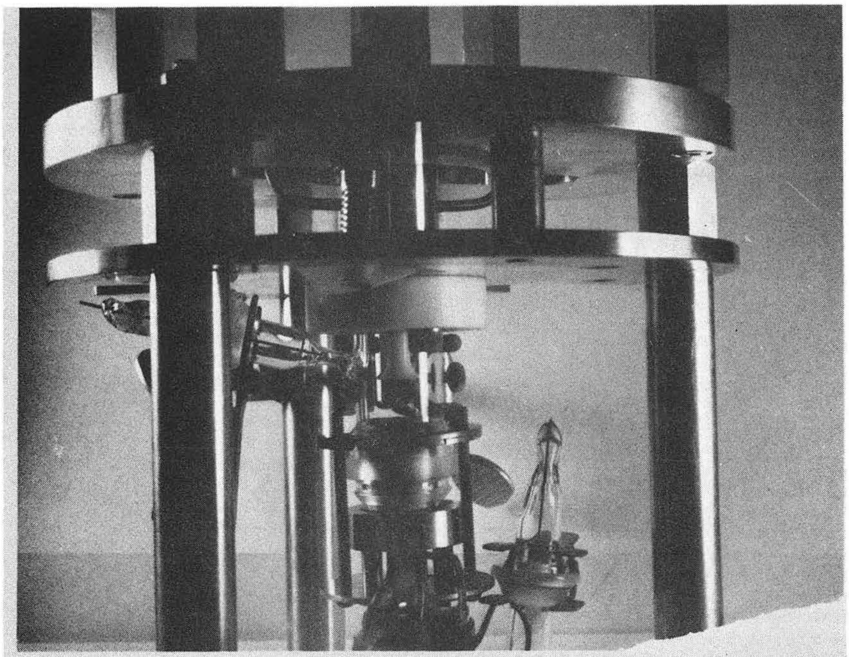

Figure 3-12. The rotating disk electrode apparatus with the cell.

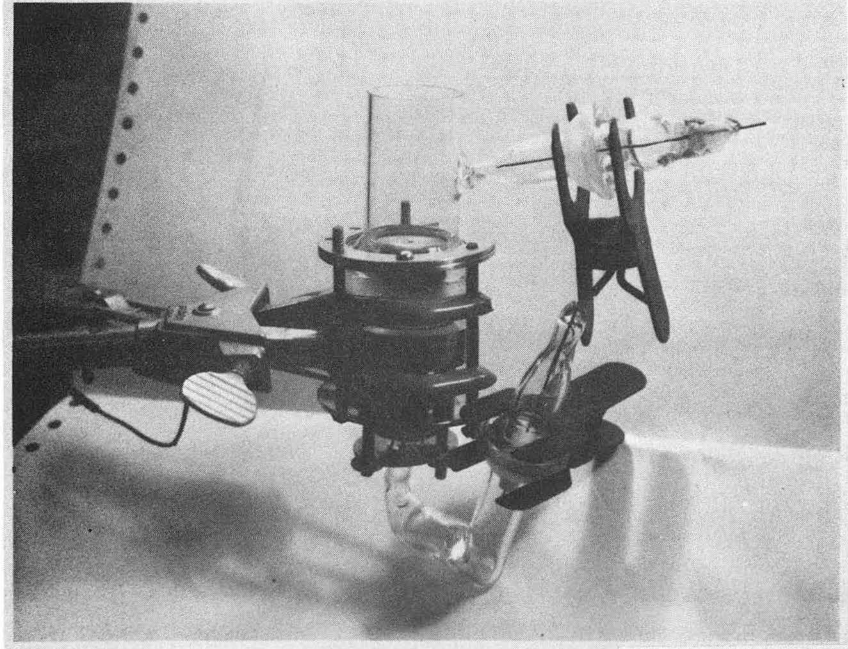

XBB 793-4110

Figure 3-13. Electrolysis cell (#6) for RDE with a stainless steel heater electrode.

combination with a center electrode having a large (15 $cm^2$) surface area. A heater (Chromalox, cartridge type, 100 watt) and a thermocouple were placed inside the center electrode to control the surface temperature. The anodic dissolution of the aluminum coil (99.9995%) made it possible to determine the current efficiency of the potassium deposition using the difference of the potassium ion concentration before and after the electrolysis and also from the weight of the potassium deposit.

#8 (Figure 3-14): This cell is similar to cell #7, except that a potassium anode replaces the aluminum coil. The anode was prepared by pouring molten potassium into a flask with a polyethylene cylinder set at the center (shown in the figure). A stainless steel screen was used as the current collector. The polyethylene cylinder was removed at about 50°C after the potassium has sufficiently hardened and yet did not stick to the polyethylene cylinder. Only 30 ml of electrolyte were used. At a temperature higher than the melting point of potassium, the cell was placed inside an aluminum block cooled by a solid state cooler and stirrer (Thermoelectric Unlimited Co.), so that the temperature of the potassium anode was kept below the melting point and the solution was stirred at the same time.

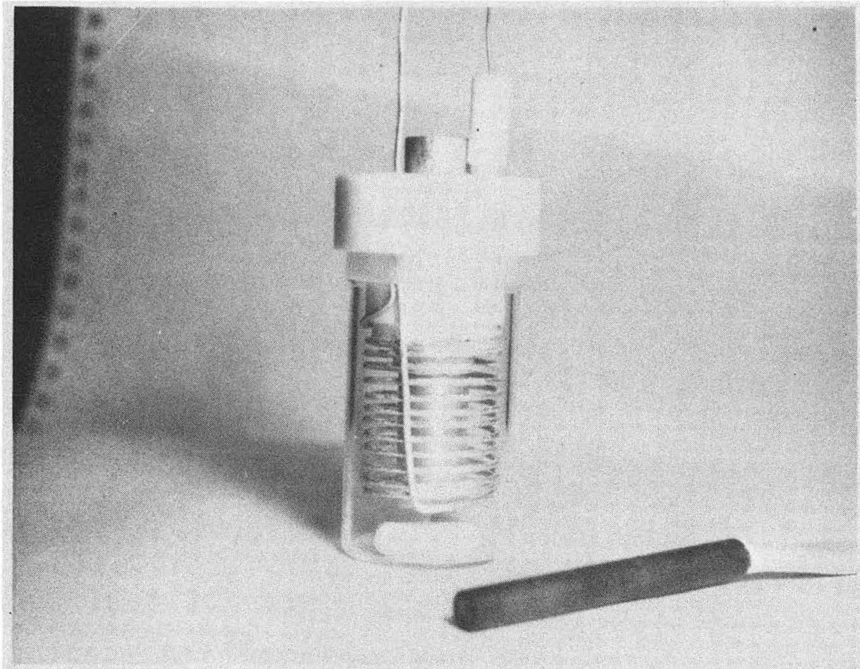

Figure 3-14. Electrolysis cell (#7) with the heater for determining the current efficiency of potassium deposition.

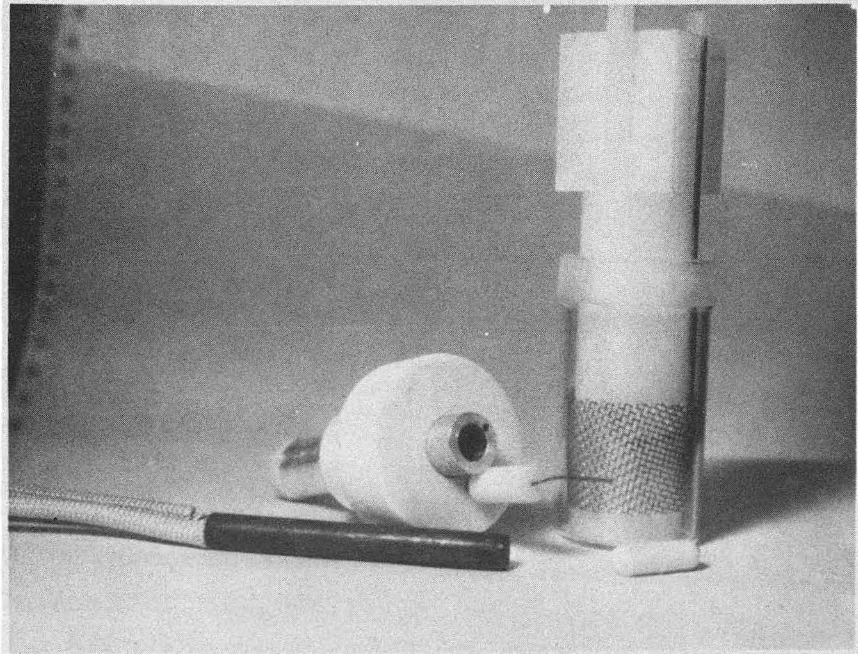

Figure 3-15. Electrolysis cell (#8) with the apparatus for making the potassium anode in measuring overpotential.

XBB 793-4106

#9 (Figure 3-16): This membrane cell was designed to determine the compatability of the Dupont Nafion membrane with PC electrolyte. The type tested was Membrane 425, a 5 mils thick homogeneous film of 1200 equivalent weight perfluorosulfonic acid resin laminated with T-12 fabric of Teflon TFE resin. Before use, the membrane was treated with KOH solution, washed with distilled water and dried under vacuum. The electrochemical characteristics of the Nafion membrane were not determined. Upon use in potassium deposition experiments, the membrane did not show any visible physical change, and the deposition process was not affected to any noticeable degree when these membranes were used to separate the electrode compartments.

## 3.6. Instrumentation

Instruments employed in this study served two functions, supplying the power for the electrochemical reaction, and measuring and recording transient and steady state potentials, current, and temperature. The first group consisted of potentiostats and function generators. The second group included digital multimeters, strip chart (X-time) recorders, X-Y recorders , and a data acquistion system involving a computer controlled digital oscilloscope. A coulometer (Princeton Applied Research, Model 379) was also employed. Figure 3-17 shows the

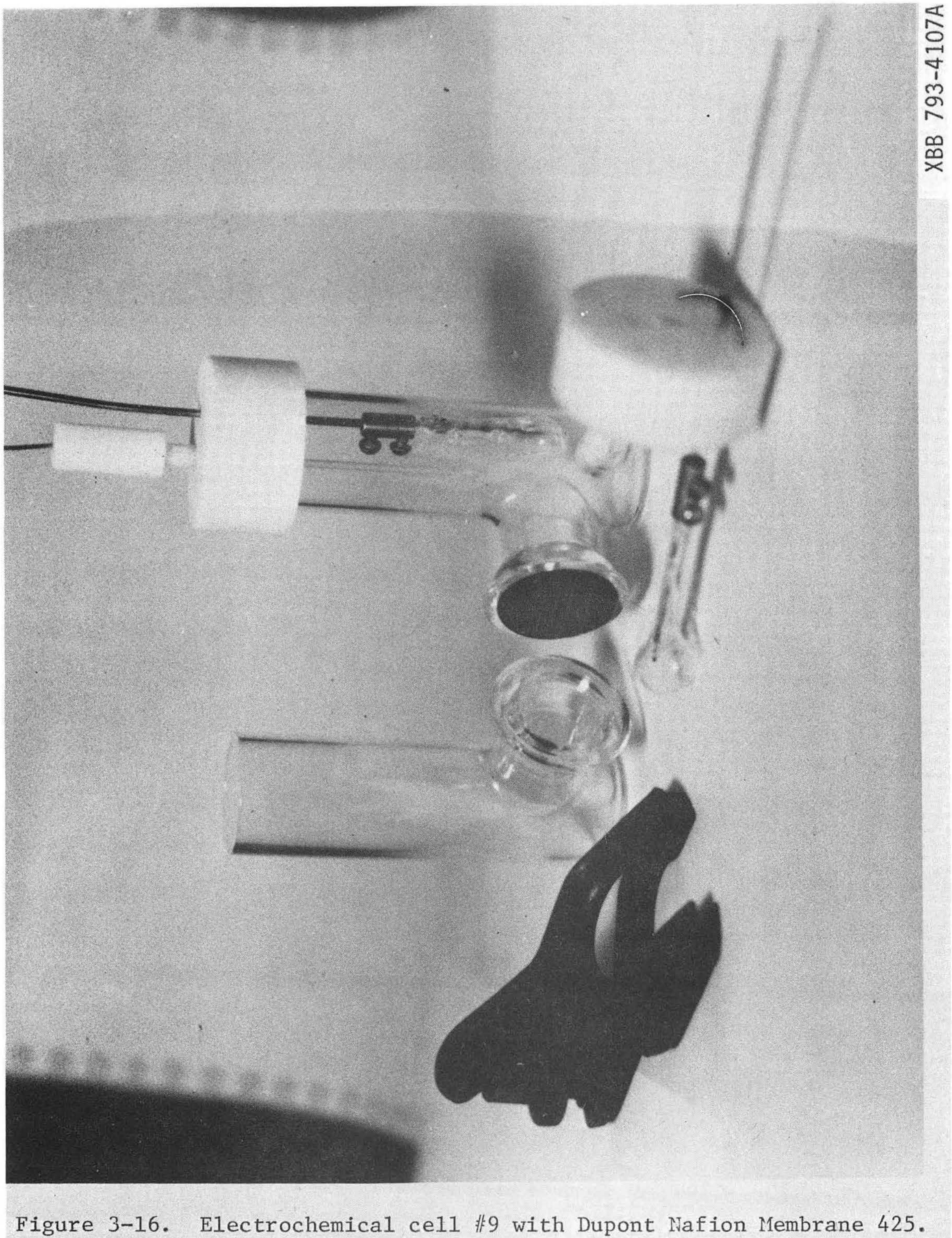

Figure 3-16. Electrochemical cell #9 with Dupont Nafion Membrane 425.

author sitting near one of glove boxes and some of instruments used.

The potentiostats/galvanostats used were Princeton Applied Research (PAR) Model 173/176, Amel Model 551, and Wenking models 66TS1 and 61RS. The output of these instruments can be modified by external function generators to give the various waveforms required; for example, a square pulse for current interruption and current pulse experiments or a triangular wave for linear sweep and cyclic voltammetry. A custom-made pulse generator and Exact models 250 and 255 function generators were used initially. These were later replaced by a Universal Programmer (PAR model 175).

In order to minimize the disturbance on the electrochemical system when making a measurement, only high input impedances devices were employed. The digital multimeters used (Weston model 4444 and Keithley model 172) had input impedance higher than $10^9$ ohms. When necessary, low input impedance instruments, such as a potentiometric recorder or an oscilloscope, were coupled with a custom-made differential voltage follower to provide an input impedance of $10^{10}$ ohms. The strip chart (X-time) recorders used were Linear model 300 series and Hewlett-Packard model 7100B. The X-Y recorder was a HP

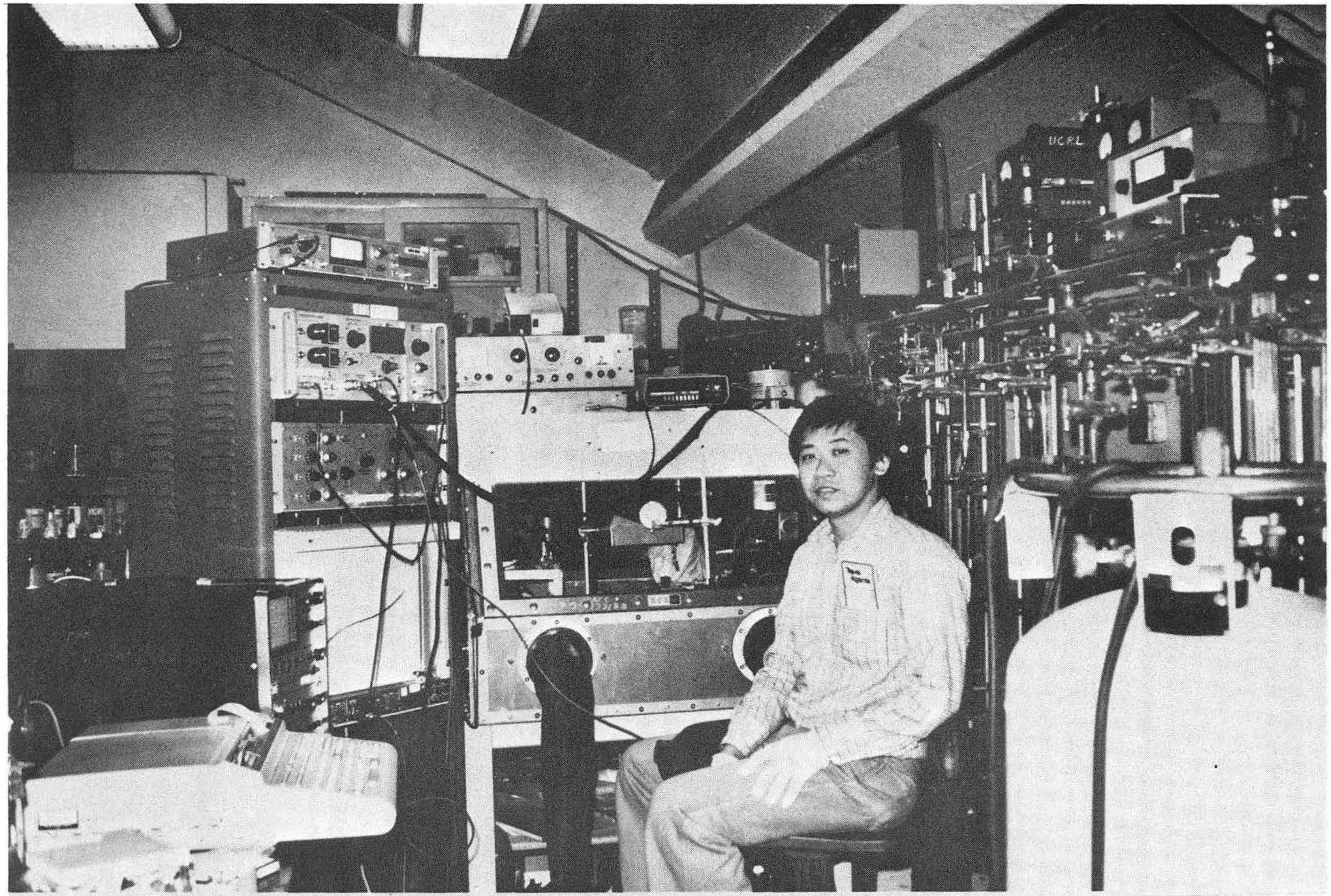

CBB 792-2603

Figure 3-17. The author with the glove box and some of the instruments used.

model 7447A with a time base option.

The data acquisition system consisted of a Nicolet digital oscilloscope model 1090A interfaced with a Hewlett-Packard model 9825A desk computer. The digital scope has a memory space of 4096 12-bit words. It can take data as rapidly as 0.5 microsecond/point and as slowly as 200 seconds/point. The data can be stored on a data cartridge and can be plotted by a HP 9862A plotter or an X-Y recorder through the oscilloscope. This system also provides convenient means to perform routine data reduction.

## 4. Electrolyte Preparation and Determination of Impurities

Impurities in any electrochemical system often change the true picture of what is happening. A process that might otherwise have occurred may not proceed at a significant rate. The K/PC system is no exception. An effect of impurities on the electrochemical behavior of potassium is illustrated in Figure 4-1. Cyclic voltammograms (A) and (B) contrast responses of a potassium electrode in a contaminated electrolyte before and after electrolysis involving potassium dissolution and deposition at 1 mA for 11 hours. The electrolyte was inside the glove box exposed to the helium atmosphere when air was accidentally introduced. It is difficult to estimate the amount of impurities absorbed. Cyclic voltammograms (A) show negligible current at a potential as cathodic as -400 mV relative to a potassium reference electrode. If the electrolyte we prepared had the same level of impurities, potassium deposition would not have occurred at all. After the electrolysis removes impurities, potassium deposition does occur, as shown by cyclic voltammograms (B). This distinctive change demonstrates the necessity to have an electrolyte as free of impurities as possible. Therefore, it is essential to

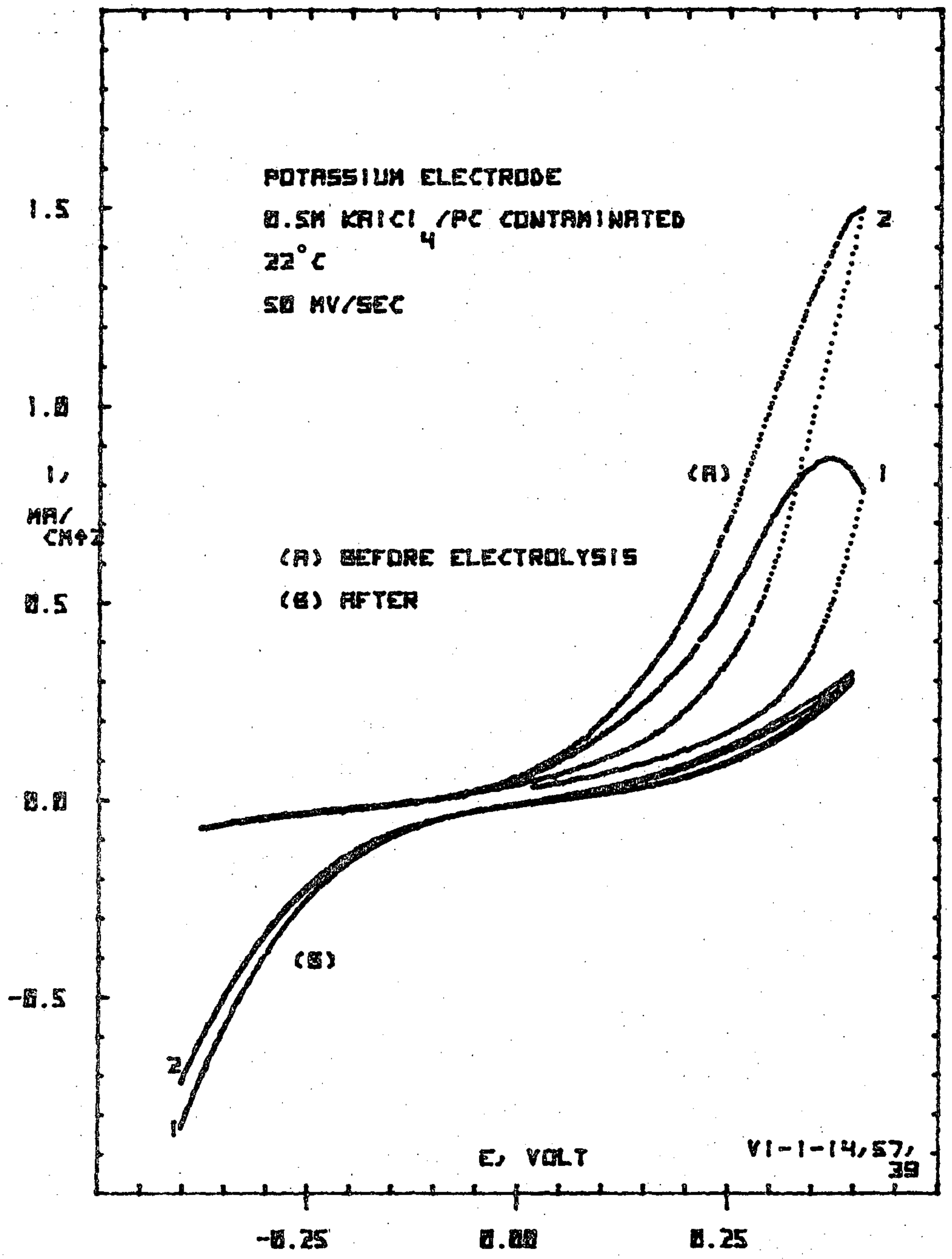

Figure 4-1. Cyclic voltammograms of a potassium electrode in a contaminated $KAlCl_4$ solution: (A), before the electrolysis at 1 $mA/cm^2$ for 11 hours; (B), after; (1) 1st sweep, (2) 2nd sweep, cell #2, reference electrode: $K/K^+$.

XBL-792-8463

purify the solvent and the solute with great care. The amount of water present in the solvent has also been determined because such a reference condition is needed for meaningful comparisons of results obtained by different researchers.

## 4.1. Solvent Purification

Propylene carbonate, as received, contains numerous impurities: water, propylene oxide, propylene glycol, allyl alcohol, etc. Many of these are known to react with potassium.

The flow diagram of our purification procedure is shown in Figure 4-2. Commercial grade PC, containing 0.1 - 1 % of water and 2 % of propylene glycols, was selected as the starting material because problems that could be encountered in a scaled-up operation would be revealed. At these concentrations, the common purification method--vacuum distillation--is not sufficient to remove impurities to ppm level by itself. Additional purification is necessary. For example, Chacon[C2] treated the distilled PC by passing it through a column of dried molecular sieves and alumina to reduce the impurity content further. But we determined that a post-distillation solvent purification step is not as effective as a pre-distillation one. Accordingly, our method

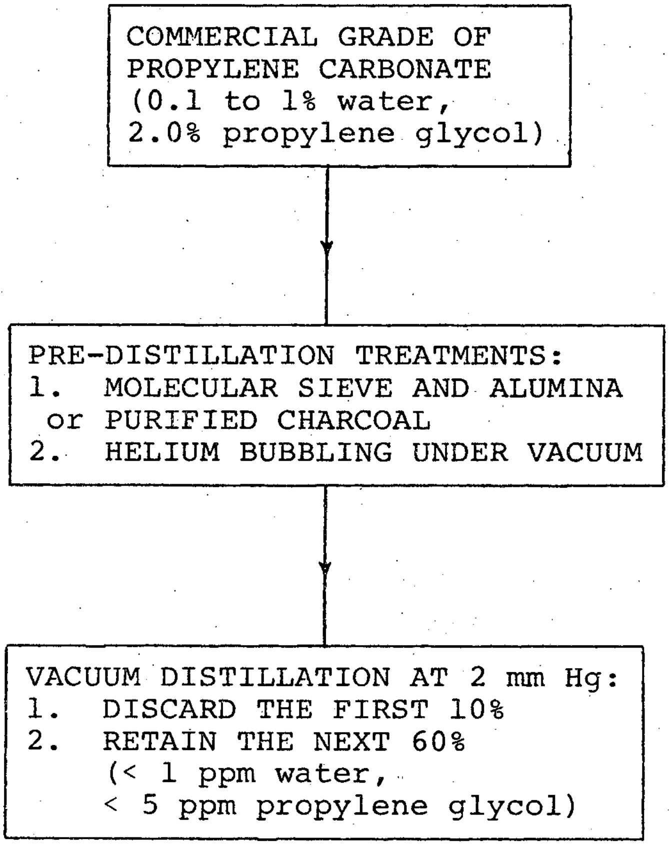

Figure 4-2. Flow diagram for the purification of propylene carbonate.

employs purification steps before distillation. Two treatments have been found satisfactory: (1) continuously passing through a column of molecular sieves and alumina, or (2) batch-wise mixing with purified charcoal. After this treatment, the solvent is transferred to the boiler pot of the distillation column. The bubbling of pure helium through the treated PC under 3 mm Hg vacuum removes the bulk of the volatile impurities. The remainder is eliminated by discarding the first 10% of the distillate. Only the middle 60% is collected for use. The purified PC, analyzed by gas chromatography, has less than 1 ppm of water and less than 5 ppm of propylene glycol. Other impurities have not been detected.

This procedure for purifying propylene carbonate avoids any inorganic and organic contaminant from materials used in a post-distillation treatment. Because distillation is the final step, the quality requirement of the absorbants used before distillation is less demanding. Also, the scale-up of this procedure shouldn't involve major difficulties.

## 4.2. Salt and Electrolyte Preparation

The potassium salt used in the present study is selected for its suitability in scaled-up operation. Important criteria are solubility, cost and abundance.

Solubilities of selected potassium salts reported in the literature are listed in Table 4-1. Although PC is capable of ionizing various inorganic salts, it does not dissolve potassium halides readily. From the solubility consideration, the choice is then limited to either $KPF_6$ or $KCl+AlCl_3$. The availability and cost of $KPF_6$ make it unattractive. We use KCl as the source of potassium because it is cheap, abundant and available at high purity ($40 per ton, 99.9% pure[C6]). Due to the low solubility of KCl, aluminum chloride is used to increase the potassium concentration and the electrolyte conductance by forming complexes with KCl. But the use of aluminum chloride also creates a problem. Because $AlCl_3$ is such a good complexing agent, the dissolution process is highly

Table 4-1

Solubilities of Potassium Salts in Propylene Carbonate at 25°c

| Salt | Concentration | Reference |
|---|---|---|
| KCl | 0.000352 m | C3 |
| KBr | 0.006 m | H1 |
| KI | 0.23 M | W1 |
| KI | 0.223 m | H1 |
| $KBF_4$ | 0.012 m | H1 |
| $KPF_6$ | 1.2 M | E1 |
| $KCl+AlCl_3$ | >1.0 M | J3 |

exothermic. The heat of solution is so large that it can decompose the solvent easily to undesirable products. Without a simple procedure for solution preparation, the use of KCl as the source of potassium would not be practical.

Several procedures were reported for the preparation of $AlCl_3$/PC solution. All are tedious and have to be carried out with extreme care. Keller et al.[K2] prepared the $AlCl_3$/PC electrolyte in this manner: they cooled $AlCl_3$ in a volumetric flask to liquid nitrogen temperature, added the solvent and allowed the mixture to thaw with repeated partial refreezing. Jorne[J3] reported the preparation of $AlCl_3$/PC solutions inside a glove box with argon atmosphere. The solutions were cooled with a chloroform--carbon tetrachloride--dry ice bath mixture. Finely powdered $AlCl_3$ had to be added carefully to avoid local heating and darkening of the solution. Chacon[C2] devised the most sophisticated procedure to prepare the $AlCl_3$ electrolyte. Besides adding $AlCl_3$ slowly to a well cooled solvent with potassium chloride, the solution was further purified by passing it through an absorption column of alumina. However, none of the procedures could easily be simplified to prepare large quantity of $AlCl_3$/PC solution in a straight-forward manner.

The key to simplifying electrolyte preparation is to avoid the large heat of solution of aluminum chloride and hence the thermal decomposition of PC. The problem is solved by synthesizing the double salt--potassium tetrachloroaluminate, $KAlCl_4$. The rationale for its use is as follows. According to Keller et al.[K2], the reaction upon dissolving $AlCl_3$ in PC proceeds as follows:

$$4\ AlCl_3 + 6\ PC \rightarrow Al(PC)_6^{3+} + 3\ AlCl_4^- . \qquad (4\text{-}1)$$

Addition of KCl results in the formation of the $AlCl_4^-$ ion, and the potassium ion:

$$4\ KCl + Al(PC)_6^{3+} \rightarrow 4\ K^+ + AlCl_4^- + 6\ PC. \qquad (4\text{-}2)$$

Each $K^+$ ion is expected to be solvated in average by 2.4 molecule of PC.[G2] The complete reaction is:

$$KCl + AlCl_3 \rightarrow K^+ + AlCl_4^- . \qquad (4\text{-}3)$$

Because the dominant species in the KCl + $AlCl_3$ solution are $K^+$ and $AlCl_4^-$, it is logical then to believe the dissolution of $KAlCl_4$ would avoid the exothermic reaction (4-1) and would create the same ionic species.

The $KAlCl_4$ salt dissolves readily in PC; the saturation concentration was determined to be approximately 2 M at room temperature. Its heat of solution is much smaller than that of $AlCl_3$ though it is still exothermic. Dissolving $KAlCl_4$ in PC does not cause any darkening or decomposition of the solution. Using the double salt provides us two additional advantages besides simplifying electrolyte preparation steps. First, no purification of KCl and $AlCl_3$ is needed. Even though $AlCl_3$ is very hygroscopic, the moisture remaining in $KAlCl_4$ does not require removal. In fact, the solution prepared from $KAlCl_4$ and purified PC contains less than 1 ppm of water (see next section). Second, traces of inorganic impurities present in KCl and $AlCl_3$, such as $FeCl_3$ in $AlCl_3$, are also removed during the synthesis of the double salt. This is because a side reaction occurring at about 500°C concentrates the impurities in a dense black precipitate in the molten double salt. Our analyses showed that the black material contained carbon; the iron and silicon content are at least one order of magnitude higher in the black precipitate than those of the double salt.

In summary, a straight-forward procedure to prepare pure electrolyte has been developed. This involves addition of $KAlCl_4$ instead of $AlCl_3$ and KCl in sequence.

## 4.3. Water Determination

In the electrodeposition of potassium in PC solutions, the most damaging impurity is water, even at the ppm level. Water initiates and catalyzes the decomposition chain reaction of PC and also reacts with potassium metal directly. Therefore, the amount of water present in PC has to be known and carefully controlled.

Cyclic voltammetry was employed to determine quantitatively the amount of water in PC electrolytes. By using a vibrating platinum electrode and by limiting the range of potential scan from 0.03 volt to 1.1 volt, we relate the change of cyclic voltmammograms to the presence of water in $KPF_6$ solution. By avoiding potassium deposition, the electrode can be used repeatedly without removal from the electrolyte. This eliminates the possibility of contamination by additional impurities adsorbed on the electrode surface. This procedure is in contrast with that employed by Jansta et al's work[D3] where each potential-current curve was obtained on a new Pt electrode by a single linear potential sweep to the potential beyond that of potassium deposition.

We have extended the use of cyclic voltammetry to the determination of water in $KAlCl_4$ solutions. The Pt electrode is not satisfactory in detecting the presence of water. A stainless steel electrode was found to be more sensitive, probably because an anodic reaction involving water occurs on the stainless steel electrode and not on the Pt electrode. The magnitude of the peak current could be used to correlate the amount of water in solution.

### 4.3.1. $KPF_6$ solution

Typical changes of the voltammograms of a vibrating Pt electrode in $KPF_6$ solution when 1 ppm of water was added are shown in Figure 4-3. The electrolyte was pre-electrolyzed with a potassium anode and a platinum screen cylinder as cathode for two days before the experiment. Curve 1 was recorded immediately before the addition of 1 ppm of water; curve 2 represents the tenth cycle after the addition. The important feature of the voltammogram is the appearance of an incompletely developed peak at 0.3 volt. A reaction with water in the potential range from 0.25 volt to 0.5 volt in PC was reported previously.[E2,G1,D3] The difference between the background current and the current at the shoulder (0.3 volt) is 60 microamperes. If there is a linear relationship between the water concentration and the peak current, we would detect water at a level at least one order of magnitude lower than 1 ppm. This means that less than 0.1 ppm of water is present in the system before the addition of 1 ppm water.

The effect of continuously cycling of the potential is shown by curve 3 in Figure 4-3. The curve, taken at 75 minutes (350 cycles) after water was added, approaches the same shape as before the addition. A new addition of 1 ppm of water results in a voltammogram similar to curve 2. Thus, cycling of the potential removes water from the

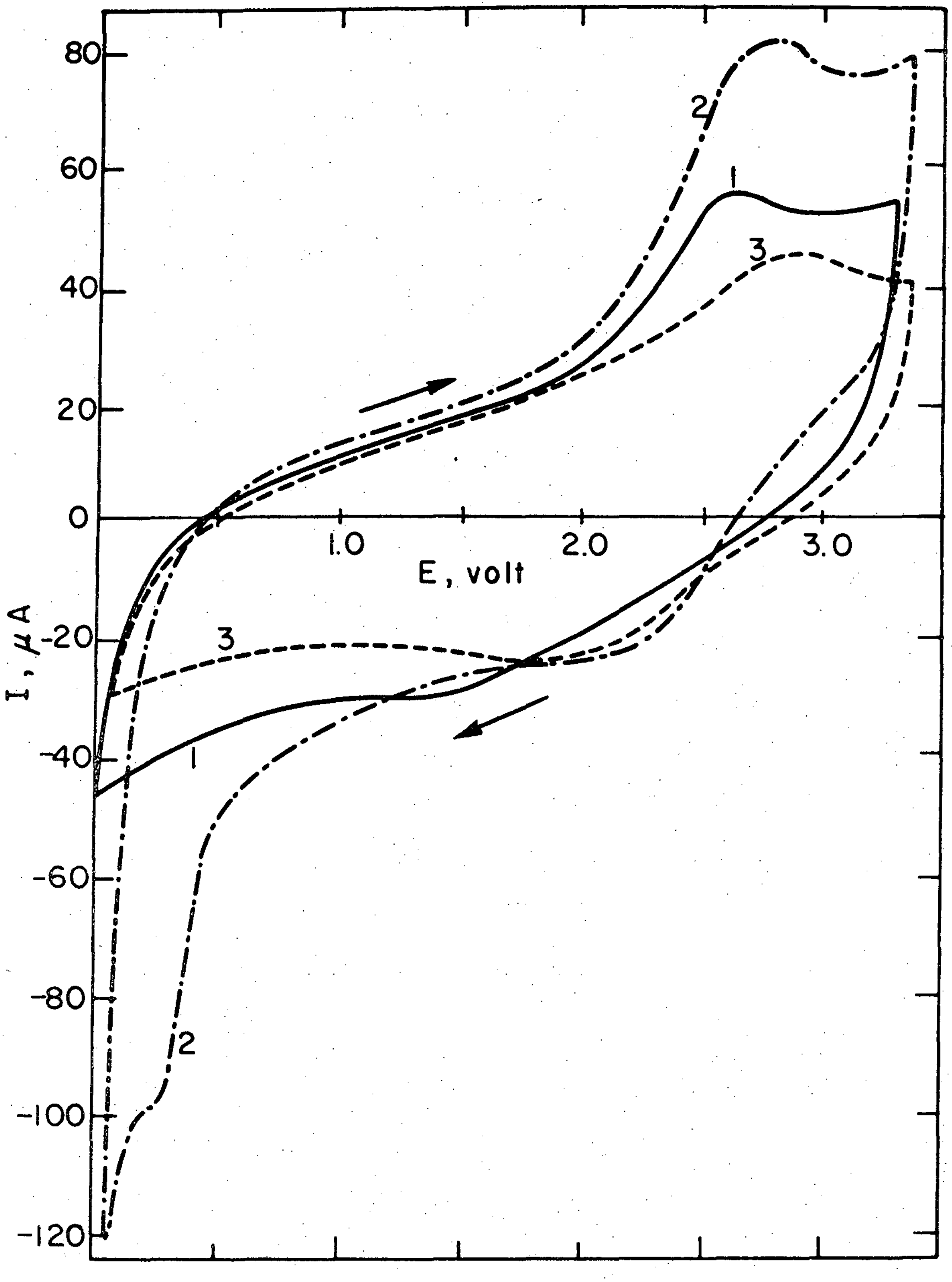

XBL 7812-6244

Figure 4-3. Effect of adding 1 ppm of water; indicating electrode: Pt wire, 1.3 mm diameter, 1.14 $cm^2$; 0.5 M $KPF_6$/PC, stirred; sweep rate: 260 mV/sec; curve 1 was taken before the addition; curve 2 was the 10th cycle after the addition; curve 3 was after 75 minutes of cycling (350 cycles) following the addition, cell #1, reference electrode: $K/K^+$.

electrolyte without changing the electrochemical behavior of the system. Fully developed cyclic voltammograms (those with largest current peaks) at three different potential sweep rates are compared in Figure 4-4.

The development of current peaks from the addition of only 0.33 ppm water to the same electrolyte is depicted in Figure 4-5(a). The background current was recorded after the working electrode had been kept at 0.25 volt for 48 hours, followed by cycling the potential for approximately 1 hour until the voltammograms show no further change. There is no pronounced peak in the background. Current peaks created by the addition of water become more pronounced with each additional cycle. The anodic and cathodic peaks appear to be mutually influencing each other even though they are 2.5 volt apart.

The influence of the range of the potential scan on the voltammograms is shown in Figure 4-5(b). In another experiment, after the maximum peak height is reached, the upper bound of the potential scan is lowered. Immediately the height of the cathodic peak decreases. Within eight cycles, the curve shows no sign of any electroactive impurity.

No conclusion concerning this behavior is offered although the reactions of potassium propylene glycolate on

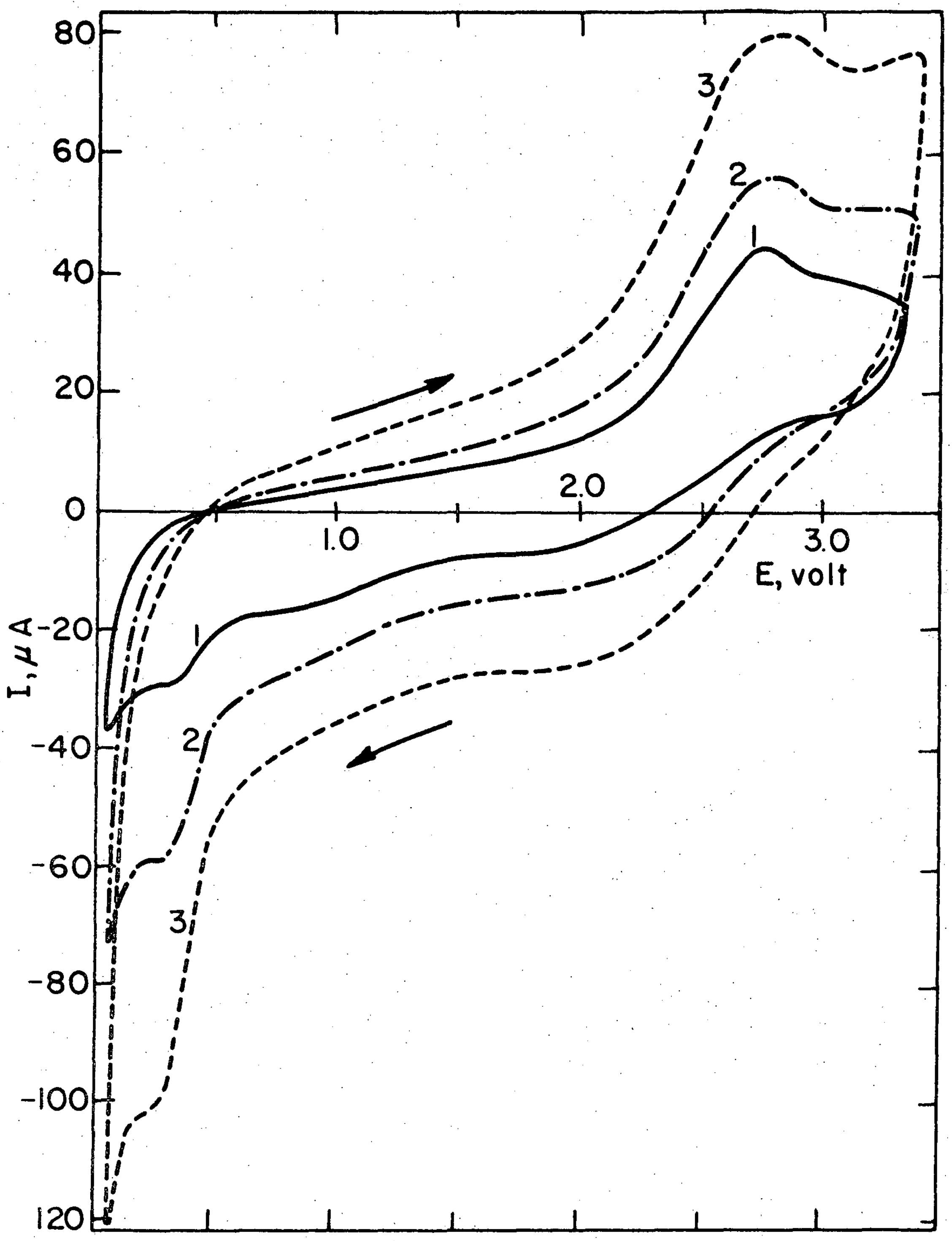

XBL 7812-6243

Figure 4-4. Influence of the potential sweep rate on cyclic voltammograms (the 10th cycle after adding 1 ppm of water to the system described in figure 4-3): curve 1, 65 mV/sec; curve 2, 130 mV/sec; curve 3, 260 mV/sec, reference electrode: $K/K^+$.

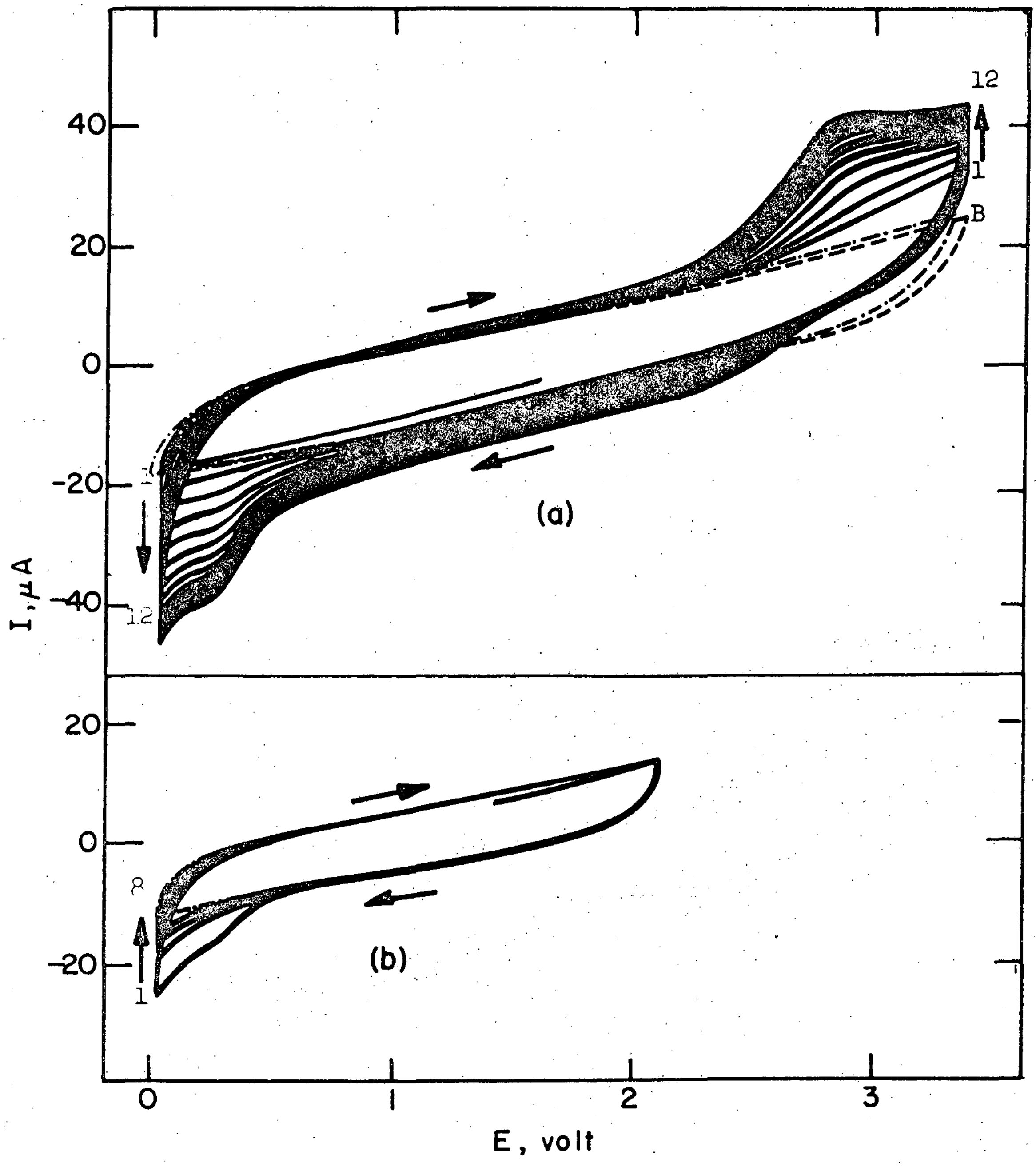

XBL771-7249

Figure 4-5. Cyclic voltammograms with the addition of 0.33 ppm of water; same system as in figure 4-3; sweep rate: 260 mV/sec; The curve (-•-•-) is the steady state voltammogram after the addition.

(a) Developments of the peaks, curve B is taken before the addition, curves 1 to 12 are the first twelve cycles after the addition.

(b) Influence of the potential range on the cyclic voltammograms, curve 1 is the first cycle after decreasing the upperbound of the potential range and curve 8 is the eighth cycle.

amalgam electrodes[D1] and the oxidation of hydrogen[G1] on platinum in $EtNClO_4$ systems was reported to occur at about 3 volts. The amount of charge passed in the cathodic region (Figure 4-5) is much smaller than that required for the reduction of 0.33 ppm water. The active sites on the electrode surface may be blocked, but the electrode resumes its activity with each addition of water (up to 20 ppm were added in this series of experiments).

The method of determinating water quantitatively involves relating the magnitude of the cathodic current peak at 0.5 volt (Figure 4-6) to the amount of water added. In order to avoid possible interference from anodic reactions, the upper bound of the potential range was limited to 1.1 volt. Over a period of 2 days at selected intervals, water was added only after the effect of the previous addition completely disappeared. A current extremum was always observed after each addition of water, from 0.3 to 3 ppm. The difference between that current and the background current at the same potential is a linear function of the water added to the system (Figure 4-7). The linear relationship is expected at this low concentration and is in agreement with the finding of Jansta et al.[D3]

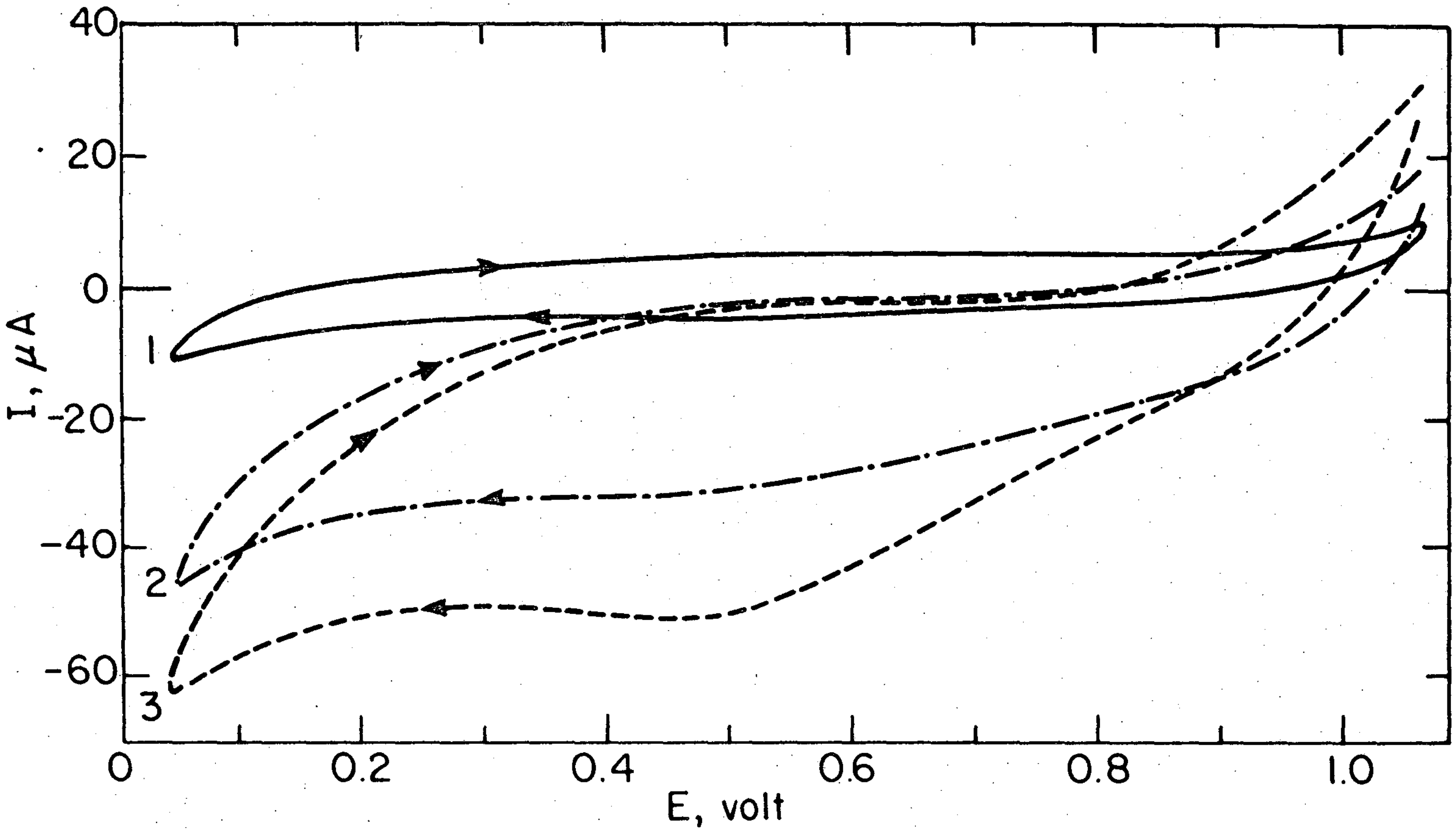

XBL 7812-6245

Figure 4-6. Cyclic voltammograms for quantitative determination of water; same system as in figure 4-3; sweep rate: 200 mV/sec; curve 1, before the addition of water; curve 2, after the addition of 1 ppm of water; curve 3, after the addition of 2.33 ppm of water, reference electrode: $K/K^+$.

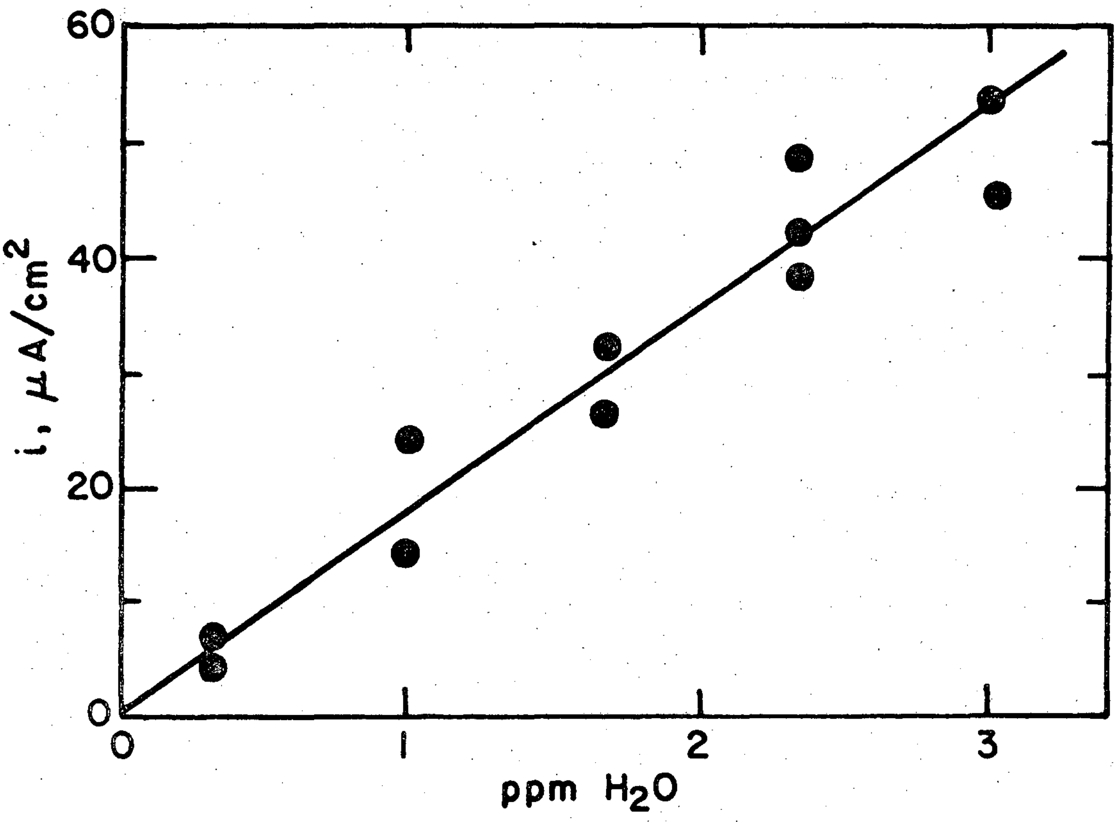

XBL 771-7100

Figure 4-7. Change of current density of the cathodic peak at 0.48 volt (figure 4-6) as a function of the amount of water added; sweep rate: 200 mV/sec; same system as in figure 4-3.

These results mean that no water is found to be present in the purified electrolyte at concentration above 0.1 ppm. Furthermore, the system consumes water in such a way that no sign of its presence could be noticed by the potential sweep method. Blockage of the electrode surface probably does not occur since the electrode is sensitive to new additions of water. Possibilities which should be further explored are (i) a slow chemical reaction between PC or some other organic component catalyzed by the presence of water and (ii) hydration of the ions resulting in water molecules bound in a way that would change their chemical activity.

As mentioned earlier, intense agitation of the working electrode during the experiment is necessary to get a response on the cathodic side of the cyclic voltammograms to the addition of water. The response of a stationary Pt electrode to the addition of water in an unstirred electrolyte is shown in Figure 4-8. An increase in the current passed on the cathodic side and a pronounced peak on the anodic side results. However, no characteristic peak appears at the potential near that of potassium reduction. The dependence of the peak on the sweep rate is similar to that presented in Figure 4-4. The cycling of the potential after the addition of water

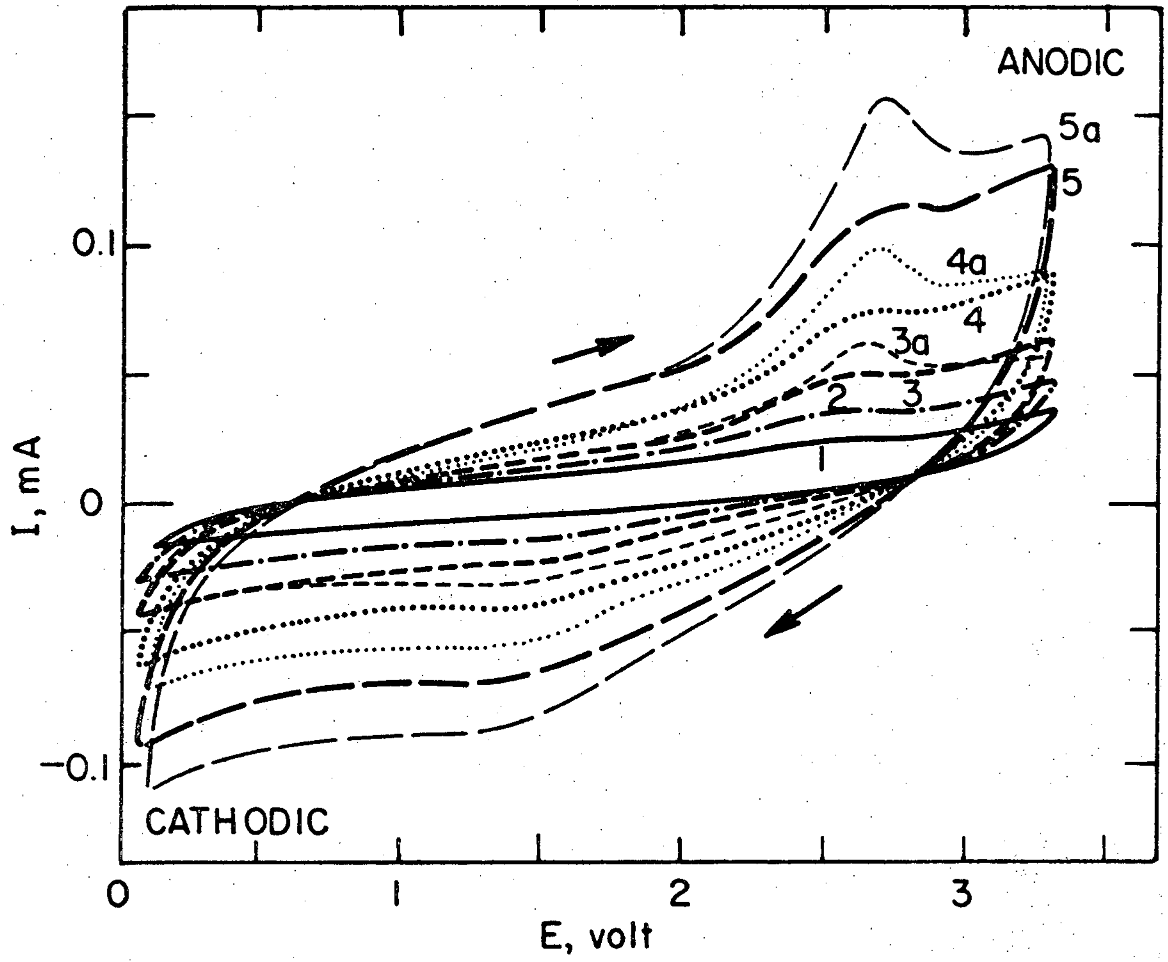

XBL7812-6249

Figure 4-8. Influence of the sweep rate on cyclic voltammograms obtained before and after the addition of 1 ppm of water in an unstirred solution; indicating electrode: cylindrical Pt electrode, 0.85 cm$^2$; 0.5 M $KPF_6$/PC; curves 1 to 5 are taken before the addition; curves 3a, 4a and 5a are after the addition; sweep rate: curve 1, 33 mV/sec; curve 2, 65 mV/sec; curves 3 & 3a, 130 mV/sec; curves 4 & 4a, 260 mV/sec; curves 5 & 5a, 520 mV/sec; cell #1, reference electrode: K/K$^+$.

brings the curves down to their original shape, and the peaks are reproduced.

### 4.3.2. $KAlCl_4$ solution

Cyclic voltammograms were obtained on platinum and stainless steel electrodes to provide a perspective on the background current. Curves in Figure 4-9 are voltammograms taken on a fresh Pt surface in 0.1 M $KAlCl_4$ solution with the potential scanned from 0.15 to 4.0 volt. A rather high activity with several distinct current peaks is shown on the first scan of potential. However, continuous cycling of the potential leads to a decrease in the current peaks on each subsequent curve, which eventually results in a reproducible voltammogram, one that is smoother than the cycle recorded initially. Similar voltammograms were obtained on a fresh stainless steel surface (Figure 4-10). The same results were reproduced in $KPF_6$ solutions in PC.

Although the background current behaves similarly, a vibrating Pt electrode is less sensitive to the presence of water in $KAlCl_4$ than in $KPF_6$ solution. The characteristic cathodic peak at 0.5 volt is not detected. The difficulty is similar to that of a stationary Pt electrode in $KPF_6$ solution. In contrast, a distinctive

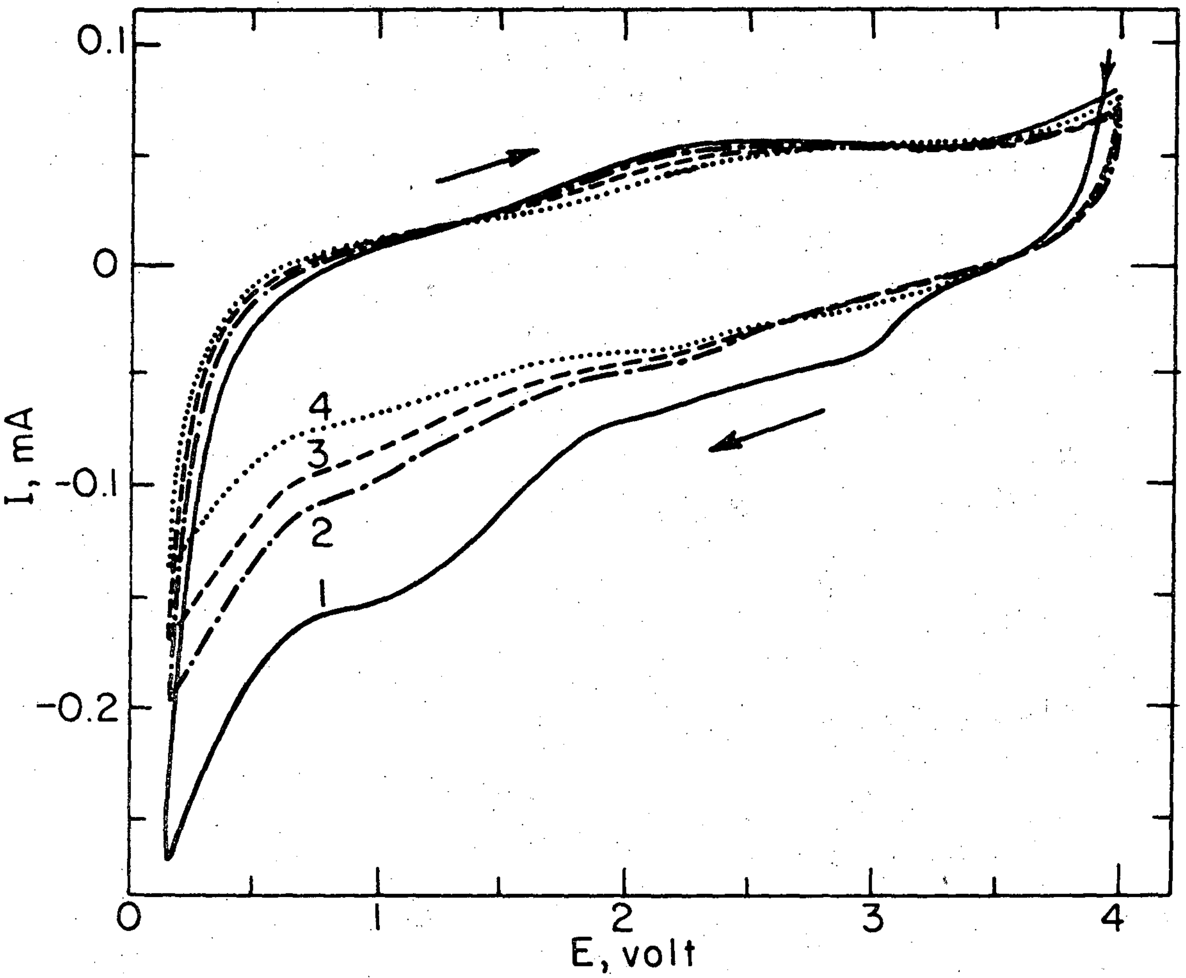

XBL7812-6246

Figure 4-9. Cyclic voltammograms on a fresh cylindrical platinum electrode, 0.85 $cm^2$; 0.1 M $KAlCl_4$/PC, unstirred; sweep rate: 110 mV/sec; curves 1, 2, and 3 are the first three cycles; curve 4 is the 6th cycle; cell #1, reference electrode: $K/K^+$.

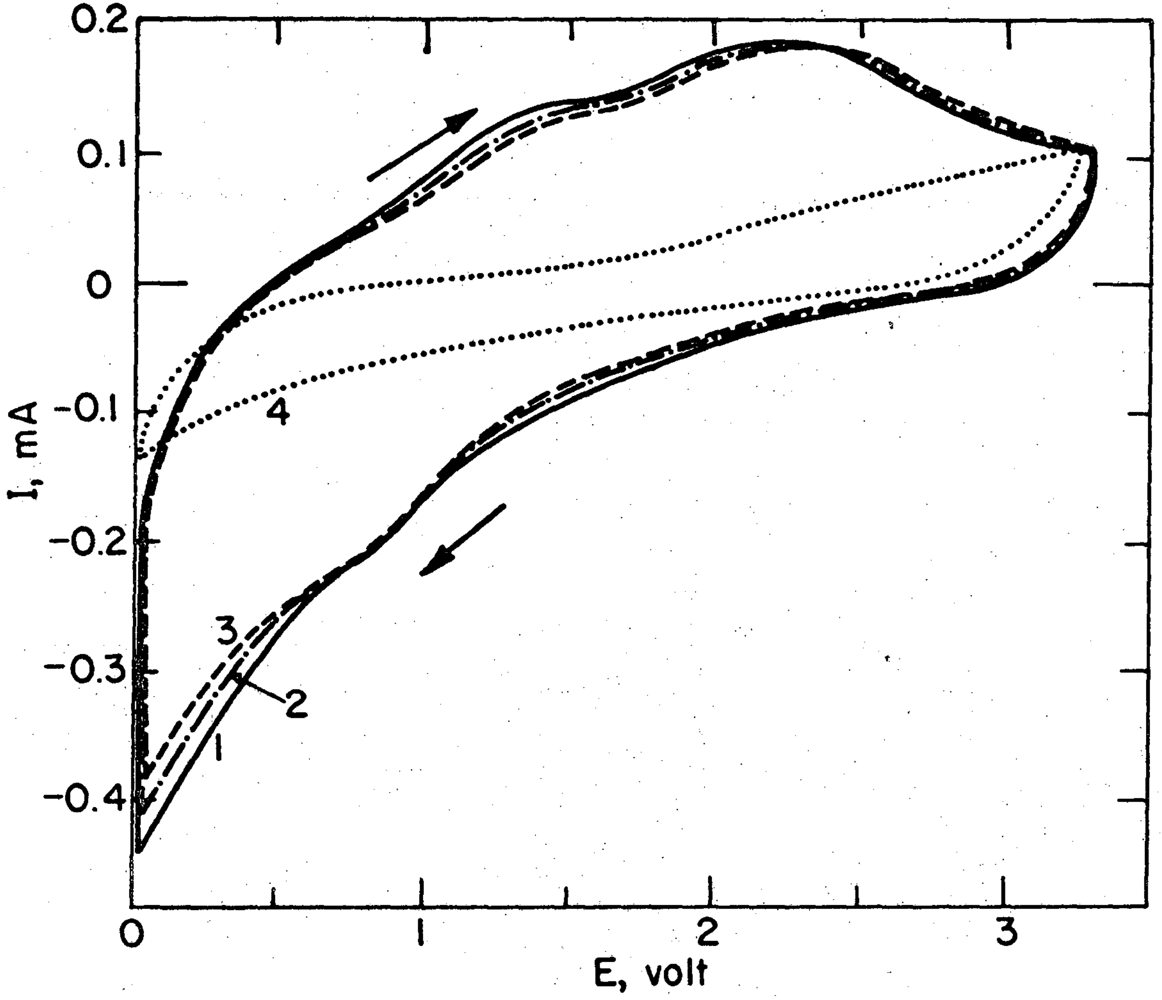

XBL 7812-6247

Figure 4-10. Cyclic voltammograms on a fresh cylindrical stainless steel electrode, 1 $cm^2$; 0.1 M $KAlCl_4$/PC, unstirred; sweep rate: 260 mV/sec; curves 1, 2 and 3 are the first three cycles and curve 4 is the 24th cycle; cell #1, reference electrode: $K/K^+$.

anodic current peak due to the presence of water was observed on a stainless steel electrode. Figure 4-11 presents the cyclic voltammograms before the addition of 1 ppm of water (curve 1) and the seventh cycle after (curve 2), as well as the recovery of the system by continuously cycling the potential (curve 3). As the water is added, a large anodic current appears at 3.5 volt with a shape similar to that of the dissolution of a metal with a passive layer on its surface, and the cathodic activity does not increase. This experiment shows that less than 1 ppm of water is present in $KAlCl_4$/PC solutions, a level similar to that in $KPF_6$/PC solutions.

Figures 4-9 and 4-10 show that no component in the $KAlCl_4$/PC system should react in the same potential region. The dissolution of some of the constituents of stainless steel therefore must occur. For instance, Dousek et al[D2] have reported that the dissolution of nickel started at about 3.8 volt in $KPF_6$ solution in PC. The water in the system merely modifies the process of dissolution. A probable scheme might involve the hydrolysis of $AlCl_4^-$ giving HCl, which might act as a breaking agent, destroying the protective layer on the stainless steel surface. Once the water is used up, a new passive film (perhaps formed by PC decomposition)

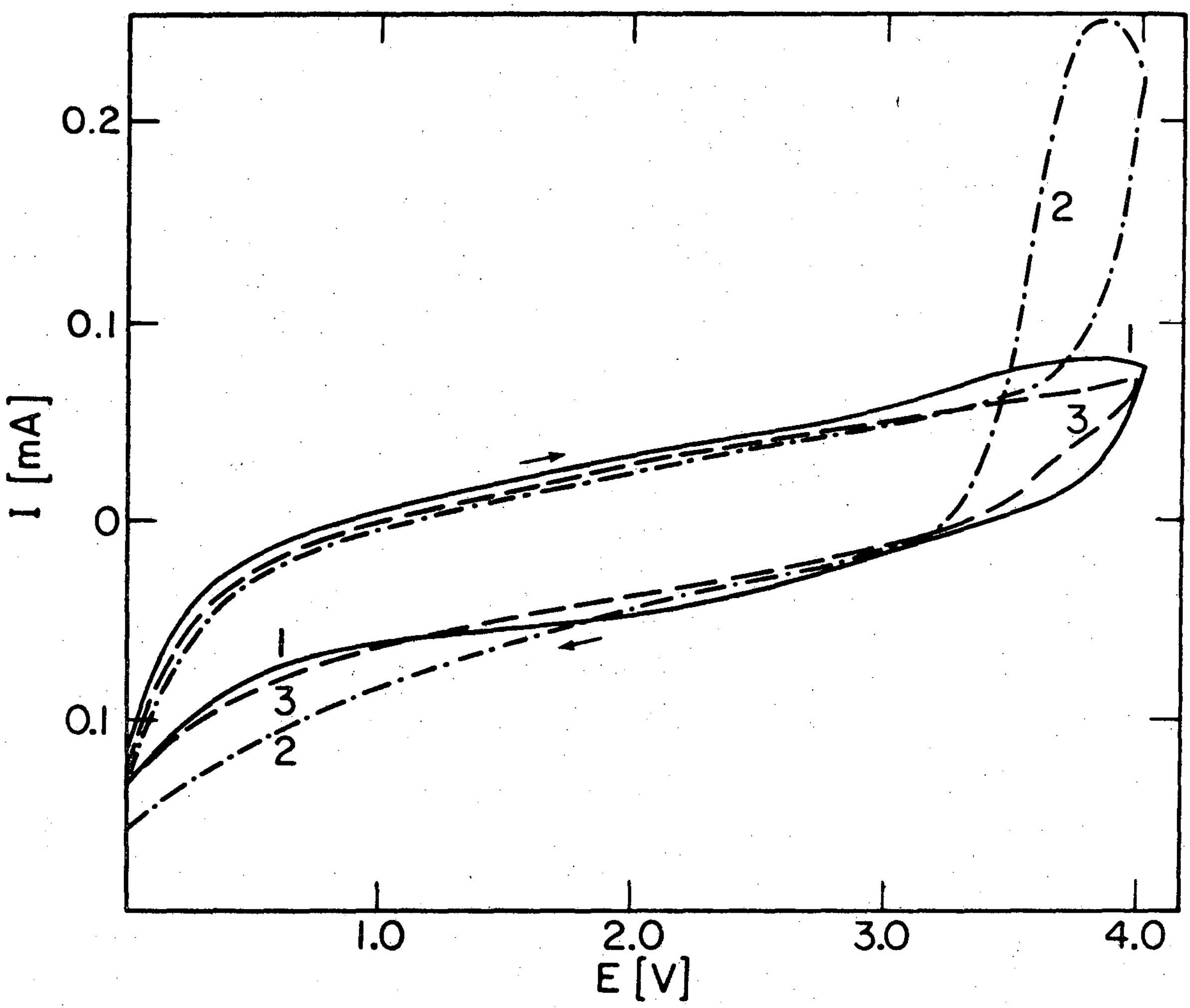

XBL 764-2697

Figure 4-11. Effect of 1 ppm of water in unstirred 0.1 M $KAlCl_4$/PC; indicating electrode: cylindrical stainless steel electrode, 1 $cm^2$; sweep rate: 260 mV/sec; curve 1, before the addition; curve 2, 7th cycle after the addition and curve 3, 25th cycle; cell #1, reference electrode: $K/K^+$.

gradually protects the electrode from further dissolution.

In summary, less than 1 ppm of water was shown to be present in the electrolyte prepared by our technique. The blockage of the electrode surface by inert materials in PC is confirmed. The breakage of the passive layer on the stainless steel surface is responsible for the anodic peak at 2.8 volt. In $KAlCl_4$ solutions, the stainless steel electrode is more sensitive than the platinum electrode for the detection water at the ppm level.

## 5. Stability of Potassium in Propylene Carbonate Electrolyte

Compatibility of PC with potassium is a crucial question which needs to be answered because solvent stability is a necessary criterion for the success of any practical electrochemical process. In the case of potassium deposition in PC electrolyte, any solvent decomposition reaction can decrease the current efficiency. Decomposition products can inhibit the potassium reduction by either changing the state of the electrode surface or by reacting with the potassium deposits. The accumulation of these decomposition products would also require costly reprocessing of the electrolyte.

Despite extensive research efforts on the use of propylene carbonate in recent years, the free energy of formation of PC has not been determined as yet. As shown by our analysis in Appendix I, PC and potassium are not expected to be thermodynamically stable. Therefore, we are interested in the kinetic behavior. Given a reactive metal like potassium, a satisfactory kinetic stability criterion would be that the decomposition reaction should proceed at a negligible rate when compared to that of electroreduction of potassium under practical operating conditions.

Often impurities or decomposition products form a film on the electrode surface. Such a surface layer would hinder any reaction occurring on the surface. The system would then appear to have no stability problem. For processes involving continuous renewal of the surface, as in metal dissolution and deposition, such a false stability assumption would only lead to erroneous conclusions. Thus, observing no reaction upon physical contact is not sufficient for establishing stability. In the present study, cyclic voltammetry and chronopotentiometry were employed to study the stability of PC in contact with potassium.

## 5.1. Surface Layer

The existence of a passivating layer on potassium was demonstrated by the response of a potassium electrode to two consecutive current pulses. Figure 5-1 depicts the duration of anodic current pulses (1 $mA/cm^2$) and the corresponding change of electrode potential. The electrode approached steady state in about six seconds after the initiation of the first pulse, while this occurred after less than one second during the second pulse at the same current. After the anodic pulses, two cathodic pulses were applied. Figure 5-2 shows the chronopotentiogram. The electrode responded similarly, but the change was less dramatic. The potassium surface

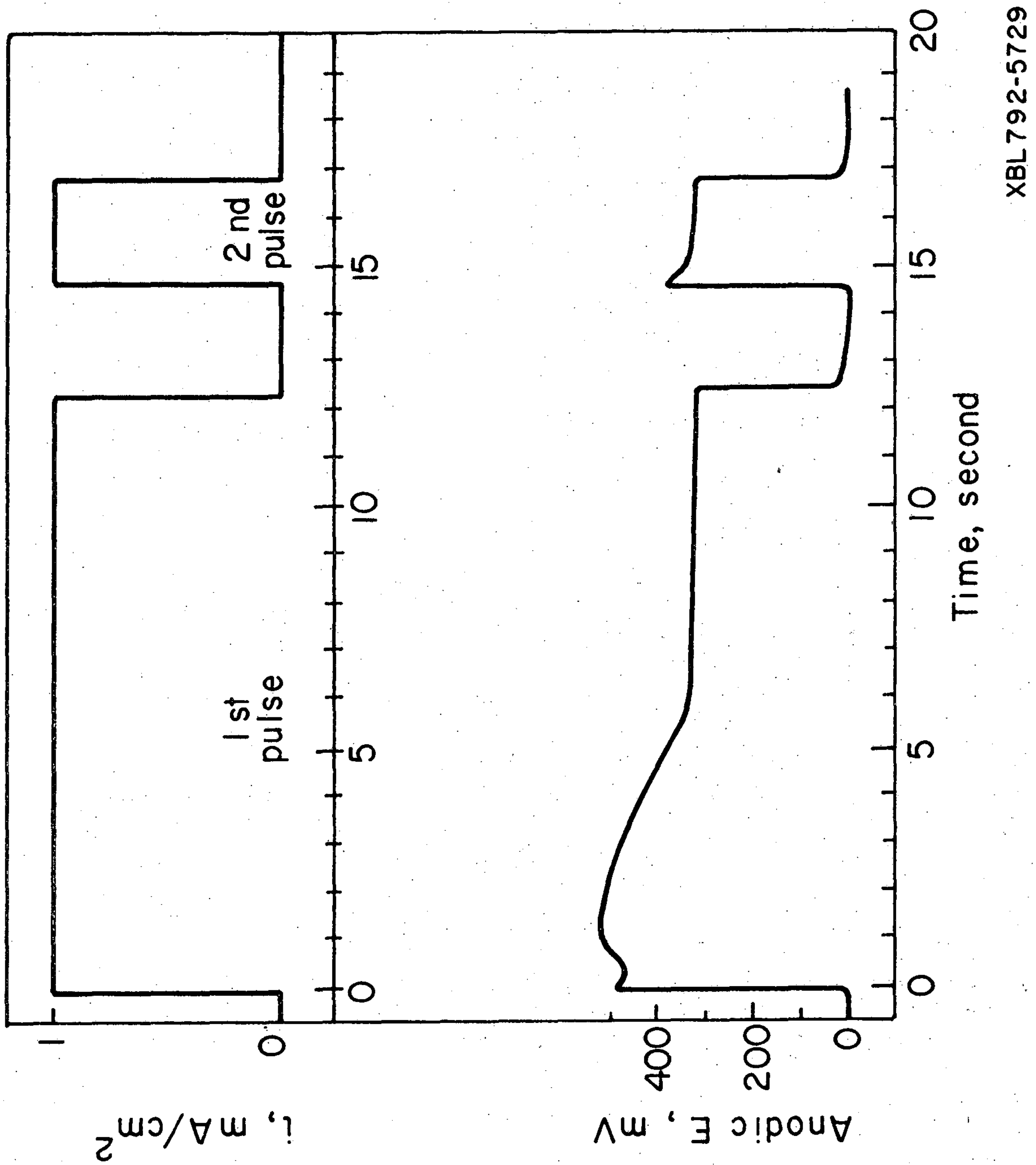

Figure 5-1. Chronopotentiogram of a potassium electrode in 0.5 M KAlCl$_4$/PC solution for two cathodic current pulses at 27°C, cell #2, reference electrode: K/K$^+$.

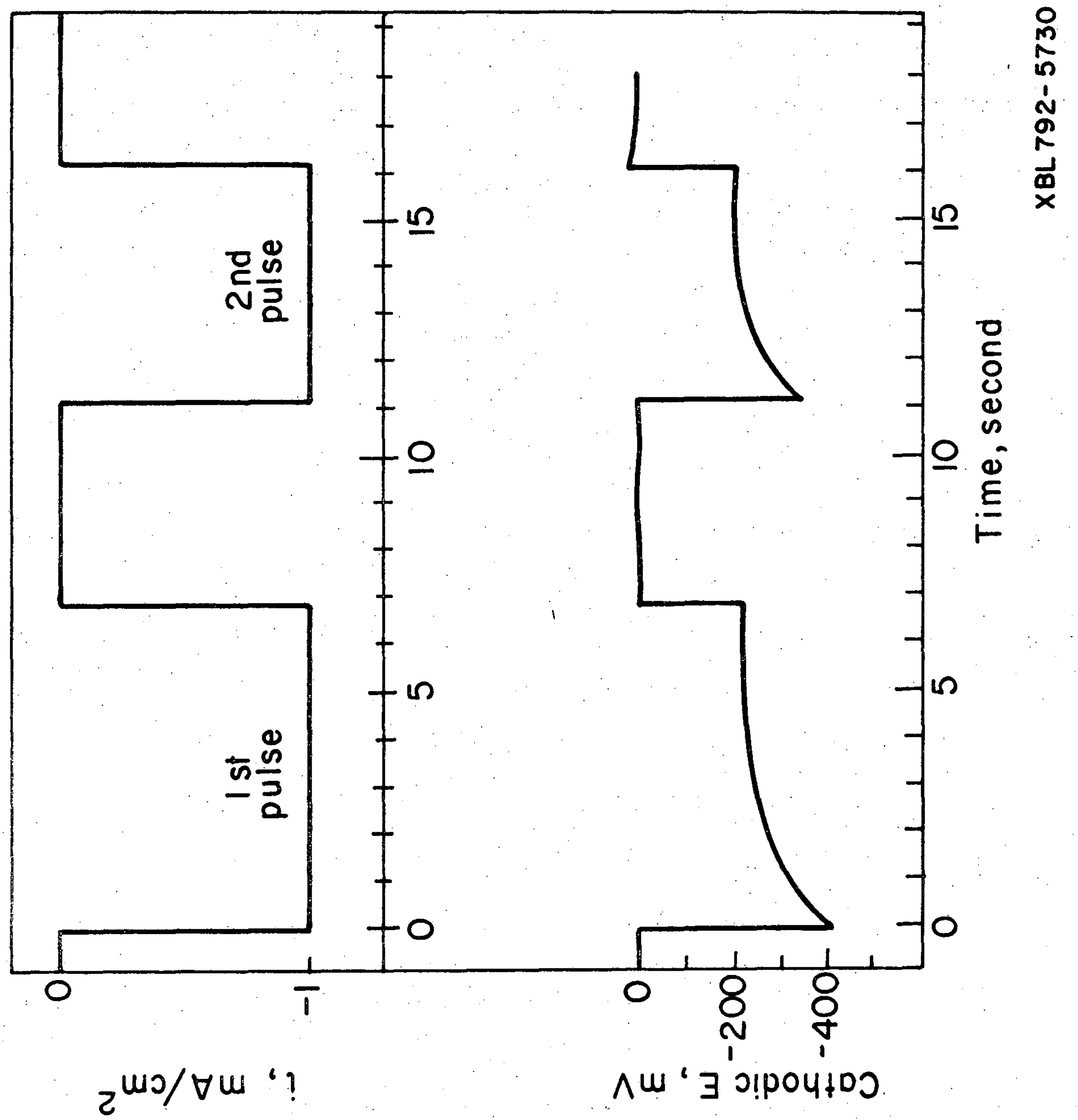

Figure 5-2. Chronopotentiogram of a potassium electrode in 0.5 M $KAlCl_4$/PC solution for two anodic current pulses at 27°C, cell #2, reference electrode: $K/K^+$.

appears to be activated by either an anodic or a cathodic current pulse although the surface layer may not be the only reason for these responses.

Even if the surface is passivated, potassium behaves rather symmetrically in $KAlCl_4$ electrolyte. Cyclic voltammograms in Figure 5-3 show the response of potassium deposited on a Pt electrode at $30^oC$ at four different sweep rates: 10, 20, 50 and 100 mV/sec. For sweep rates higher than 10 mV/sec, there was no significant influence of the sweep rate in the potential region ranging from -0.38 volt to +0.38 volt. No side reaction occurred. The anodic current reached 0.80 $mA/cm^2$; this was slightly smaller than that of the cathodic current. Only at 10 mV/sec did the surface passivation influence the voltammogram. Nevertheless, cyclic voltammograms of potassium approach that of a chemically reversible electrode.

The electrodeposited potassium remains shiny when stored in the electrolyte over extended periods of time. Cyclic voltammograms taken after 22 months of storage indicate that the deposit may be protected by a very thin surface film. The open-circuit potential measured between a fresh potassium reference electrode and the 22 months old potassium deposit was 14 mV. Figure 5-4 depicts the

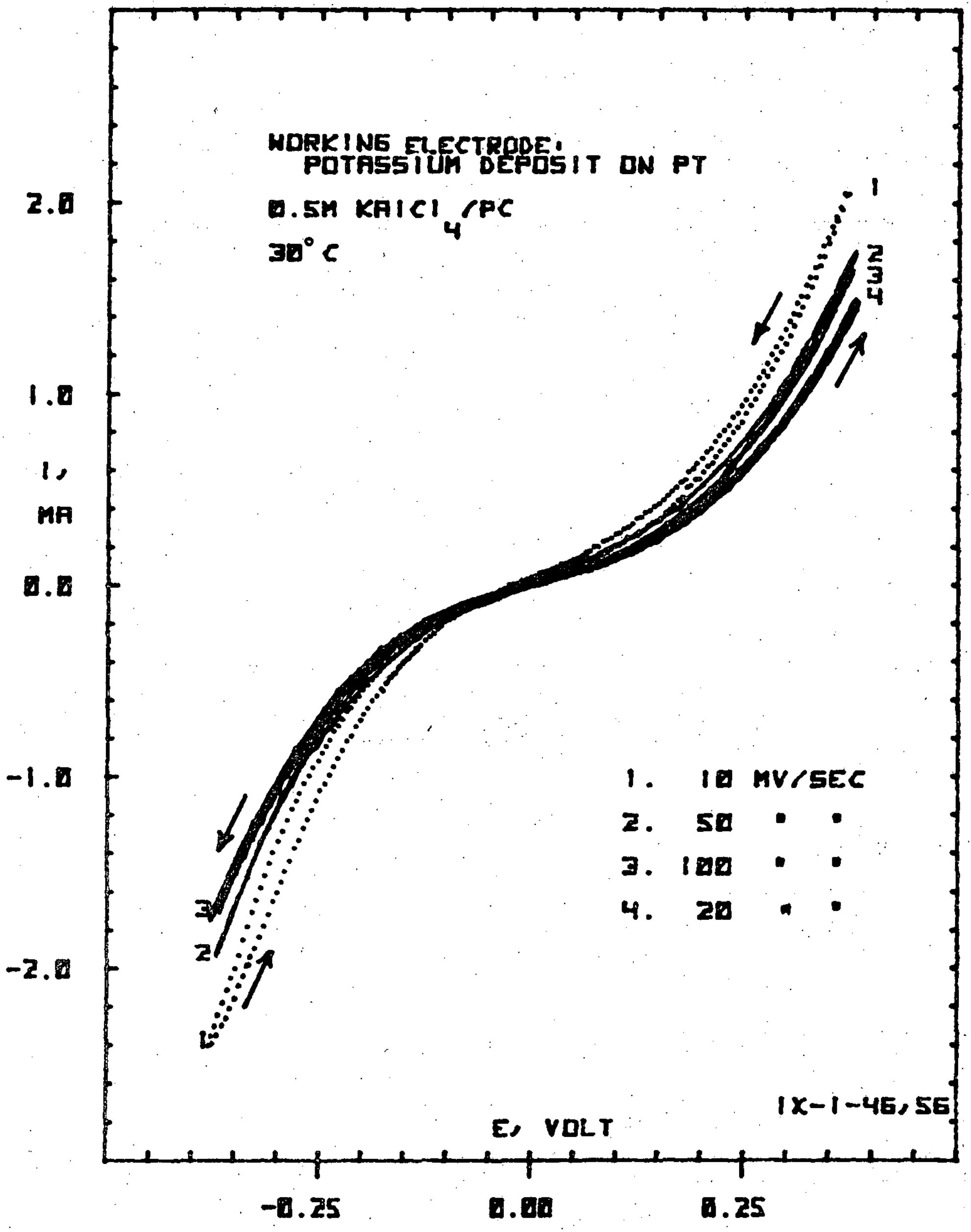

Figure 5-3. Cyclic voltammograms of potassium deposit on Pt in 0.5 M $KAlCl_4$/PC solution at 30°C, cell #1, reference electrode: $K/K^+$.

XBL 792-8459

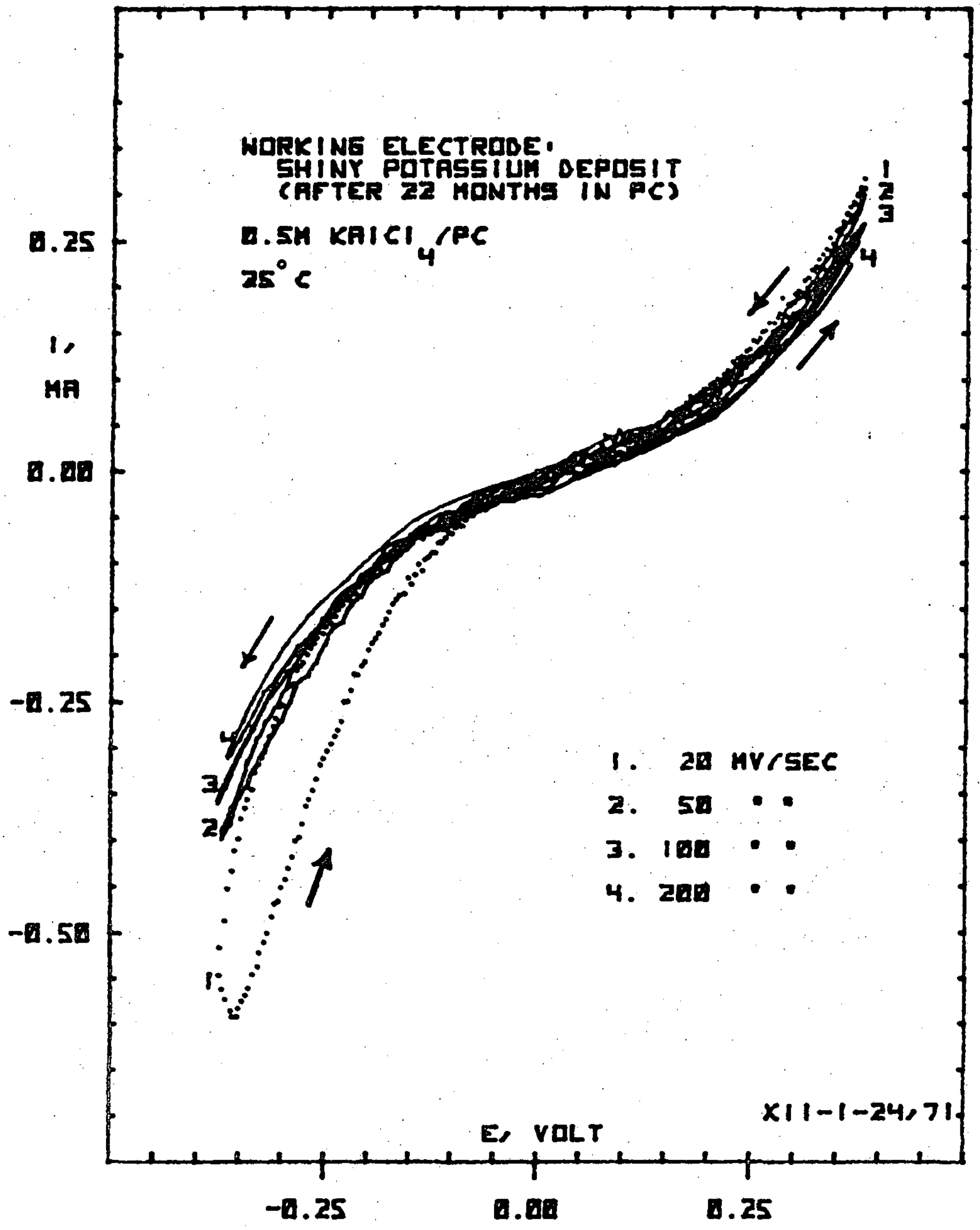

Figure 5-4. Cyclic voltammograms of potassium deposit (after immersion in PC for 22 months) in 0.5 M KAlCl$_4$/PC solution at 25°C, cell #2, reference electrode: K/K$^+$.

XBL 792-8461

cyclic voltammograms measured on this deposit at four different sweep rates in this chronological order: 20, 50, 100, and 200 mV/sec. Each curve represents the first two sweeps. At 20 mV/sec, and then only in the cathodic polarization region, the electrode behaved like one with a passivated surface: when the change of potential (absolute value) with time, $d|E|/dt$, is positive, the surface is first activated; as $d|E|/dt$ becomes negative, higher current passes through because of larger active area. At sweep rates higher than 20 mV/sec, the deposit behaved symmetrically, rather similar to the one depicted in Figure 5-3. It is likely that the surface was sufficiently activated by the initial sweeps at 20 mV/sec to give symmetrical curves at higher sweep rates.

In summary, the formation of a thin surface film on potassium deposits was detected by the response of the potential to galvanostatic pulsing. That this surface film inhibits further chemical attack of potassium is evidenced by the similar behavior of a freshly prepared deposit and a deposit stored for more than 22 months in the same electrolyte. Since the presence of a surface layer is a necessary but not sufficient condition for establishing the incompatibility of PC with potassium, surface reactions have to be studied.

## 5.2. Decomposition Reactions

Many impurities may lead to the passivation of a reactive surface like potassium. To attempt to assess every possible reaction would be a futile exercise. The most likely reactions expected to occur are as follows:

$$2K + H_2O \rightarrow K_2O + H_2 \qquad (5\text{-}1)$$

$$K + R\text{-}OH \rightarrow KOR + 1/2\ H_2 \qquad (5\text{-}2)$$

$$K + PC \rightarrow CO_2 + C_3H_5OK + 1/2\ H_2. \qquad (5\text{-}3)$$

$$PC + 2\ K \rightarrow K_2CO_3 + C_3H_6 \qquad (5\text{-}4)$$

$$PC + 2\ e^- + 2\ K^+ \rightarrow K_2CO_3 + C_3H_6 \qquad (5\text{-}5)$$

Since the major reactive impurities in PC are water and alcohols, reactions (5-1) and (5-2) are the most likely to occur. Even though we keep impurities at the ppm level, we cannot prevent these reactions from proceeding and influencing the electrochemical behavior of potassium. For example, if one ppm of water in one ml of electrolyte were to react with one $cm^2$ potassium electrode surface, this would mean that the layer of potassium reacted is about 200 Angstroms thick.

Reactions (5-3), (5-4) and (5-5) represent the electrochemical and chemical reduction of PC. Reaction (5-5) is not likely to proceed appreciably because the cathodic current efficiency of potassium deposition is close to 100% (see section 6). To differentiate reactions (5-3) and (5-4), electrolyses under 60 mm Hg vacuum were carried out to detect the presence of propylene and carbon dioxide. Gas samples from anodic and cathodic chambers were characterized by mass spectroscopic analyses.

Mass spectroscopic analysis was chosen as the analytical method because propylene (b.p. $-47.4^{\circ}C$) and carbon dioxide (b.p. $-78.5^{\circ}C$) are in gaseous phase at room temperature. However, mass spectroscopy gives only relative amounts of each component present. We are still interested in these qualitative results because they can provide an insight into the decomposition reactions. Before discussing the results, it is instructive to examine the mass spectra of carbon dioxide and propylene. Such spectra indicate the fragmentation of these compounds and hence give a basis for comparison. Figure 5-5 shows no interference between mass peaks from fragmentation of carbon dioxide and propylene. The mass spectrum of propylene shows that the hydrogen atom breaks off easily and the predominating species are $C_3H_6$, $C_3H_5$, $C_3H_4$, $C_3H_3$ and $C_2H_3$. Thus the sum of mass peaks 27, 39, 40, 41 and 42 represent the major part of propylene. The spectrum of $CO_2$ indicates that it breaks down only to CO and oxygen. Peaks 28 and 44 have been assumed to originate from carbon dioxide. Although we expect no reaction yielding CO, its

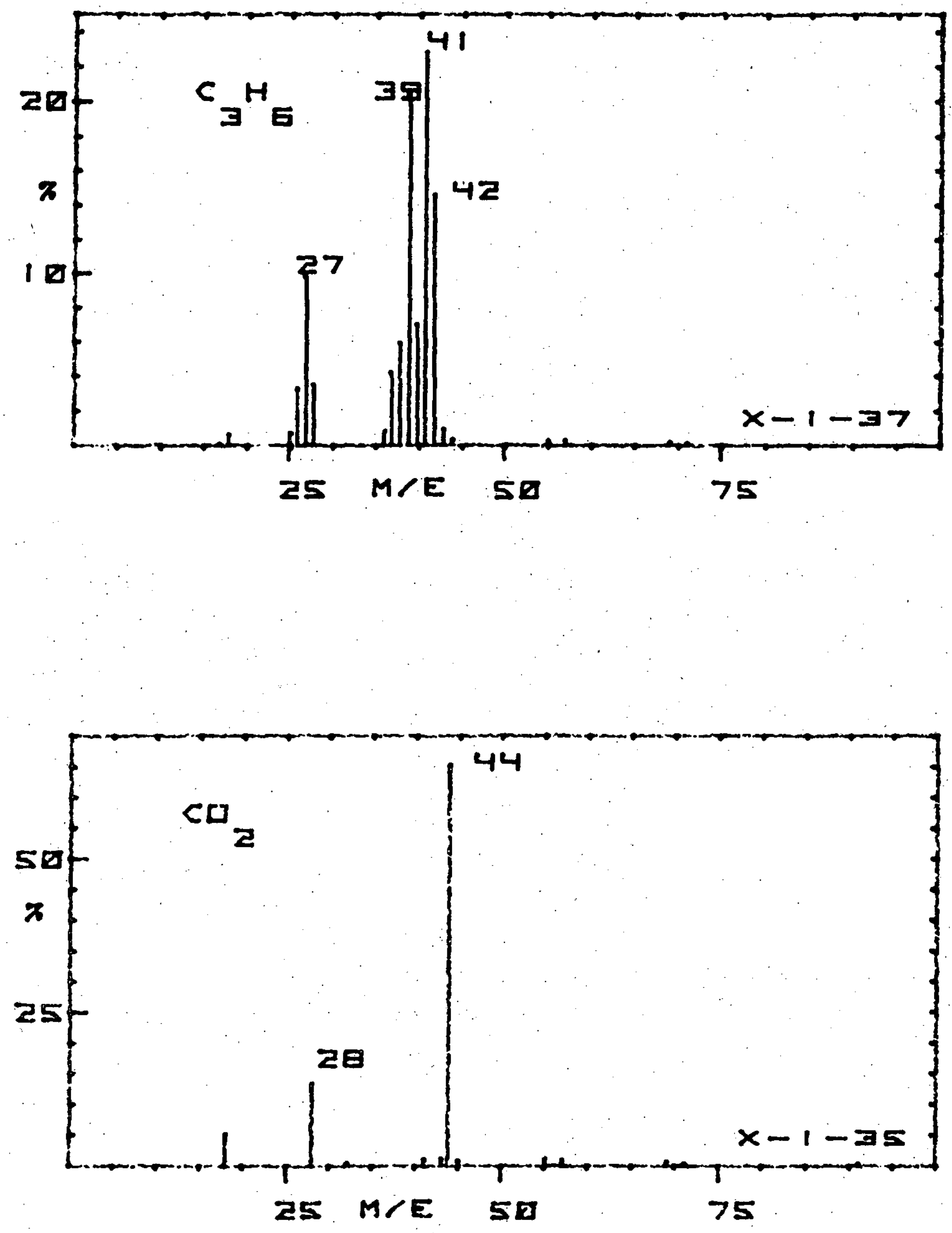

XBL 793-9114

Figure 5-5. Mass Spectra of Carbon Dioxide and Propylene.

presence cannot be distinguished from that of carbon dioxide fragmentation.

Table 5-1 shows the composition of gas samples by mass spectroscopic analyses. The percentage expressed is the percentage of total ionization detected including all the fragments of molecules. It is not the mole percentage of gas sample. Typically, the fraction of predominating species is about 70%. Other small peaks in the background are usually less than 1%. The mass spectrum of the gas sample in experiment #45 in the cathodic chamber was an exception. It was surprisingly clean, and more than 95% was observed. The gas samples from the aluminum dissolution experiment also have similar decomposition

Table 5-1

Mass Spectrum Analyses of Gaseous Samples

| Reaction (Expt #) | Carbon Dioxide (#28+44) | Propylene ($C_3H_6$) (#27+39+40+41+42) |
|---|---|---|
| Al dissolution (#18) | 49.9% | 22.4% |
| K dissolution (#43) | 62.9 | 3.0 |
| K deposition (#45) | 92.7 | 3.0 |

Cell #4

products. The high percentage of propylene components in experiment #18 proves that the presence of propylene can be detected.

These qualitative results clearly indicate the predominance of carbon dioxide in gas samples. Thus reaction (5-3) is more likely than (5-4) and (5-5) to represent the main PC decomposition reaction.

Since reaction 5-3 is by no means the unique decomposition reaction, a more interesting question is how fast the potassium passivation occurs. The upper limit of the rate has been estimated by passing a small current and measuring the potential on stainless steel, aluminum and platinum electrodes. The chronopotentiogram of a stainless steel electrode with a current density of 20 microamp/cm$^2$ is shown in Figure 5-6. The open circuit potential was 3.05 volt. When the current was switched on, the potential dropped rapidly to 2.5 volt and then declined more gradually. The potential kept on decreasing with time but stayed above 2.2 volt for 28 hours. Then the potential decreased rapidly; it took only two hours (32th to 34th hour) to decline to -200 mV from 1.7 volt. Chronopotentiograms of an aluminum cathode with a current density of 5.5 microamp/cm$^2$ are depicted in Figure 5-7. The duration of the pulse was long, about 9 minutes. The initial value was 2.55 volt. For a charge of $4.3 \times 10^{-2}$

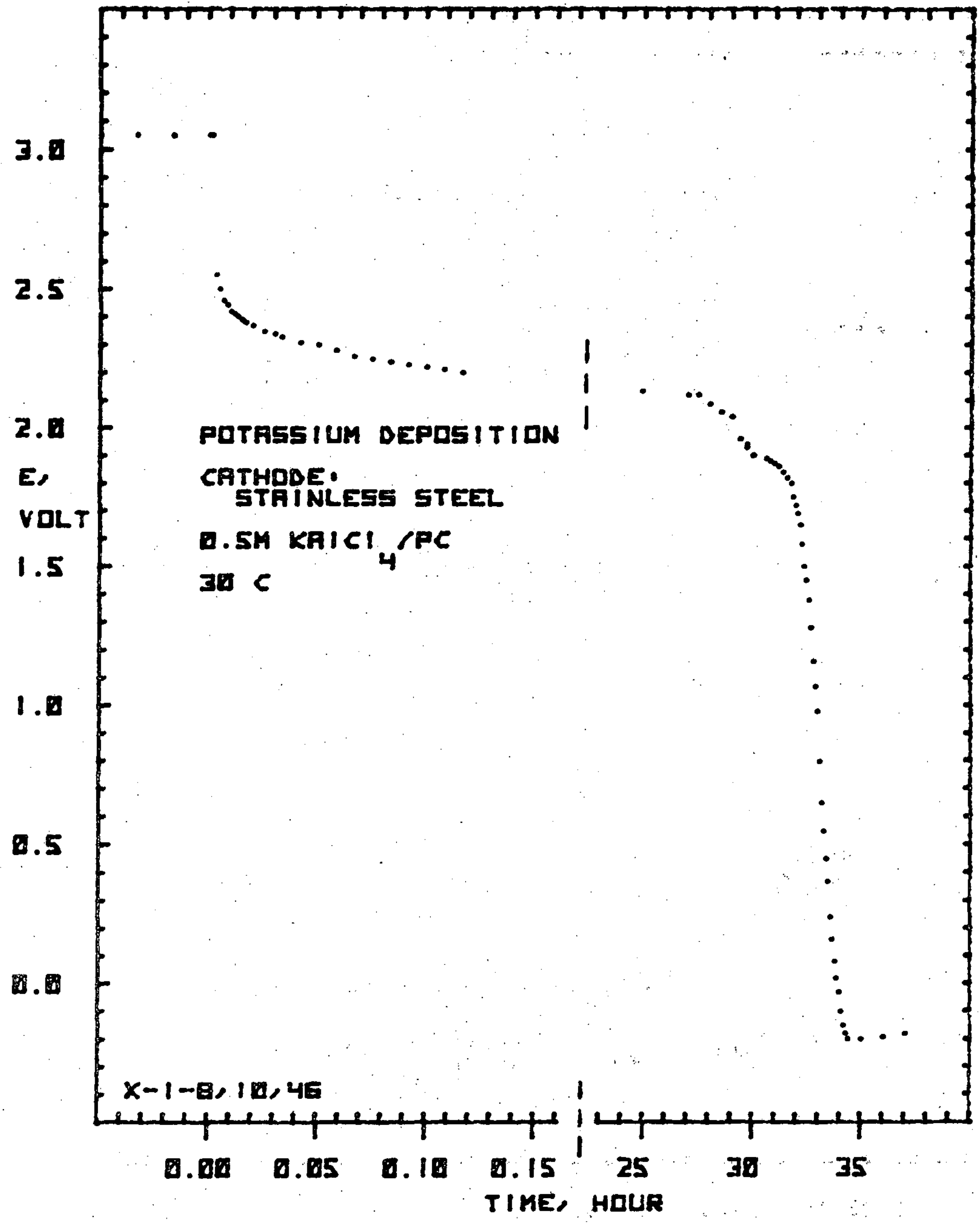

Figure 5-6. Chronopotentiogram of a stainless steel (304) electrode in 0.5 M $KAlCl_4$/PC solution at 30°C with a current density of 20 microamp/$cm^2$, cell #5, reference electrode: $K/K^+$.

XBL 792-8458

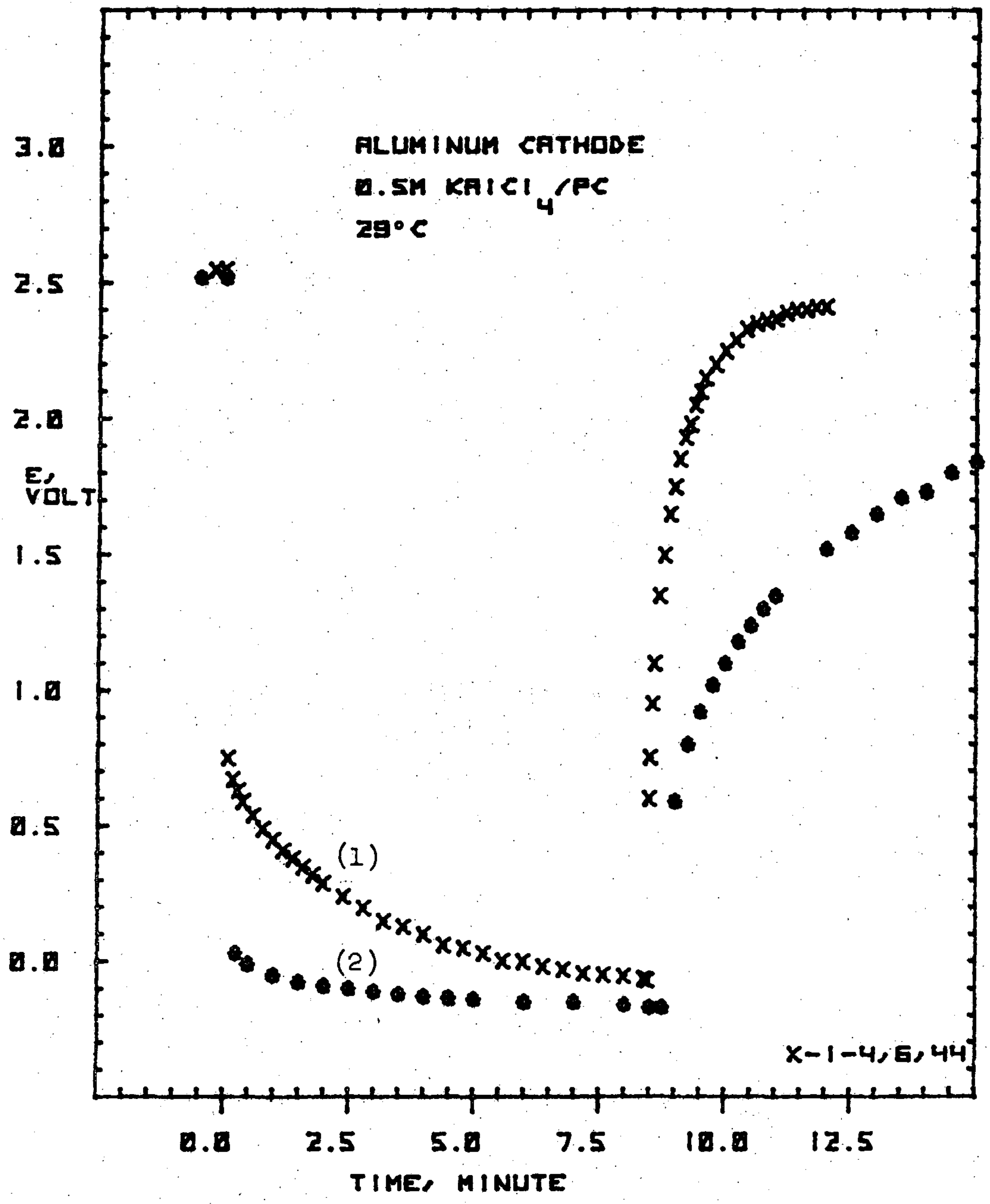

Figure 5-7. Chronopotentiograms of an aluminum cathode in 0.5 M $KAlCl_4$/PC solution for two consecutive cathodic current pulses (5.5 microamp/cm$^2$) separated by a 70 minutes zero current interval; curve 1 was measured before curve 2, cell #7, reference electrode: K/K$^+$.

XBL 792-8460

coulomb, the potential (curve 1) declined to zero, but it rose rapidly to 2.4 volt as soon as the current was off. After remaining at zero current for seventy minutes, another cathodic current pulse was passed. The potential (curve 2) reached a negative value much faster and yet, as the pulse ended, it increased more slowly than the potential in curve 1. Chronopotentiograms of the Pt gauze cylinder (40 $cm^2$) were measured with a cathodic current of 0.1 mA (Figure 5-8). Curve 1 represents this development for an electrode with a relatively fresh surface (several cyclic voltammograms and several potential step measurements in the same solution were obtained on this surface prior to this particular sweep). After making several current pulses on this Pt electrode with a net cathodic charge of 0.6 coulomb, a new Pt electrode was used. Curve 2 depicts the electrode response to the same current in same electrolyte. Over the first half hour, the decline of potential in the two experiments was quite similar; however, from then on (below 1.6 volts), the potential reached zero much more rapidly on the fresh platinum surface.

These chronopotentiograms on stainless steel, aluminum and platinum electrodes suggest the reaction of potassium deposit with impurities rather with the solvent.

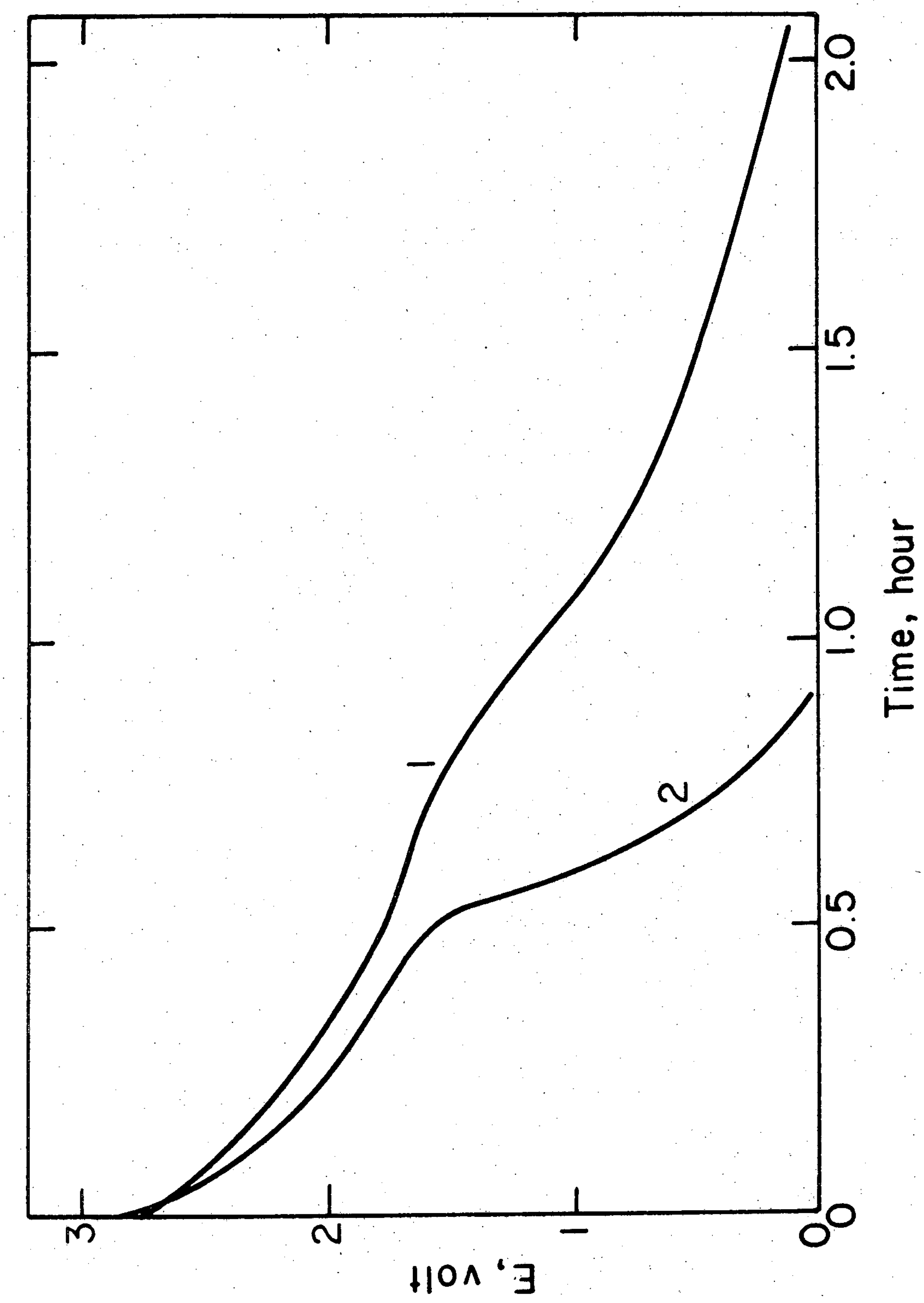

Figure 5-8. Chronopotentiograms of fresh Pt gauze cylinders in 0.5 M $KAlCl_4$/PC solution at 25°C with a cathodic current of 0.1 mA, cell #1, reference electrode: $K/K^+$.

The abrupt drop of the potential on a stainless steel electrode to a negative value after 32 hours indicates that the potassium reduction depletes the impurities in the electrolyte. This is also supported by the response of the aluminum electrode. In that experiment, the cell contained 50 ml electrolyte. Thus the charge passed in one current pulse represents a concentration change of $9 \times 10^{-6}$ equivalent/liter. All the potassium reduced in a single current pulse can react with impurities present in the solution. A water concentration of $9 \times 10^{-6}$M is equivalent to 0.16 ppm by volume, an amount likely to be present. The chronopotentiograms of the Pt electrodes has similar implication. In the initial period, the two curves are closely similar, suggesting the cathodic reaction involves an oxide on the fresh Pt surface. The difference between the chronopotentiograms in the potential region less than 1.6 volt implies the reduction of the impurities. On a fresh Pt surface (2nd electrode), once the participation of the surface in the reaction ceases, the potassium potential is reached much more rapidly than in the case of the first platinum electrode.

Although these chronopotentiograms show that impurities contribute to the formation of a surface layer, they do not demonstrate that PC decomposition by potassium can be neglected. The contribution of each reaction to the passivation of potassium is difficult to estimate. Whichever is the dominant reaction, the potassium corrodes very slowly, at a rate less than 20 microamp/cm$^2$.

## 5.3. Conclusions

In the $KAlCl_4$/PC solution, a thin surface layer exists on a potassium electrode. This layer does not appreciably distort the symmetrical electrochemical behavior nor does it cause large cathodic or anodic overpotentials. Thus, the use of potassium as a reference electrode is meaningful, provided high input impedance instruments are used. The surface layer is most likely formed by the reaction of potassium with impurities present in the solvent. Chronopotentiograms obtained on various electrode substrates show the depletion of impurities as potassium is deposited. Although there is no firm proof that the solvent itself does not react with potassium, all evidence indicates that this attack, if it occurs at all, proceeds at a negligible rate, below that corresponding to 20 microamperes/cm$^2$.

It is interesting to note that some of the results presented here do not agree with Eichinger's recent findings.[E2] In his investigation of the cathodic decomposition of PC, Eichinger found that the solvent was reduced electrochemically to propene at active electrodes with large surfaces, such as sintered nickel and copper- or steel-felt. In Eichinger's experiments, the amount of electroactive species (impurities) did not decrease as potassium was deposited. Although the water content was "estimated" to be less than 10 ppm, it is likely that the actual concentration was higher. From the brief description of his experimental procedures, we believe that not only water but perhaps other impurities as well were present at appreciable concentrations. Based on our experience, a membrane (Dupont's Nafion #425) does not stop the passage of water from the aqueous chamber to the non-aqueous section. It is doubtful that the diaphragm Eichinger used (the type was not described) was adequate to prevent the movement of water in some of his long experiments. In addition, he changed measuring electrodes several times during a single run in open air. Although the degree of contamination of the electrolyte by moisture from the air is impossible to estimate, we believe that this source of water, together with the passage of moisture through his membranes raises serous doubts about the validity of his observations.

### 6. Current Efficiency

Knowledge of the current efficiency of potassium deposition is important, not only because the energy efficiency of the process depends on it, but also because alternate reactions would involve either the decomposition of the solvent or contamination of the deposit with another metal (when $KAlCl_4$ electrolyte is used). Three methods were used jointly to determine the current efficiency: (1) measurements of the change in the potassium content of the electrolyte upon passage of known amounts of charge, (2) weighing the potassium deposit, and (3) detection of the possible presence of aluminum in the deposit by atomic absorption spectroscopy.

Based on thermodynamic considerations alone, aluminum should be reduced at a potential more than one volt positive than that of potassium. However, according to all evidences, the aluminum reduction does not occur from $KAlCl_4$ dissolved in PC. The stability of the chloroaluminate complex, $AlCl_4^-$, is most likely responsible for the absence of Al in the deposit. The amount of Al was measured by atomic absorption spectroscopy. After repeated washing with the pure solvent, the potassium deposit (either in powdery form or as a large globule) was dissolved in iso-propyl alcohol. After evaporating the alcohol, an aqueous solution was prepared for analysis using a spectrophotometer (Perkins-Elmer model 360) according to the standard atomic absorption procedure. The aluminum content was always less than 0.1% by weight, just about corresponding to the limit of detection of this method. It is likely that a slight inclusion of $KAlCl_4$ electrolyte would result in this level of aluminum. This is also supported by Chacon's work[C2]: no aluminum was detected by powder X-ray diffraction and emission spectroscopy.

Table 6-1

Current Efficiency of Potassium Deposition From the Change of K Concentration in Solution

| Experiment (cell #7) | Change of [K] coulombs | Charge Passed coulombs | Efficiency col.2/col.3 |
|---|---|---|---|
| #35 | 5049 | 4980 | 101% |
| 47 | 1240 | 1280 | 97 |
| 49 | 1119 | 1134 | 99 |
| 50 | 1090 | 1145 | 95 |

One of the methods available for determining the cathodic current efficiency is to measure the change in the potassium concentration of the electrolyte. With an anodic reaction that does not introduce potassium into the system, the difference of potassium concentration before and after the electrolysis should directly correspond to the charge passed. Table 6-1 shows the total charge passed and the current efficiency for several experiments that involved aluminum dissolution as the anodic reaction. These data imply, within experimental error, 100% current efficiency. This is in agreement with Jansta et al.[D2]

In one run, the potassium ion concentration was depleted to such a low level that the current set became larger than the limiting current. Figure 6-1 depicts the corresponding rise of cathodic potential. Still, the current efficiency of this experiment was 99%. This along with the abrupt potential change indicates that no side reaction occurred in the potential region ranging from that of potassium reduction to 2 volts more negative.

Two procedures have been used for the determination of the amount of potassium deposited. One involved directly weighing the deposit. The other required the transfer of the deposit into an aqueous solution where the potassium was determined gravimetrically.

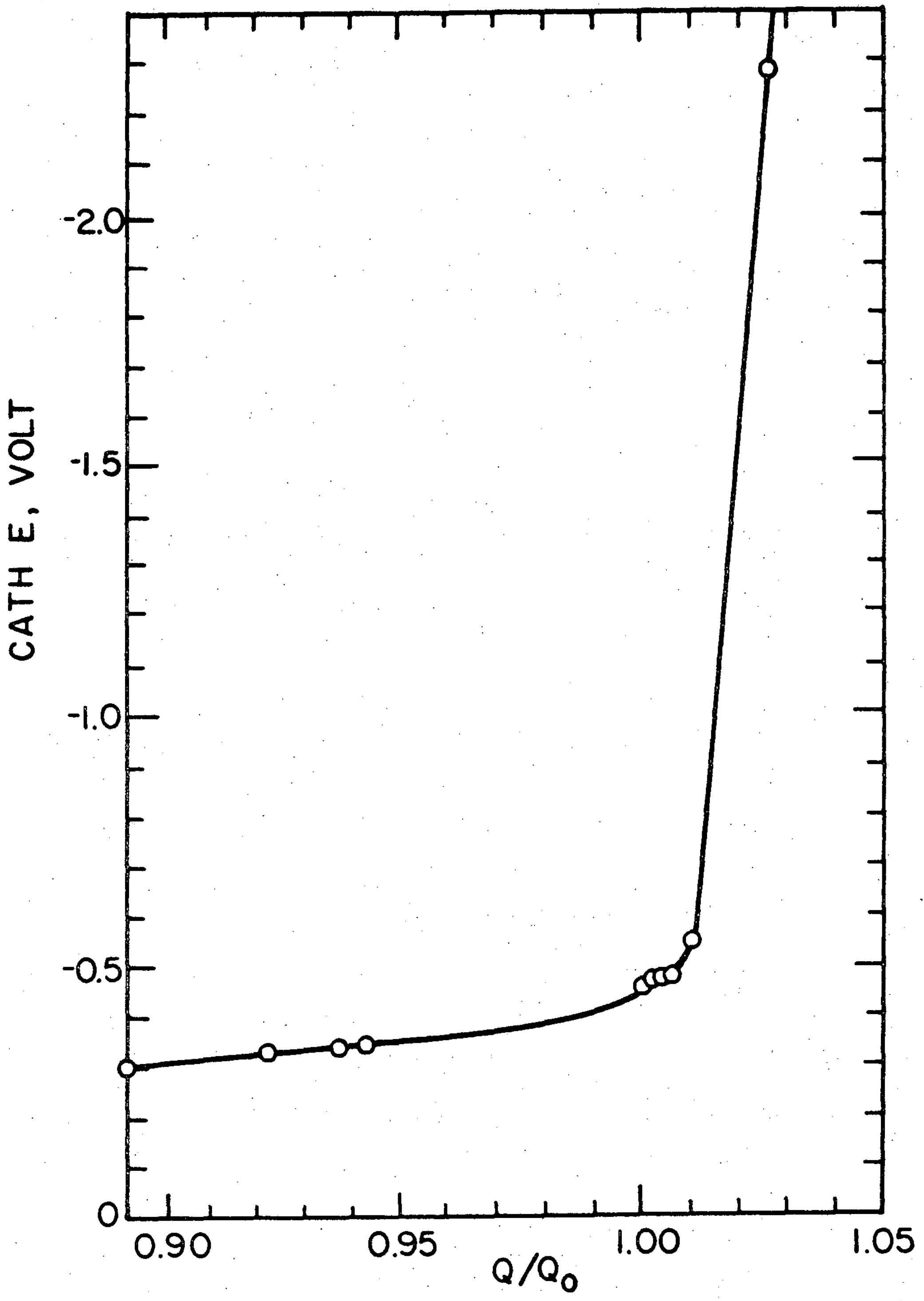

Figure 6-1. Change of cathodic potential due to the depletion of potassium ions; Q, amount of charge passed; $Q_0$, amount of potassium in solution expressed in coulombs.

Table 6-2

Change of the Weight of Potassium Deposit with Time

Expected Weight: 0.519 gram; cell #8.

| | Weight, gram |
|---|---|
| a. After washing twice with PC | 1.077 |
| b. After pumping vacuum for | |
| 20 minutes | 0.564 |
| 50 minutes | 0.514 |
| 5 hours | 0.539 |

The weighing method requires a compact deposit. Loose potassium particles which float around in the electrolyte decrease the amount of deposit collected, while the absorption of PC electrolyte by spongy deposits and the oxidation of potassium (by impurities present in the dry box) increase the weight. These error sources cause the weighing method to be unreliable. Nevertheless, the results obtained give a practical perspective. Table 6-2 illustrates two difficulties in weighing the deposit. First, the entrainment of the solvent by the deposit increased the weight substantially. Second, even in a

Table 6-3

Current Efficiency of Potassium Deposition

From the Weight of Deposit; cell #8.

| Experiment | Q passed, coulombs | Weight of Potassium, gram | Efficiency % |
|---|---|---|---|
| #47 | 1280 | 0.514 | 99 |
| 49 | 1134 | 0.494 | 107 |

vacuum atmosphere of 5 micron Hg, the potassium deposit was oxidized and its weight increased after a few hours. Table 6-3 shows the results of directly weighing the deposit. The results deviate within the expected error limits on either side of 100% efficiency.

In the gravimetric determination of potassium the deposit is transferred into an aqueous solution where the potassium ions form a precipitate with the sodium tetraphenylboron. The amount of potassium was computed from the weight of precipitate. Table 6-4 shows the results. A current efficiency higher than 95% was obtained in all these experiments. Despite the great care exercised in the collection of potassium from the cell, some potassium particles were separated from the electrode

Table 6-4

Current Efficiency of Potassiuum Deposition at 25°C

Gravimetric determination

| Charge passed, coulombs | Amount of K, milligram | Efficiency, % |
|---|---|---|
| 31.68 | 12.7 | 99.1 |
| 28.19 | 10.9 | 95.5 |
| 106.2 | 40.9 | 95.1 |
| 82.8 | 32.1 | 95.6 |

and were not included in the analysis. The deviation from 100% is contributed to these loose particles.

In summary, the current efficiency of potassium deposition was found to be very close to 100%, as determined by three independent methods. Because of the relatively small quantities of potassium on which these measurements were performed, the error limits can be estimated only very tentatively: 97.5 ± 2.5%. No co-deposition of aluminum was detectable by the atomic absorption method.

## 7. Deposit Morphology

The morphology of a metal deposit strongly affects the performance of an electrochemical system. In battery applications, the growth of dendritic deposits often cause the failure of the cell by short-circuiting the plates. In plating applications, an acceptable system will produce nothing but a smooth deposit. In the case of electrorefining or electrowinning of potassium, the deposit morphology affects the final yield. Because of the high reactivity of potassium, any additional processing step will undoubtedly result in reduction of the yield. It is then necessary to identify the important parameters that would render the deposit easily removable from the electrode and be processed into a desirable form. The influence of the temperature, the electrode substrate, and the surfactant on the deposit morphology was investigated and is discussed below.

The character of potassium deposited from $KAlCl_4$/PC strongly depends on temperature. At 30°C, the deposit tends to be powdery. The greyish-blue deposit comes off the electrode rather easily. Figure 7-1 shows the deposit on a potassium cup electrode; some of the deposit has fallen off already. At 50°C, a spongy deposit composed of

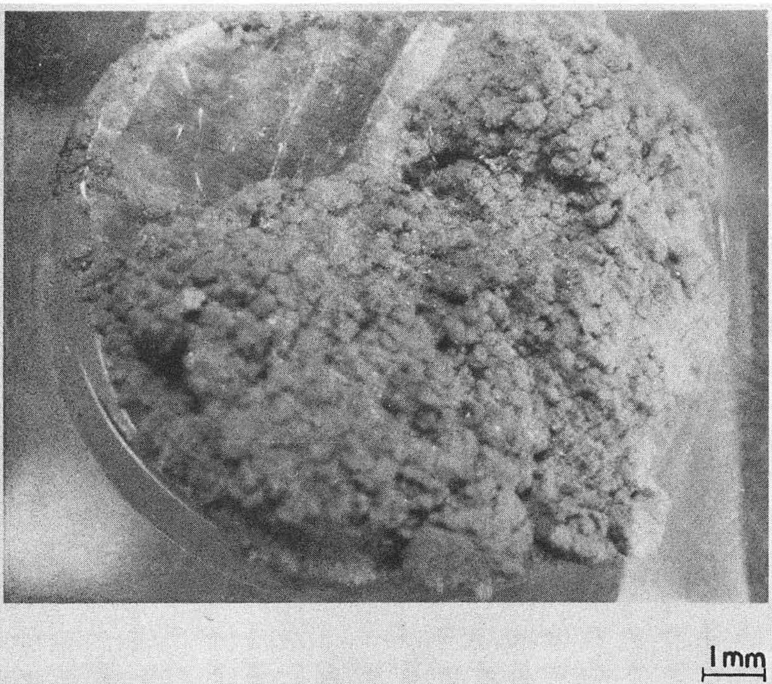

Figure 7-1. Potassium deposit from 0.5 M $KAlCl_4$/PC on a potassium cup electrode, 30°C, 2 $mA/cm^2$, cell #2, HK-27.

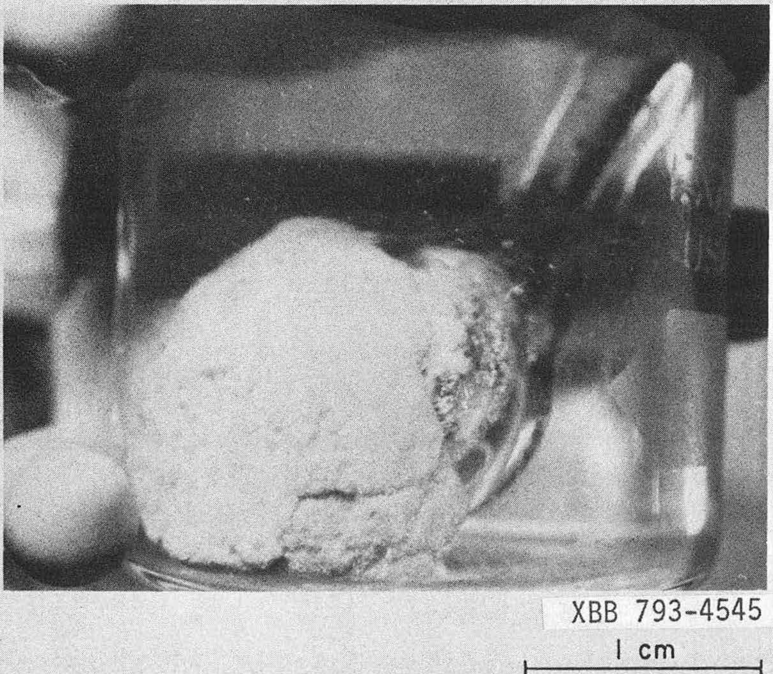

Figure 7-2. Potassium deposit from 0.5 M $KAlCl_4$/PC on a potassium cup electrode, 50°C, 2 $mA/cm^2$, cell #2, HK-27.

fine needles forms on the potassium cup electrode (figure 7-2). The electrolyte fills the pores. Upon removal from solution, the deposit volume shrinks in size. This deposit adheres more strongly to the electrode than the powdery deposit. At temperature above the melting point of potassium, small shiny metallic liquid globules are formed rather than a pool of molten potassium (figure 7-3).

The electrode substrate does not affect the nature of the deposit significantly. At 70°C, the same type of deposit, small liquid globules, are formed on flat substrates of stainless steel, platinum, or potassium. To further investigate the influence of the substrate surface on morphology, potassium was deposited at 70°C on a stainless steel screen (0.5 x 0.5 mm grid size) welded to a stainless steel wire at 70°C. Small globules filled up the holes in the screen. Figures 7-4 and 7-5 show the shiny deposit at different magnifications. This particular deposit remained shiny and metallic after storage in PC for over 22 months. At 50°C, again no difference in deposit morphology was observed on different substrates; fine needles are formed on potassium (figure 7-2), stainless steel (figure 7-6) or platinum (figure 7-7). However, the growth on Pt and stainless steel proceeds in random directions in contrast to the hemispherical deposit

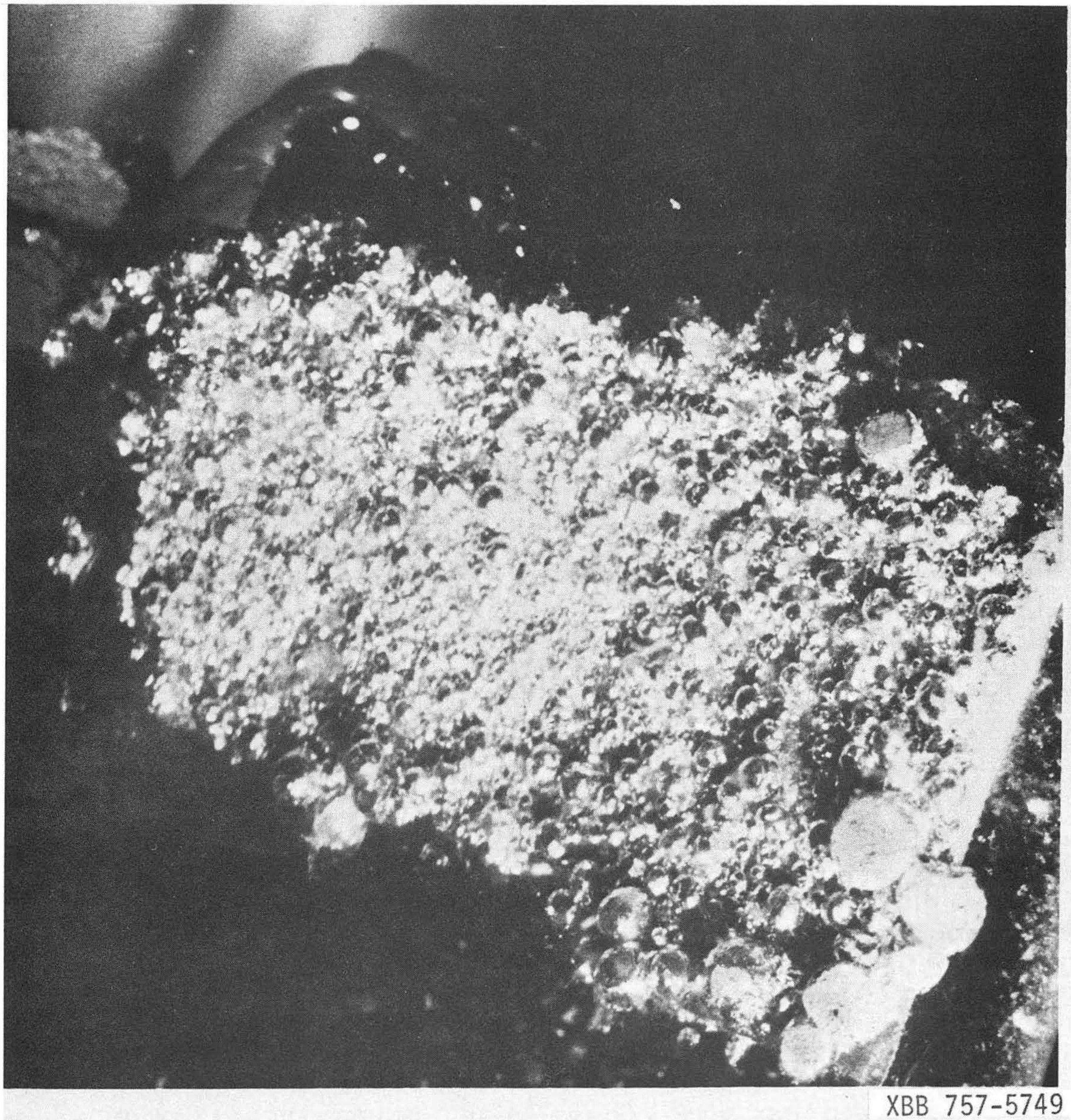

XBB 757-5749

Figure 7-3. Potassium deposit from 1.0 m $KAlCl_4$/PC on a platinum electrode with soft glass coated edges, 70-85°C, 0.3 mA/cm$^2$, 10X.

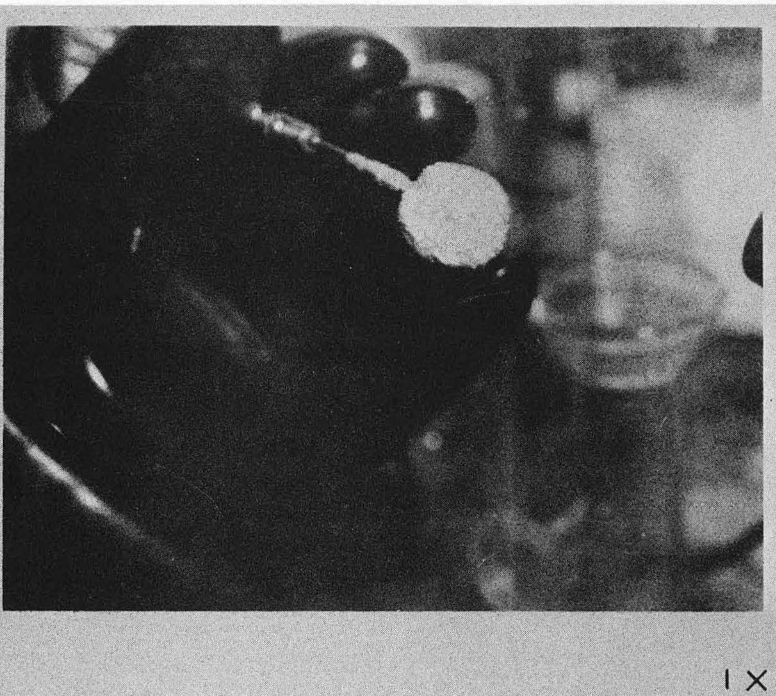

**Figure 7-4.** Potassium deposit from 0.5 M KAlCl$_4$/PC on a stainless wire screen (0.5 × 0.5 mm grid size) welded on a stainless steel wire, 70°C, 1.6 mA/cm$^2$, H-cell (#5), HK-22.

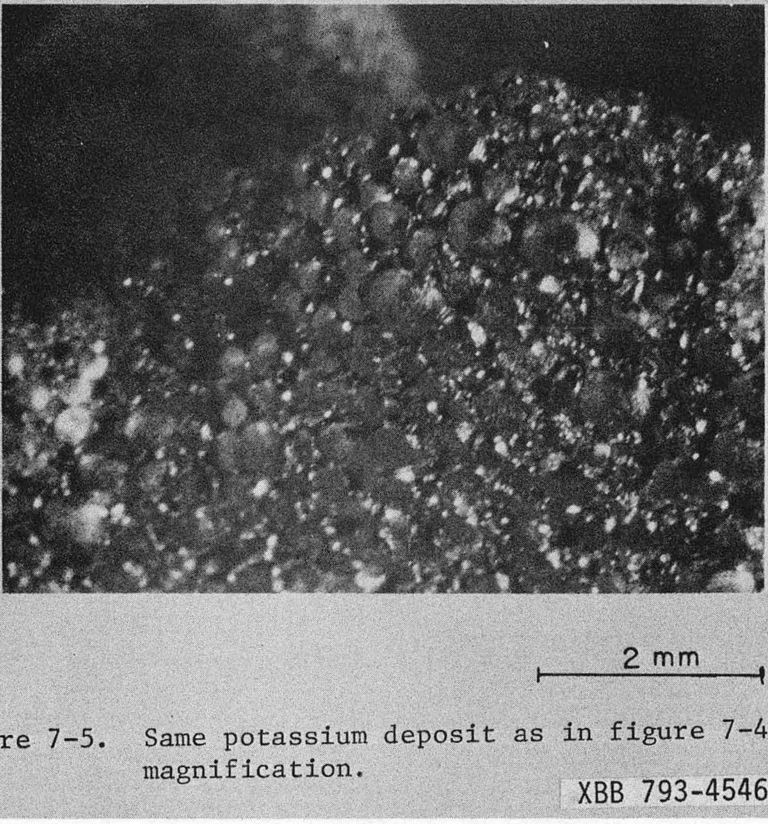

**Figure 7-5.** Same potassium deposit as in figure 7-4 with higher magnification.

XBB 793-4546

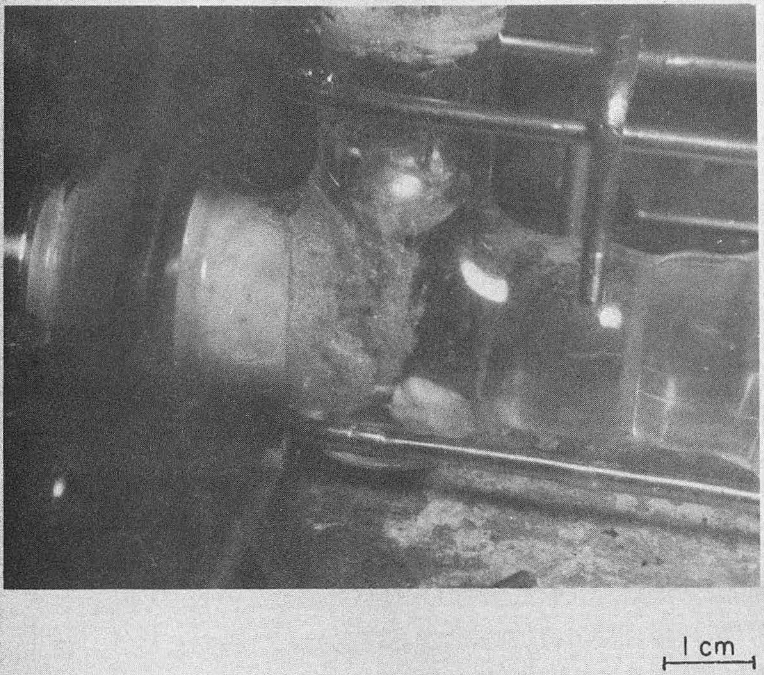

Figure 7-6. Potassium deposit from 0.5 M $KAlCl_4$/PC on a stainless steel electrode; electrolysis at a constant potential -200 mV relative to potassium in same solution, 50°C, cell #5, HK-20.

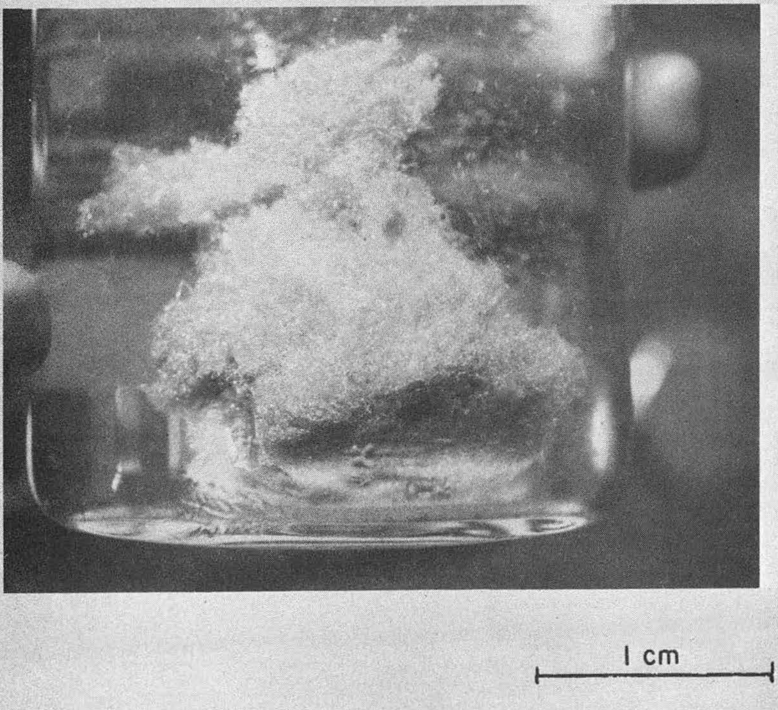

Figure 7-7. Potassium deposit from 0.5 M $KAlCl_4$/PC on a platinum electrode, 50°C, 2 mA, surface area: 1.68 $cm^2$, cell #2, HK-27.

XBB 793-4547

formed on the potassium substrate. It is not clear what are the reasons for the confinement of the deposit growth on a potassium substrate.

Organic additives are often employed for producing desirable deposit structure. For the processes of electrowinning or electrorefining of potassium, the small liquid globules and needle-like deposits are not desirable because no simple efficient method can be envisioned for removing the metal from the cell, and for separating it from the electrolyte. If potassium could be deposited to form a pool of molten metal, the liquid could be collected continuously in a straight-forward manner. Another acceptable type of deposit would be a compact solid in planar or cylindrical form.

The additive selected for the present study because of its stability is a cationic fluorosurfactant (Dupont Zonyl FSC). The influence of Zonyl surfactant was investigated with either aluminum or potassium as anode (cells #7 and #8). Most of these electrolyses were run in the same manner as the kinetic experiments described in section 8. The current was first increased from about 0.1 to 1.0 mA/cm$^2$, then kept constant at 1 mA/cm$^2$ for 1 or 2 days. After the second current scan, the deposit was removed for photographic analysis. To check whether the

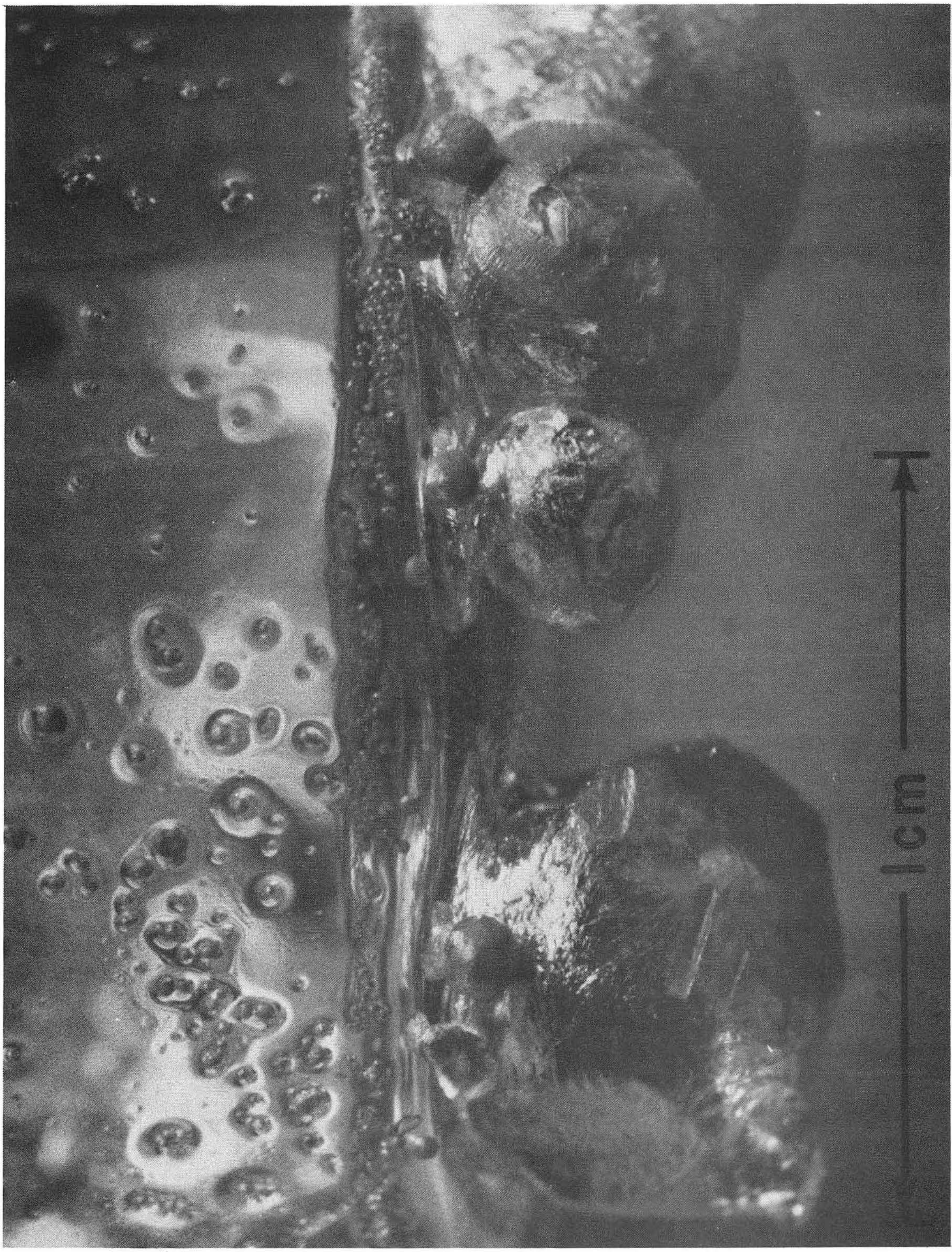

XBB 792-1609

Figure 7-8. Potassium globules from 0.5 M $KAlCl_4$/PC, 70°C, 1 mA/$cm^2$, 1.0 gram/liter Zonyl FSC surfactant, cell #8, HK-62.

current scans affect the deposit morphology, several experiments were performed at constant current density without the current scans. Deposits resembling those with the current scans were obtained.

With potassium anodes, larger globules were formed in the presence of Zonyl surfactant, but similar deposits were obtained for various surfactant concentrations of 0.167, 0.33, and 1.0 gm/liter. Perhaps the Zonyl concentration range that exerts the greatest effect on deposit morphology lies outside of the values investigated. In one experiment, potassium spheres up to 6 mm in diameter were formed (figure 7-8). The site where one sphere came off is shown in figure 7-9. The background at a higher magnification shows a range of small sizes of potassium globules (figure 7-10).

With aluminum anodes at 50°C, the Zonyl surfactant did not affect the deposit morphology in concentrations ranging from 0.0 to 0.33 gram/liter. Because PC is involved in the anodic dissolution of aluminum,[A1] the surfactant may have been rendered ineffective by products of side reactions. Figure 7-11 shows the typical compact deposit of fine needles on the surface; a section was cut away to reveal the compact texture of the solid potassium underneath the needles. Shiny metallic potassium spheres

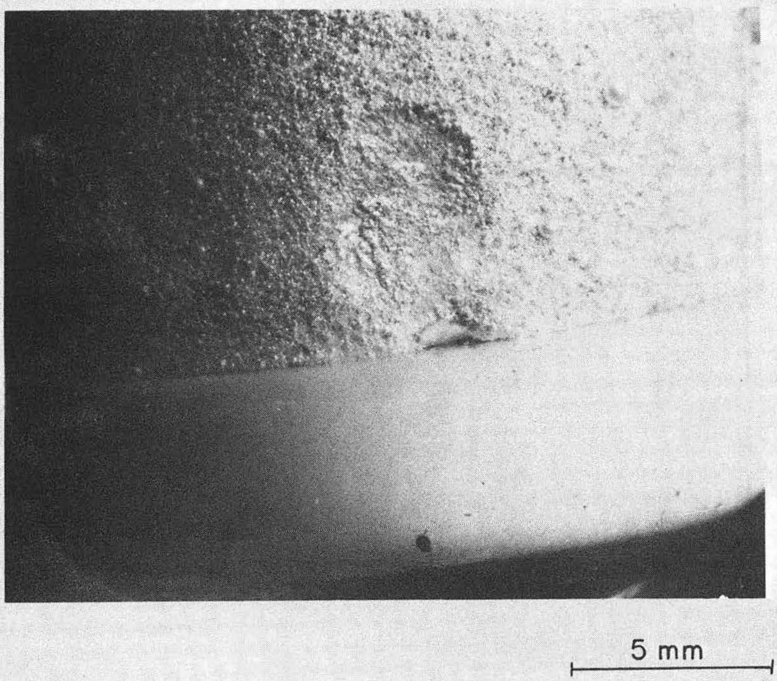

Figure 7-9. Potassium deposit from 0.5 M $KAlCl_4$/PC, 70°C, 1 mA/$cm^2$, 1.0 gram/liter Zonyl FSC surfactant, cell #8; the dented area near the teflon cap is the site where one large potassium globule came off.

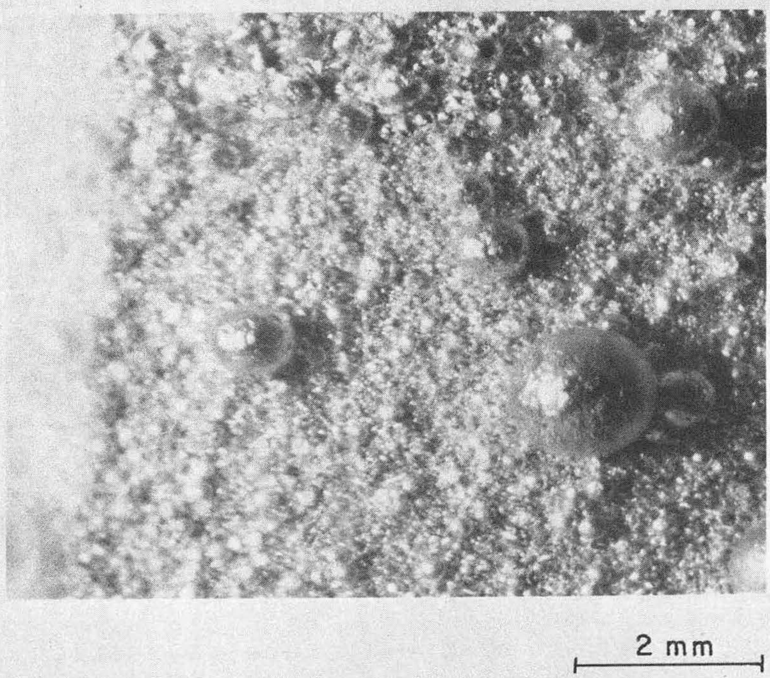

Figure 7-10. Same potassium deposit as in figure 7-9 with a higher magnification.

XBB 793-4549

were formed when this deposit was heated to 70°C after being pumped at 25°C to 10 micron Hg vacuum (figure 7-12).

The present study on the morphology of the potassium deposits is by no means complete. In spite of the qualitative nature, several conclusions can be drawn. Temperature affects the deposit morphology significantly, whereas the electrode substrate has negligible influence on the deposit structure. The Zonyl FSC surfactant also affects the shape of potassium deposit although there was no significant difference between deposits formed at concentrations of 0.167 to 1.0 gram/liter. The best deposit, in form of large globules, is obtained at 70°C in the presence of the cationic fluorosurfactant. Throughout this investigation, the effect of current density on deposit morphology has not been observed within the current range studied; hence, no systematic study was performed.

These results also raise a number of questions:

(1) Why does potassium come out as powder at 25°C and as needles at 50°C?

(2) Why do the liquid potassium globules formed at 70°C not coalesce?

(3) How does the Zonyl surfactant assist in the formation of large potassium globules?

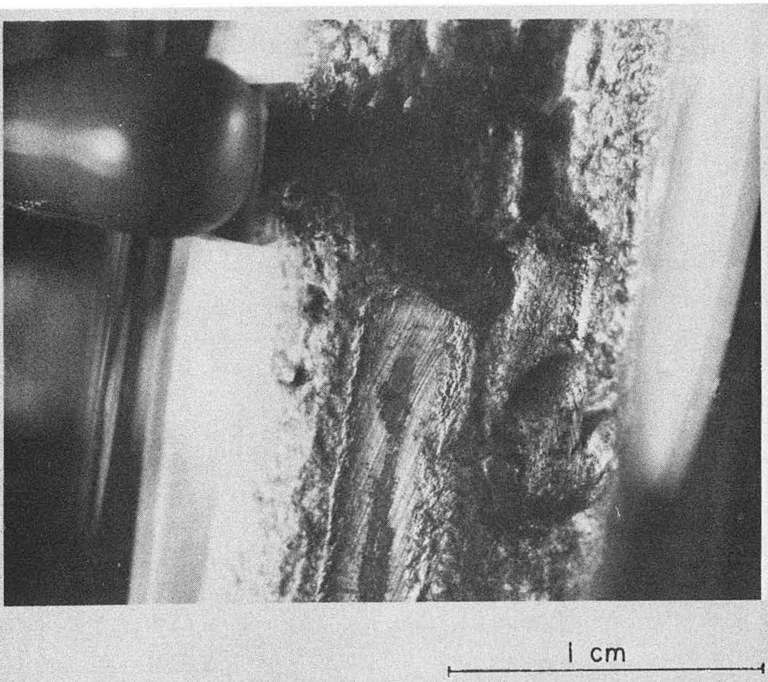

Figure 7-11. Potassium deposit from 0.5 M $KAlCl_4$/PC on aluminum, 0.4 $mA/cm^2$, 55°C, 0.064 gram/liter Zonyl FSC surfactant, cell #7, HK-35.

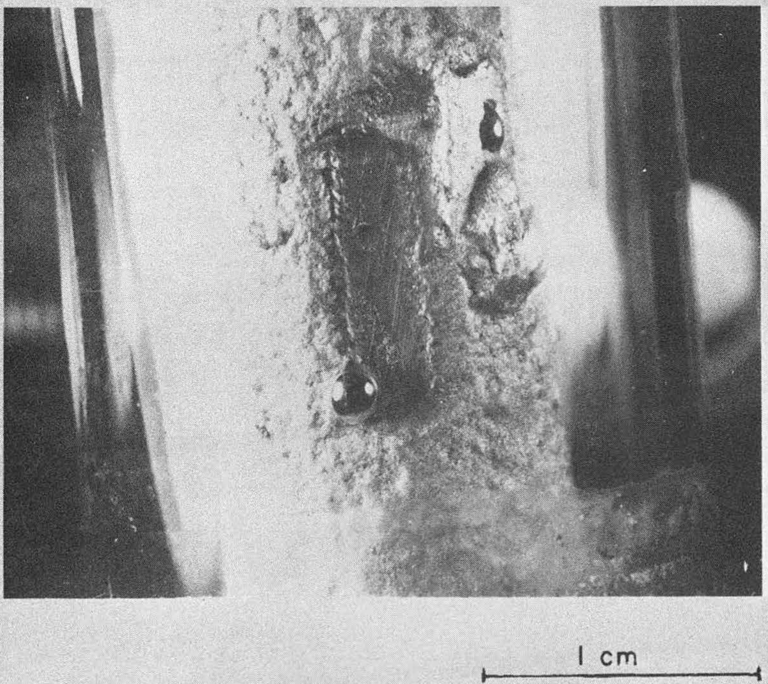

Figure 7-12. Same potassium deposit as in figure 7-11, heated to 70°C.

XBB 793-4548

These questions all address to the fundamental issues of electrocrystallization yet to be settled. An attempt to provide answers to these questions was considered to be beyond the scope of this study.

## 8. Overpotential Measurement

Before making any serious attempt to evaluate a process, thermodynamic and kinetic information is required. The influence of the operating parameters on the kinetic behavior has to be known before optimization of the system can be undertaken.

Equilibrium potentials of the alkali metals in $AlCl_3$/PC solutions, as well as electrolyte conductivities have been measured by Jorne et al.(see section 2.2.1).[J5-J7] They also explored the kinetic behavior, but by using micropolarization measurements.[J4] Thus, it is considered necessary to evaluate the kinetic parameters in a range of practical current densities.

Before discussing the results, it is necessary to digress about the basic kinetic relationships employed in this section. For a single electron transfer reaction, such as the dissolution and deposition of alkali metals, the dependence of the current density on the surface overpotential is often approximated by the Butler-Volmer equation:

$$i = i_o[\exp(a_a nFE_s/RT) - \exp(-a_c nFE_s/RT)] \qquad (8\text{-}1)$$

where $a_a$: anodic transfer coefficient

$a_c$: cathodic transfer coefficient
$E_s$: surface overpotential, mV
F: Faraday's constant
i: current density, mA/cm$^2$
$i_o$: apparent exchange current density, mA/cm$^2$
R: universal gas constant
T: temperature

Note that the values of i and $E_s$ are negative for a cathodic reaction. At low surface overpotential, equation 8-1 can be well approximated by a linear expression:

$$i = i_o(a_a+a_c)nFE_s/RT. \qquad (8\text{-}2)$$

Another method of plotting equation 8-1 deserves attention:

$$i = i_o[\exp(-a_c nFE_s/RT)][\exp(a_a+a_c)nFE_s/RT -1]. \qquad (8\text{-}3)$$

For $a_a+a_c=1$, $\ln[i/(-1+\exp(nFE_s/RT))]=\ln i_o-a_c nFE_s/RT$. (8-4) The plot of the left side of equation 8-4 versus $E_s$ yields a straight line, the slope gives the value $a_c$ and the intercept gives the value of apparent exchange current density $i_o$. The kinetic parameters to be determined from experimental data are $i_o$ and $a_c$.

Kuta and Yeager have recently reviewed the various techniques available for overpotential measurements.[K3] We will consider here the advantages and drawbacks of transient and steady state methods. For measuring the surface overpotential of potassium deposition in PC electrolyte, the transient technique was found to be less satisfactory than the steady state method. Of the two modes of electrolysis for steady state measurements, constant potential or constant current, the galvanostatic mode was preferred.

The transient technique considered involves applying a current pulse and measuring the overpotential free of ohmic drop. The steady state method involves recording the electrode potential after applying a constant current. The overpotential is obtained when the ohmic loss is subtracted from the measured potential. Each method has its own advantages. The current-pulse technique is useful for deposition and dissolution studies. The small charge passed alters the micro-structure of the surface only slightly. With a uniform current distribution, the ohmic potential drop can also be estimated. On the other hand, the steady state method, which resembles the actual operation, can reveal other facets of the electrode process.

For the study of potassium deposition, the current pulse method was found unsatisfactory. Figure 8-1 illustrates the problem: the potential drifts with time. Curves 1-11 were measured in chronological order on a Pt rotating disk electrode with the $n^{th}$ step succeeding the

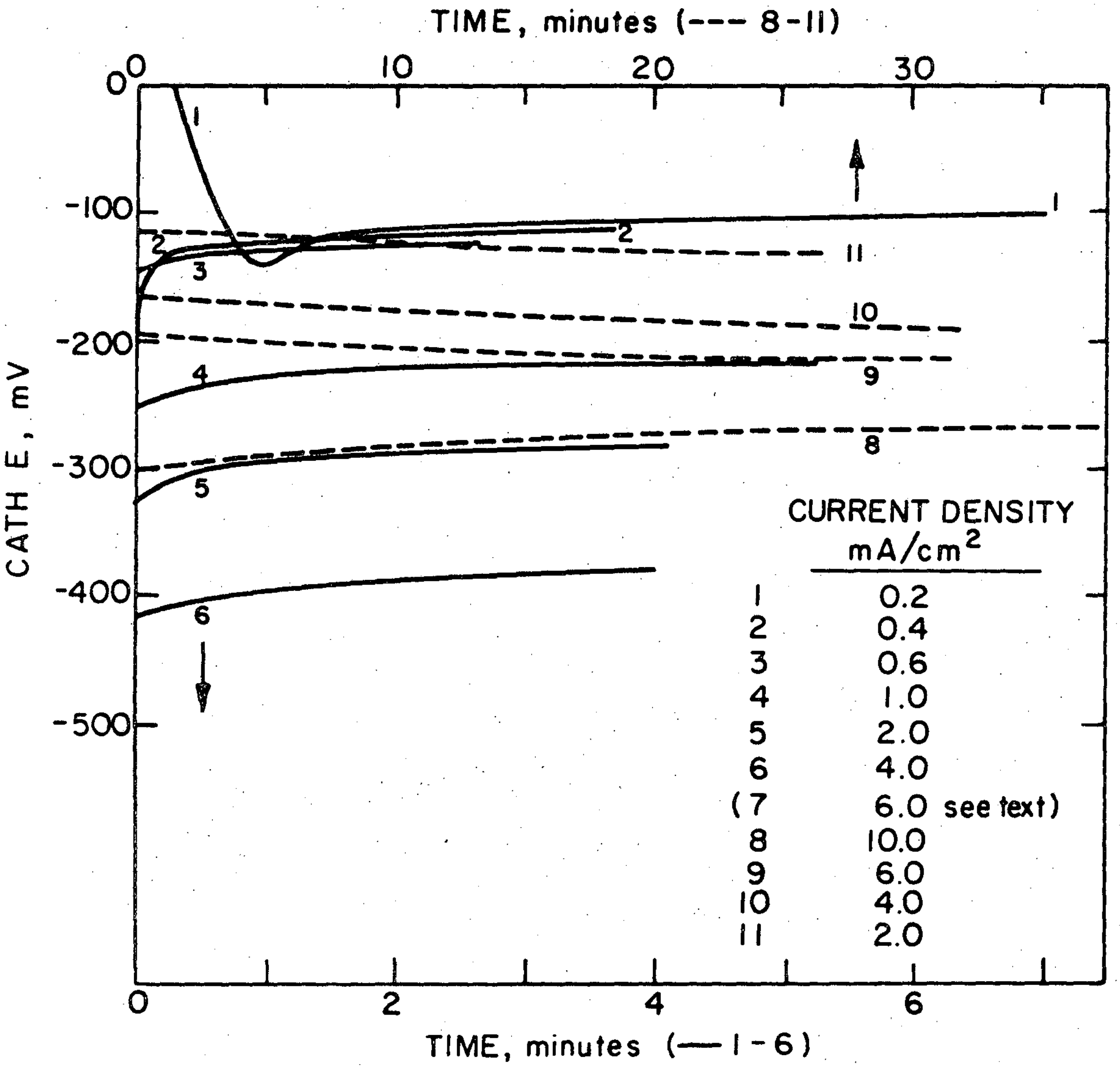

XBL 792-5812

Figure 8-1. Change of the potential of a Pt RDE at constant current densities; 25°C, 0.5 M $KAlCl_4$/PC, 1000 rpm, cell #6; Time scale: curves 1-6, bottom, curves 8-11, top; HK-24, reference electrode; $K/K^+$.

$(n-1)^{th}$, that is, the time at the end of $(n-1)^{th}$ step is the same as the time zero of the $n^{th}$ step. Curve 7 is not shown because its duration was 1.79 hours and another time scale would have been required. Its shape is similar to curve 6. The potential declines monotonically from an initial value of 376 mV relative to a potassium reference electrode to a final value of 189 mV. Curves 1-6 represent the potential responses to increasing current steps, whereas curves 8-11 involve decreasing applied currents. Note the large differences of potential between curves at the same current density. For example, curves 6 and 10 (4 mA/$cm^2$) differ by more than 200 mV.

The change of the cathodic potential during deposition may be due to the combined influences of two reactions on the surface: (1) surface activation by potassium deposition, and (2) surface de-activation by a slow passivation reaction. When the current of the $(n+1)^{th}$ curve was increased from that of $n^{th}$ curve, the change of potential with time ($d|E|/dt$) was negative. The potential decreased because of larger active area created by the higher rate of potassium deposition. When the current of $(n+1)^{th}$ curve was lower than that of $n^{th}$ curve, $d|E|/dt > 0$. The potential increased because the passivation reaction reduced the active area as a smaller current is passed.

This inherent characteristic of potassium deposition in PC electrolyte makes the transient technique for measuring overpotential unsuitable. If one is not aware of the problem, misleading results can be obtained from such a technique.

To illustrate how these surface activating and deactiviating reactions affect the overpotential data, cathodic current pulses were applied to a potassium electrode and the potential was measured. In this experiment, the current density was set in either an increasing order or in a decreasing order: 0.21, 0.42, 0.83, 1.67, 2.5, 3.33, 4.17, 8.33, 16.67, 25.0, and 33.3 mA/cm$^2$. First, pulses of 5 msec duration were applied. With current densities starting at 0.21 mA/cm$^2$ the potential reached a steady value in less than 0.5 msec. Up to 33.3 mA/cm$^2$, there was no change once the steady state was obtained. As shown in Figure 8-2, only at 41.7 mA/cm$^2$ did the potential decrease. A longer pulse (72 msec) was immediately applied and the decline became distinctive (Figure 8-3). If one were to measure overpotential data by using short (5 msec) current pulses in order to preserve the character of the electrode, the resulting overpotential would be substantially higher than the steady state value. Next 72 msec current pulses were

Figure 8-2. Potential response of a potassium electrode to a 5 msec current pulse (-41.7 mA/$cm^2$); Vertical scale: 0.2 volt/div.; Horizontal scale: 1 msec/div.; 50°C, 0.5 M $KAlCl_4$/PC, cell #3; reference electrode: $K/K^+$.

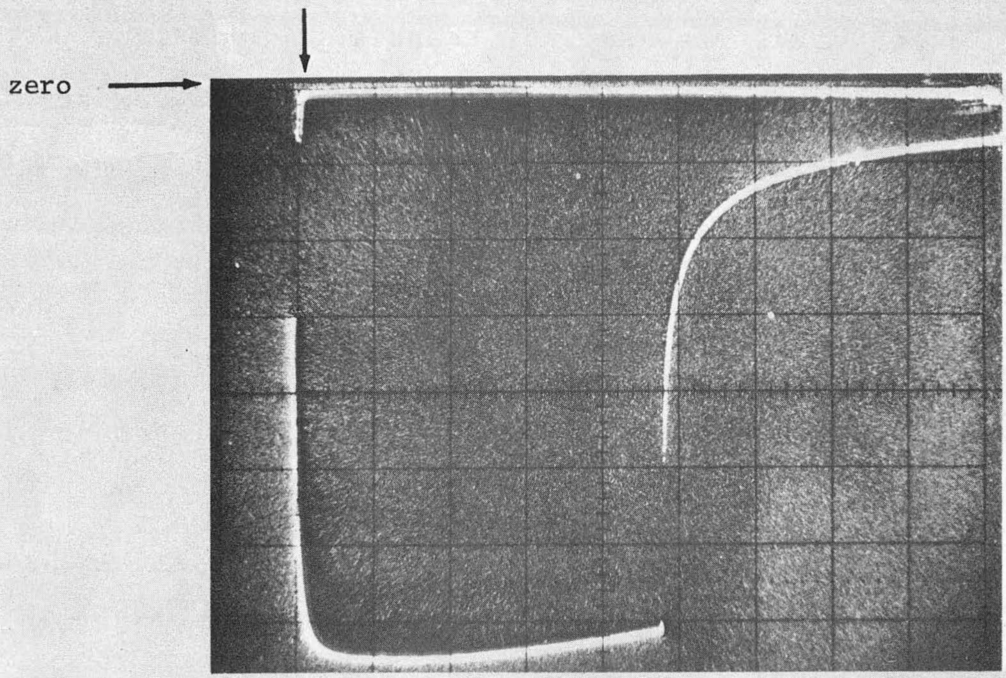

Figure 8-3. Potential response of a potassium electrode to a 72 msec current pulse (-41.7 mA/$cm^2$); Vertical scale: 0.2 volt/div.; Horizontal scale: 10 msec/div.; 50°C, 0.5 M $KAlCl_4$/PC, cell #3; reference electrode: $K/K^+$.

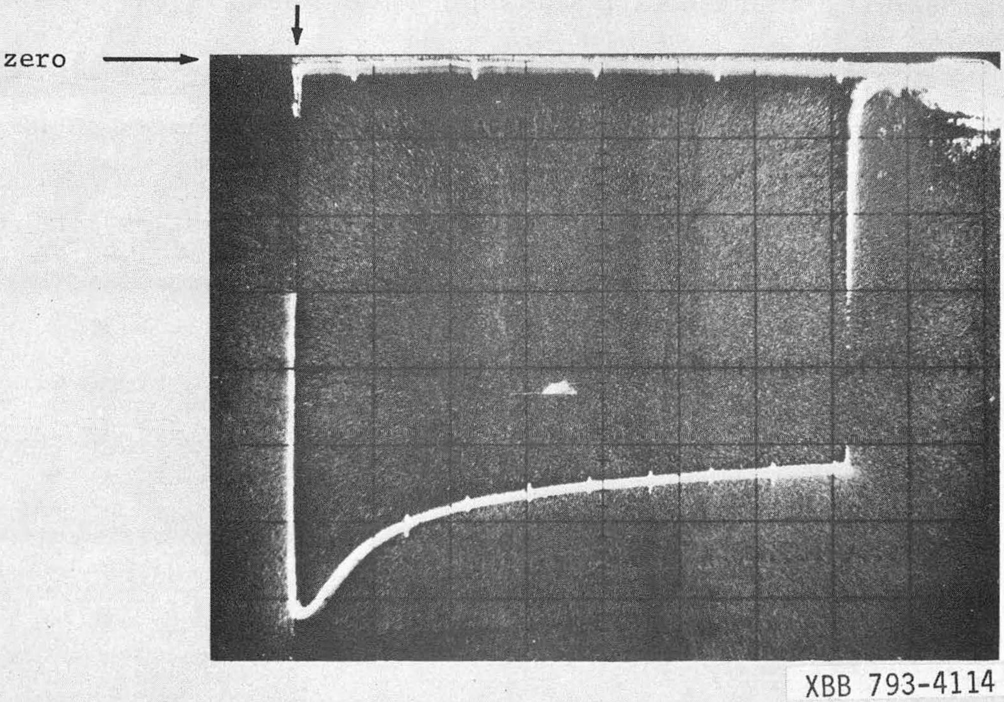

XBB 793-4114

applied with current densities decreasing from 33.3 mA/cm$^2$ to 8.33 mA/cm$^2$ in the sequence described above. The decline was clear but the change was gradual. At 4.17 mA/cm$^2$, the potential change was not noticable. Figures 8-4 and 8-5 contrast the changes of potential at 8.33 mA/cm$^2$ and at 4.17 mA/cm$^2$. A series of cathodic pulses was then passed with current densities first decreasing from 4.17 mA/cm$^2$ to 0.21 mA/cm$^2$ and then increasing back to 4.17 mA/cm$^2$. The potential of these pulses appeared to reach the steady state; no decline was observed. However, the electrode was activated by this series of current pulses. The steady state potential at 4.17 mA/cm$^2$ was 20 mV higher in the beginning (Figure 8-5) than in the end (Figure 8-6) of the series. At current densities 8.33 mA/cm$^2$ and higher, the potential drop described earlier was reproduced; Figure 8-7 shows those at 16.67, 25, 33.3 and 41.7 mA/cm$^2$.

Similar behavior was observed in longer current pulses (0.59 sec). The potential declined at current densities that previous shorter pulses gave steady state responses. The comparision of Figure 8-5 or 8-6 to Figure 8-8 illustrates the point clearly. Figures 8-8 and 8-9 depict the change of potential at current densities 4.17, 3.3, 2.5 and 1.67 mA/cm$^2$.

Figure 8.4. Potential response of a potassium electrode to a 72 msec current pulse (-8.33 mA/cm$^2$); Vertical scale: 0.1 volt/div.; Horizontal scale: 10 msec/div.; 50°C, 0.5 M $KAlCl_4$/PC, cell #3; reference electrode: K/K$^+$.

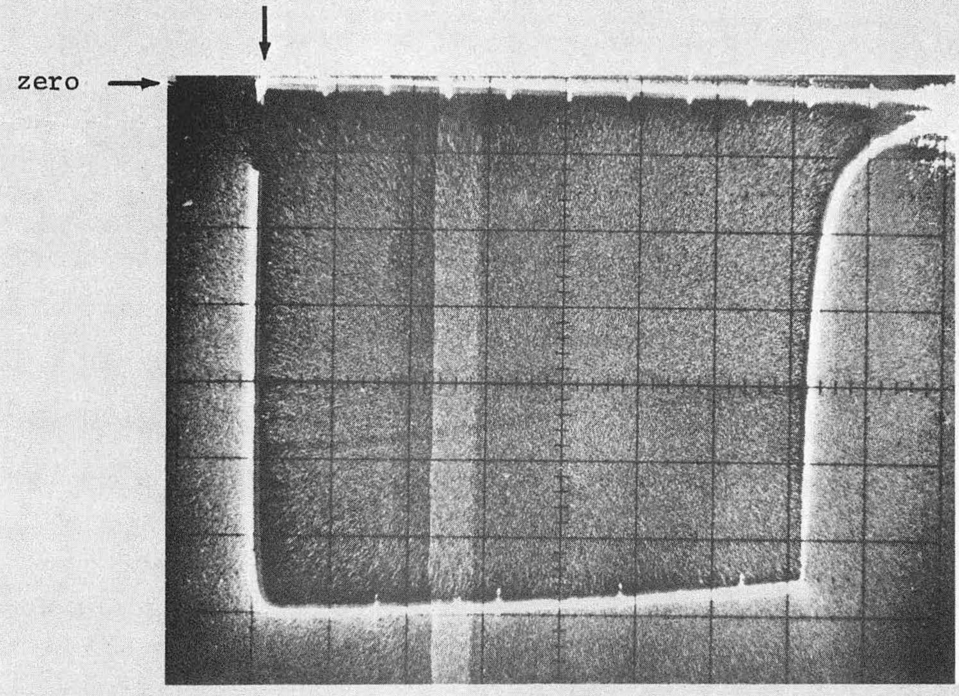

Figure 8.5. Potential response of a potassium electrode to a 72 msec current pulse (-4.17 mA/cm$^2$); Vertical scale: 0.1 volt/div.; Horizontal scale: 10 msec/div.; 50°C, 0.5 M $KAlCl_4$/PC, cell #3; reference electrode: K/K$^+$.

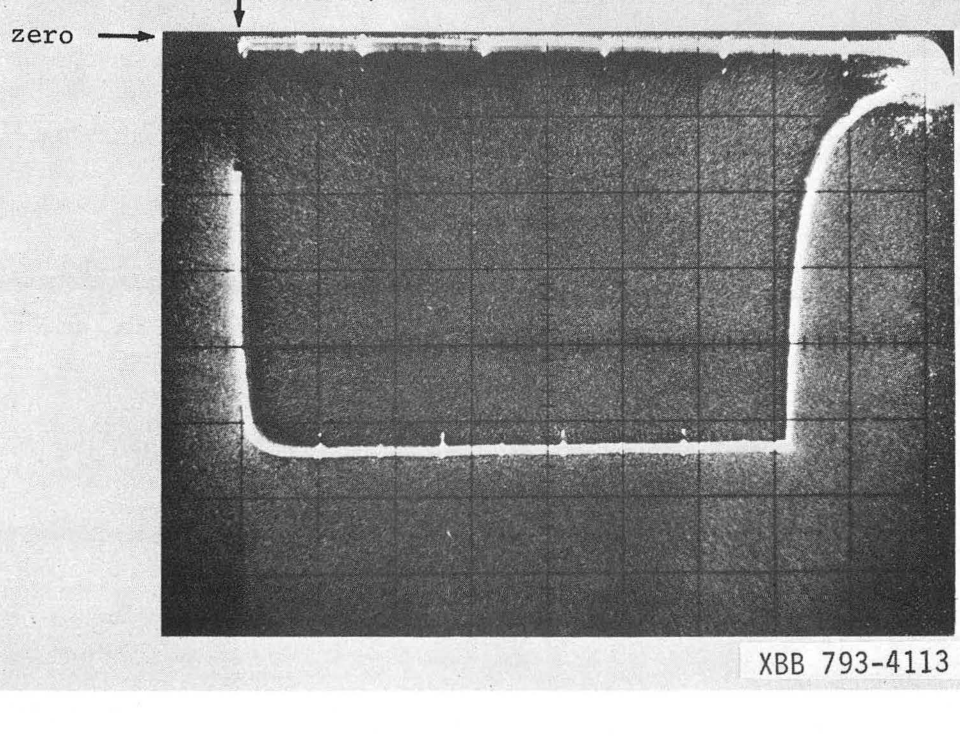

XBB 793-4113

**Figure 8-6.** Potential response of a potassium electrode to a 72 msec current pulse (-4.17 mA/$cm^2$); Vertical scale: 0.1 volt/div.; Horizontal scale: 10 msec/div.; 50°C, 0.5 M $KAlCl_4$/PC, cell #3; reference electrode: $K/K^+$.

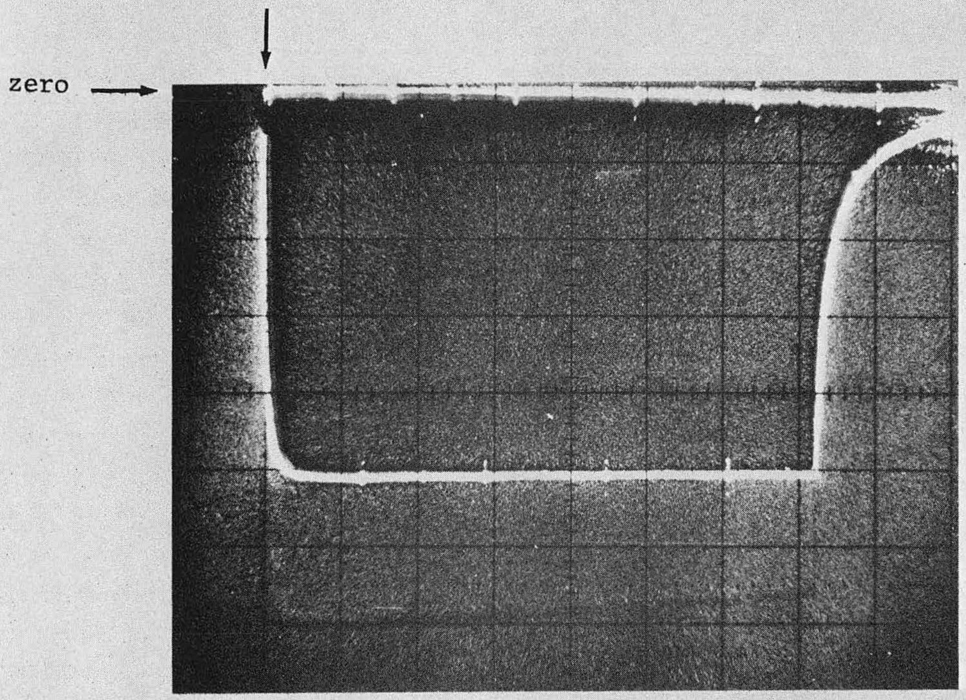

**Figure 8-7.** Potential response of a potassium electrode to 72 msec current pulses (from the top: -16.67, -25.0, -33.3, and -41.7 mA/$cm^2$); Vertical scale: 0.2 volt/div.; Horizontal scale: 10 msec/div.; 50°C, 0.5 M $KAlCl_4$/PC, cell #3; reference electrode: $K/K^+$.

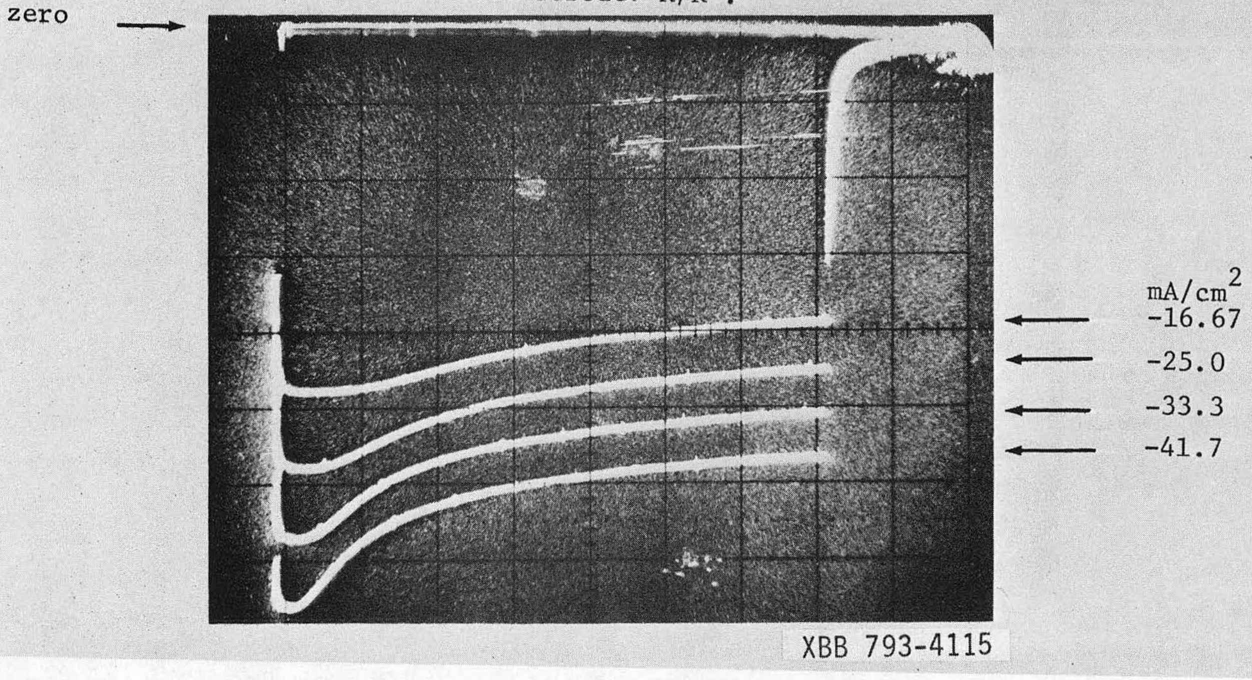

XBB 793-4115

Figure 8-8. Potential response of a potassium electrode to a 0.59 second current pulse (-4.17 mA/cm$^2$); Vertical scale: 0.1 volt/div.; Horizontal scale: 0.1 msec/div.; 50°C, 0.5 M $KAlCl_4$/PC, cell #3; reference electrode.

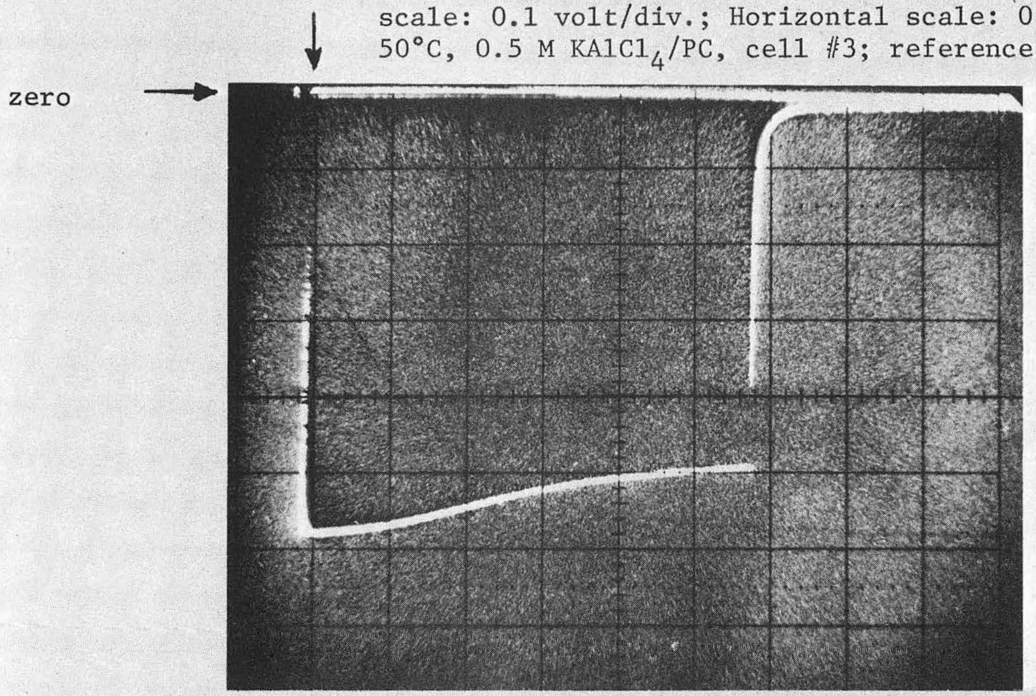

Figure 8-9. Potential response of a potassium electrode to 0.59 second current pulses (from the top: -1.67, -2.5, and -3.33 mA/cm$^2$); Vertical scale: 0.1 volt/div.; Horizontal scale: 0.1 sec/div.; 50°C, 0.5 M $KAlCl_4$/PC, cell #3; reference electrode: K/K$^+$.

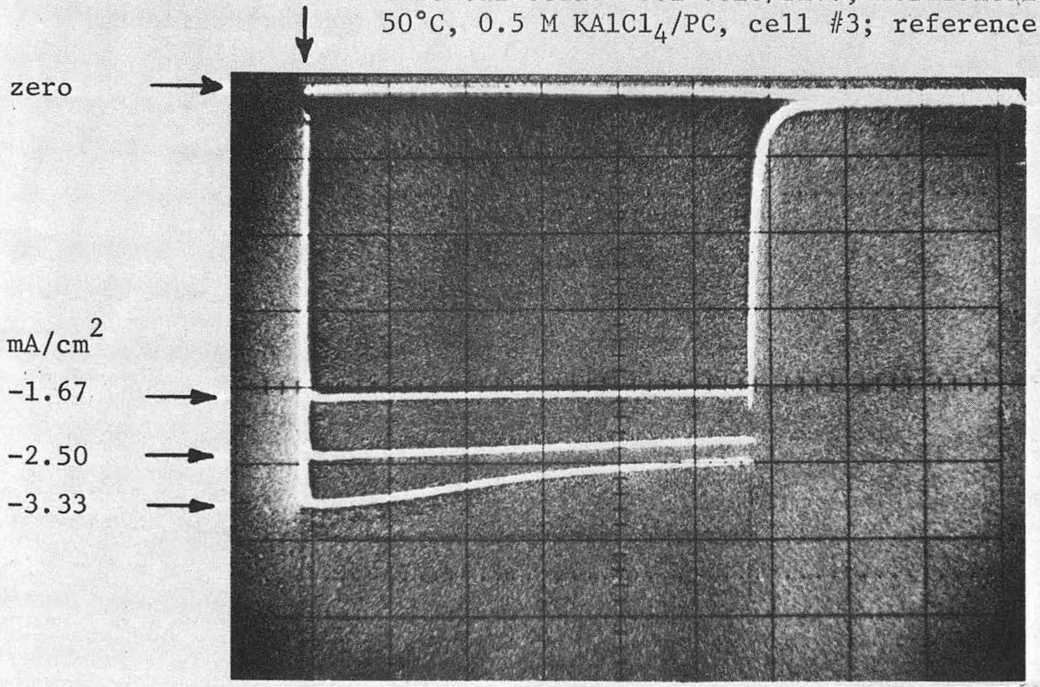

XBB 793-4116

These observations support what Figure 8-1 illustrates: the surface overpotentials are affected by the surface activating and de-activating reactions. A potassium electrode is passivated to a certain extent if no current is passed. When a cathodic current is first passed, the surface is activated by the potassium deposit. As more active area is created, the overpotential decreases. As expected, the rate of potential change depends on how fast the surface is activated, that is, on the current density. At 41.7 mA/cm$^2$, the decline is obvious in 72 msec, whereas at 4.17 mA/cm$^2$ it takes 0.59 second pulse to show the change. Clearly, using a current-pulse method is not adequate. When the examined time period of a particular current density lies in the region where the change of potential is gradual, one would believe that the "steady" overpotential was measured. The data so obtained would differ significantly from the actual steady state values.

The change of surface activity during electrolysis renders the transient technique inadequate for overpotential measurement. There are two modes available for performing the electrolysis for measurement by the steady state method: at constant potential or at constant current. We found that the galvanostatic mode was better.

Under galvanostatic condition (Figure 8-1), the change of potential is gradual, whereas under the potentiostatic mode, no steady current is obtained. Figure 8-10 depicts the change of the current with time when polarizing a rotating Pt disk electrode to -200 mV relative to the potassium reference electrode. The continuous change of current makes the potentiostatic method unsuitable for overpotential measurements.

The steady-state, constant-current technique, however, does have some drawbacks. Because of the large amount of charge passed, the physical structure of the surface does not remain the same. As the amount of deposit increases, the surface area as well as the surface activity changes. The current density based on the geometric area of the cathode becomes an apparent (or superficial) value, meaningful only for purposes of order-of-magnitude estimation. Since there is no accurate method that can continuously measure the surface area in the present system, it is doubtful that the true current density and therefore the true exchange current density can be determined by this method. However, these apparent current densities can be used to reveal relative changes that pertain to the questions we are interested in-- how do the operating parameters, such as, temperature and electrolyte concentration, affect the kinetic behavior?.

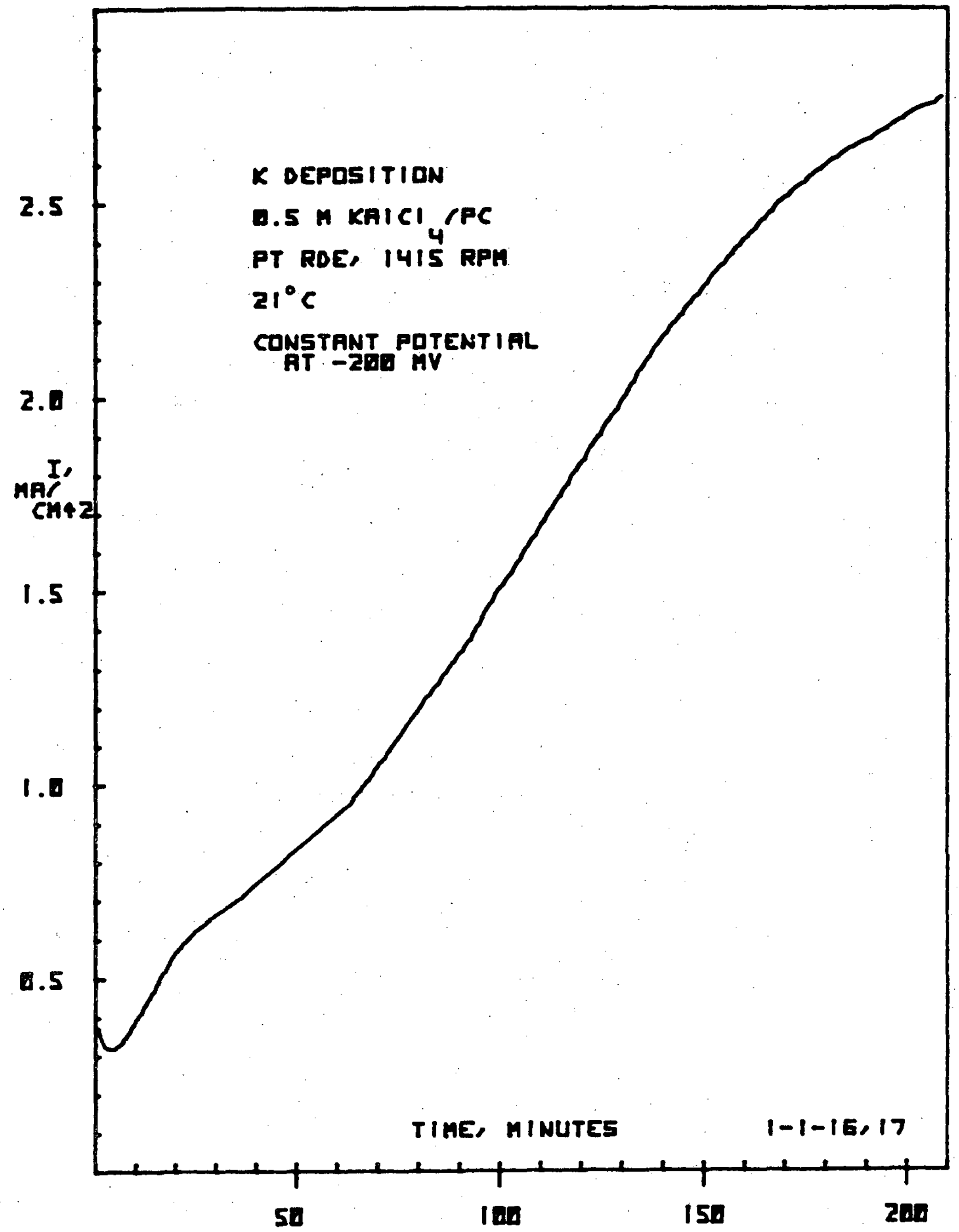

Figure 8-10. The change of current density with time of a Pt rotating disk electrode at a potential -200 mV relative to a potassium reference electrode; 21°C, 0.5 M $KAlCl_4$/PC, 1415 rpm, cell #6.

Although the steady-state, constant-current method is better than other methods, we still have to deal with the problem of the gradual change of the potential with time. When does the potential reach the steady state? The definition we adopted is that the potential is steady when it changes at a rate less than 2 mV/minute. In order to present a meaningful picture, we report a range of the cathodic overpotential for a given current density, from the initial value, when the current is first set, to the steady value. This method of presentation is especially informative when potassium is deposited on a different metal. The nucleation overpotential associated with the reduction of metal cation on a foreign metal differs from that on a potassium substrate.

The cell we employed for overpotential measurement has a cylindrical symmetry (cell #8). The cathode was an aluminum cylinder at the center, and the anode was potassium metal on the wall of the flask. The current was first increased from 0.1 to 1 mA/cm$^2$ (hereafter referred as initial scan). Then the current was kept constant at 1 mA/cm$^2$, usually for 1 day. The second scan began with the current decreasing from 1 mA/cm$^2$ down to about 0.1 mA/cm$^2$ and back to 1 mA/cm$^2$. The ohmic losses were measured by using current interruption method.

Figure 8-11 shows a typical set of data. In the inital scan, the change of overpotential for a given current density was large. The nucleation overpotential makes it difficult to deduce the charge transfer overpotential from these measurements. For example, an overpotential of 115 mV was observed at each current density considered. Thus, the initial scan does not yield any quantitative information.

Overpotentials from the second scan, however, did not change much at a given current density. Potentials from the decreasing-current part and the increasing-current part of the second scan did not deviate much from each other. Although the surface area is not known, comparative studies are now possible using data frond scan. We have studied the effect of the electrolyte concentration, temperature, the presence of cationic surfactant, and the electrode substrate on the overpotential of potassium deposition. The cathodic transfer coefficient and the apparent exchange current density were deduced by fitting the overpotentials to equation 8-4 (Appendix II). Table 8-1 lists the value obtained.

The dependence of the overpotential on the concentraton of the $KAlCl_4$ salt is complicated. Figure 8-12 depicts the data obtained from 0.1, 0.5 and 1.0 M solutions. The apparent exchange current density in 0.5 M

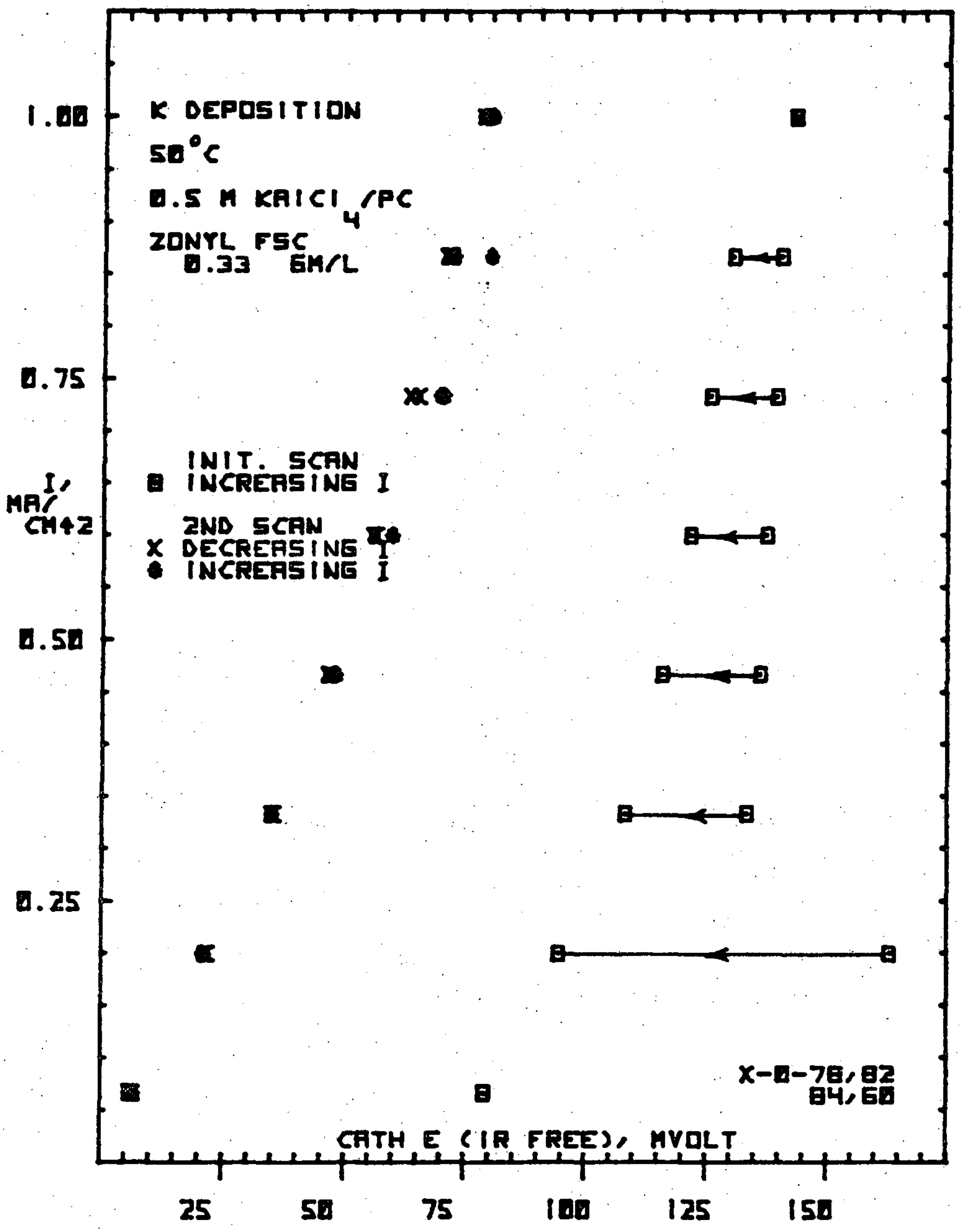

Figure 8-11. Typical set of the overpotentials of potassium deposition measured in cell #8; a range of the overpotential is presented for a given current density.

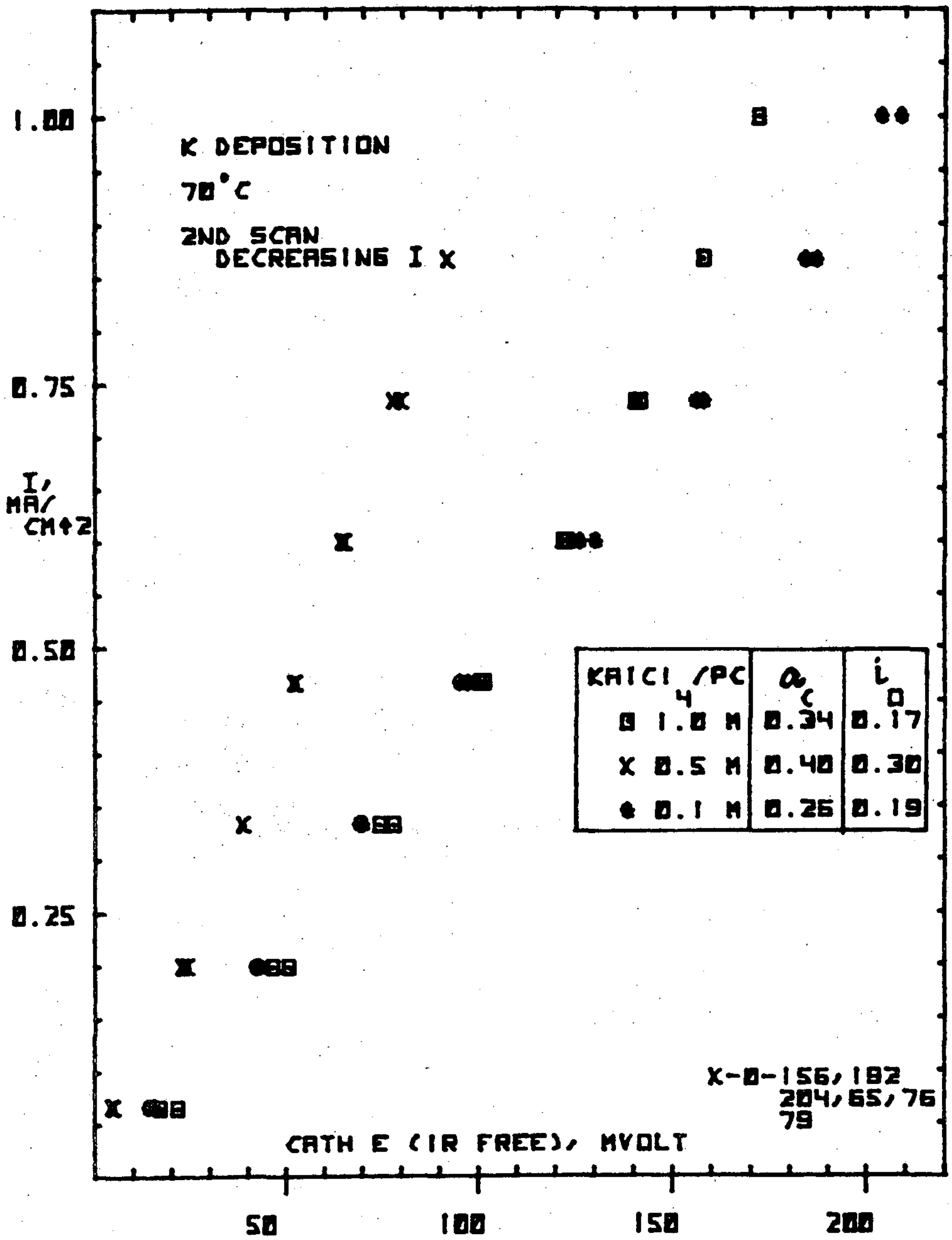

Figure 8-12. Effect of the $KAlCl_4$ concentration on the overpotentials of potassium deposition at 70°C, cell #8.

Table 8-1

Kinetic Parameters of Potassium Deposition

| Temp ,°C | Zonyl gm/l | $KAlCl_4$ M | $a_c$ | $i_o$ mA/cm$^2$ |
|---|---|---|---|---|
| 70 | 0.0 | 0.5 | 0.40 | 0.30 |
| 50 | 0.0 | 0.5 | 0.38 | 0.16 |
| 70 | 0.0 | 0.1 | 0.26 | 0.19 |
| 70 | 0.0 | 1.0 | 0.34 | 0.17 |
| 50 | 0.167 | 0.5 | 0.33 | 0.43 |
| 50 | 0.33 | 0.5 | 0.45 | 0.31 |
| 50 | 1.0 | 0.5 | 0.69 | 0.27 |

electrolyte is larger; hence, the overpotentials are higher in either 0.1 or 1.0 M electrolytes. It is difficult to interpret this strange dependence of the apparent exchange current density on the electrolyte concentrations.

Overpotentials of the potassium deposition at temperatures above and below the melting point of potassium (63°C) are appreciably different. Figure 8-13 shows that the overpotential at 70°C is lower than that at 50°C. The apparent exchange current density is higher at 70°C than at 50°C because the deposition on a liquid electrode needs a smaller activation energy than on a solid surface.

The influence of a surface-active agent on the cathodic potential has also been considered. The Dupont Zonyl cationic fluorosurfactant (FSC) was selected. The

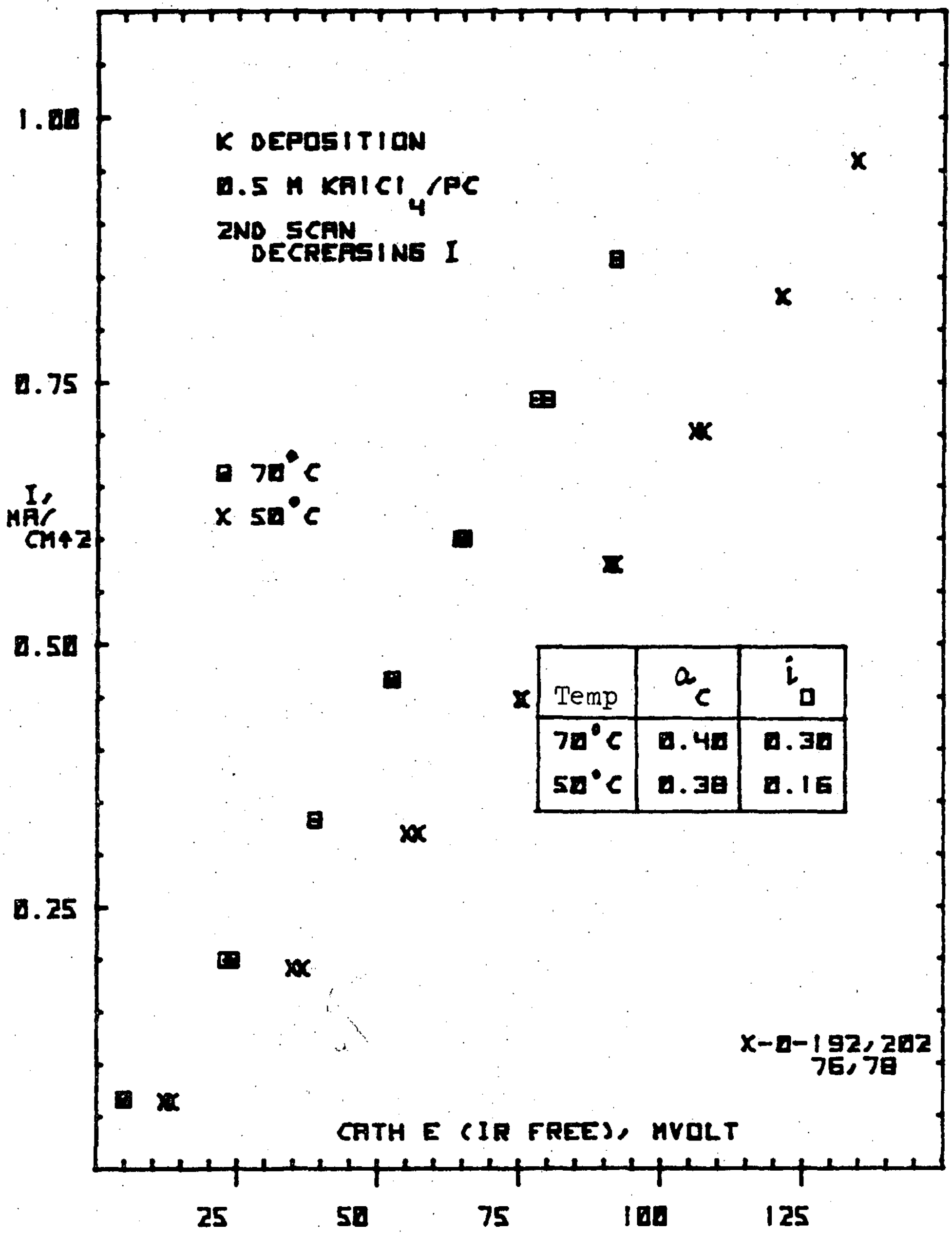

| Temp | $a_c$ | $i_0$ |
|---|---|---|
| 70°C | 0.40 | 0.30 |
| 50°C | 0.38 | 0.16 |

Figure 8-13. Overpotentials of potassium deposition at temperatures above (70°C) and below (50°C) the melting point of potassium, cell #8.

dependence of the overpotential on the surfactant concentration at 70°C is shown in Figure 8-14. The overpotential is higher in the presence of Zonyl surfactant. This is expected because the adsorption of the surfactant on the liquid electrode would increase the resistance to the reduction of the potassium ion.

At 50°C, the surfactant influences the reduction of potassium in the opposite manner. It appears to enhance the potassium deposition process; the overpotential is lower in the presence of the surfactant (Figure 8-15). In order to elucidate the influence of the Zonyl surfactant, the temperature dependence of the overpotential at a surfactant concentration of 0.33 gm/liter was studied (Figure 8-16). The overpotential increases with temperature. Similar behavior was observed at a surfactant concentration 1.0 gm/liter. This is opposite to the overpotential behavior observed in the absence of surfactant (Figure 8-13).

Results presented so far are from experiments performed with very pure aluminum cylinder (99.9995%) as a cathode. Since commercially available aluminum is an alloy (>96%), the influence of electrode substrate on overpotential was also explored. Table 8-2 lists the composition of the Al alloy studied. Figure 8-17 shows

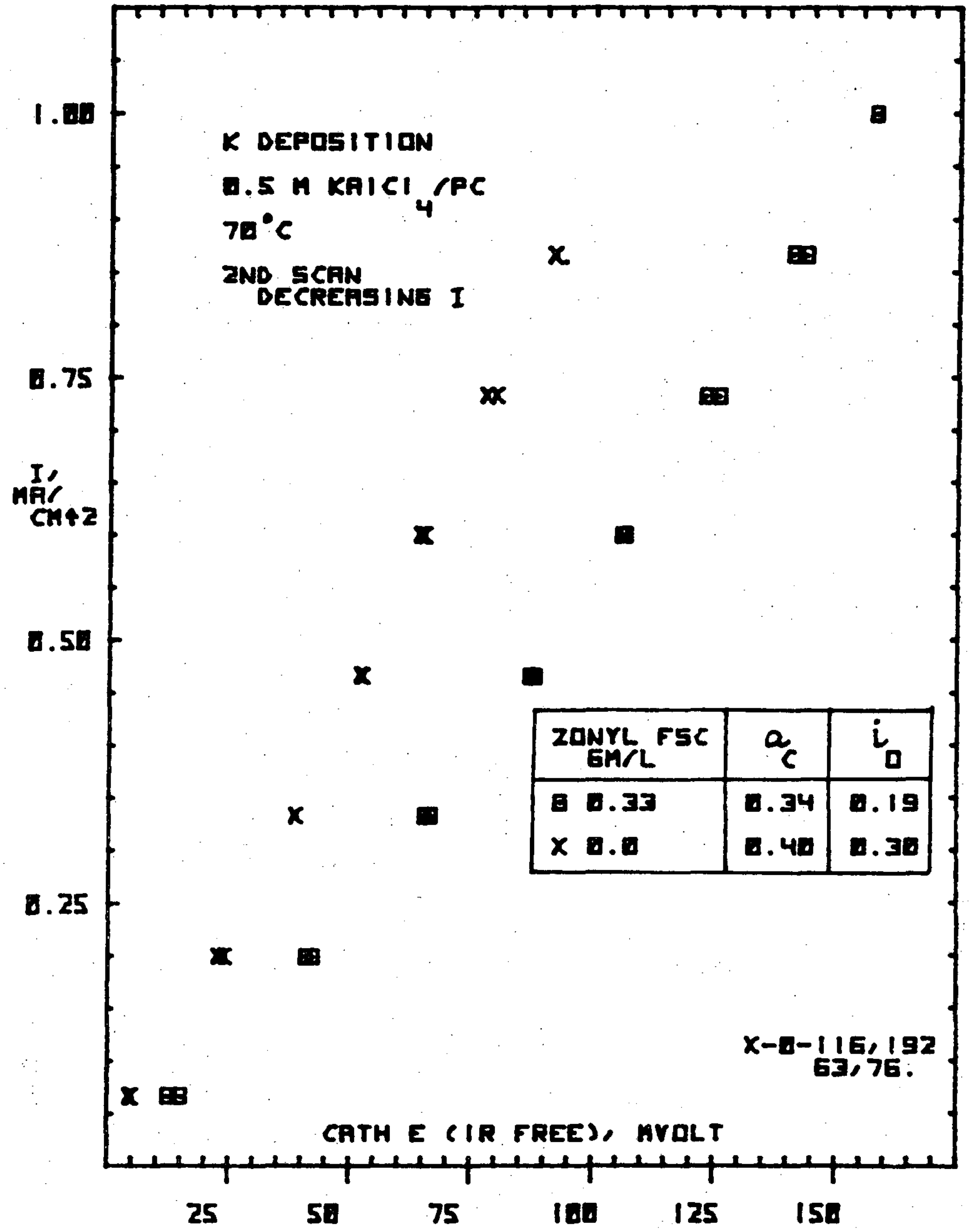

Figure 8-14. Overpotentials of potassium deposition at different surfactant concentrations at 70°C, 0.5 M KAlCl$_4$/PC, cell #8.

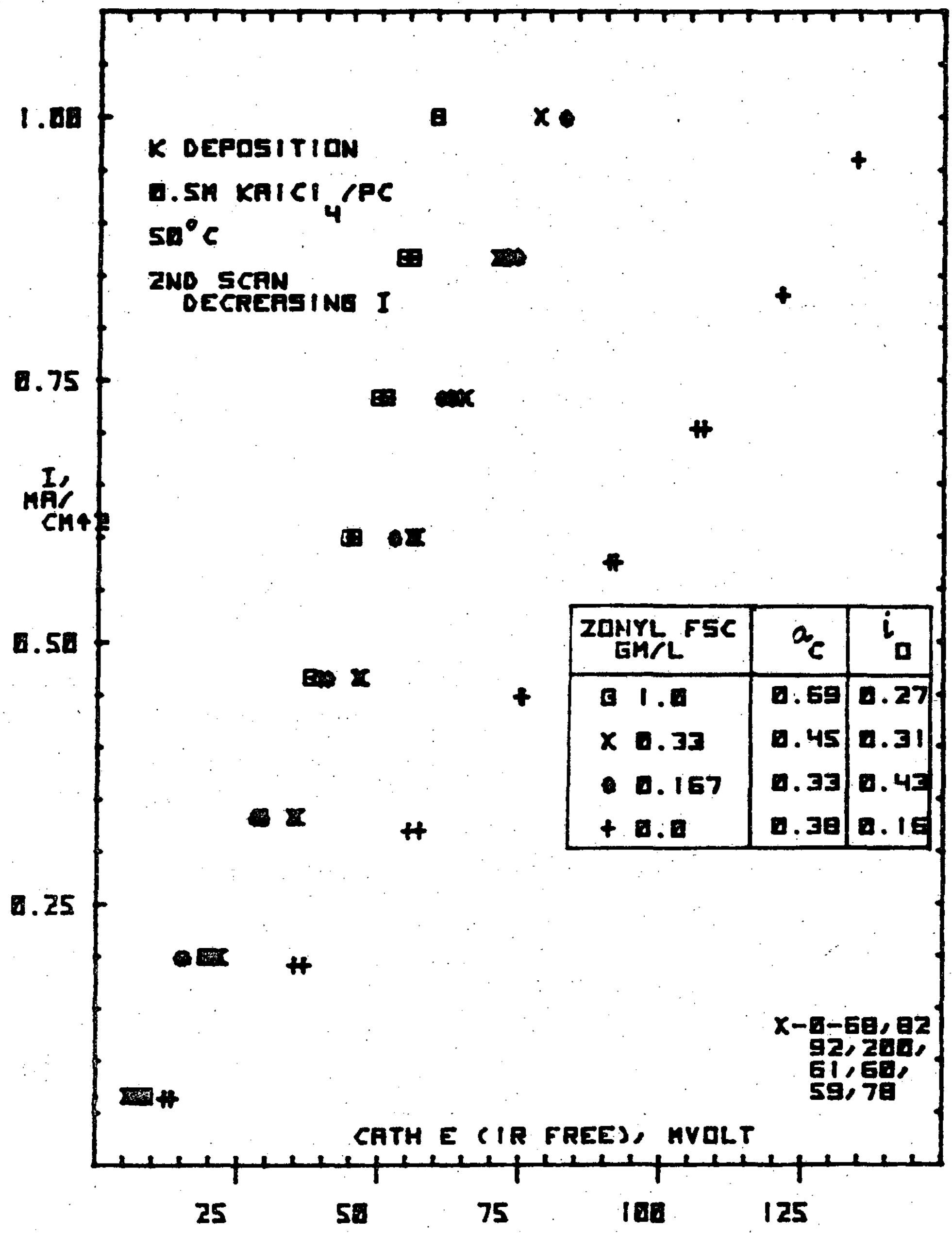

Figure 8-15. Influence of the surfactant concentration on the overpotential of potassium deposition at 50°C, 0.5 M $KAlCl_4$/PC, cell #8.

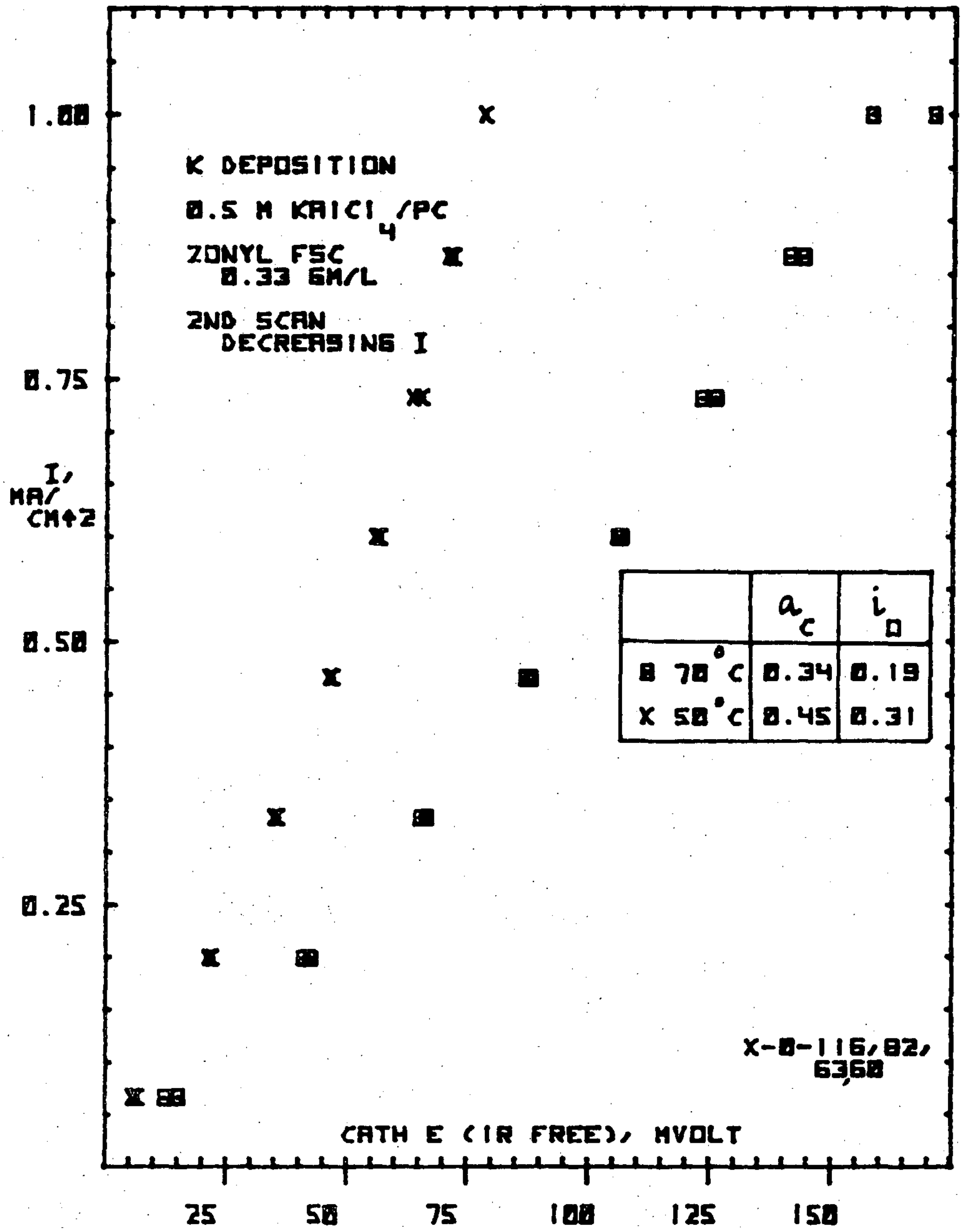

Figure 8-16. Effect of temperature on the overpotentials of potassium deposition, 0.33 gram/liter surfactant, 0.5 M $KAlCl_4$/PC, cell #8.

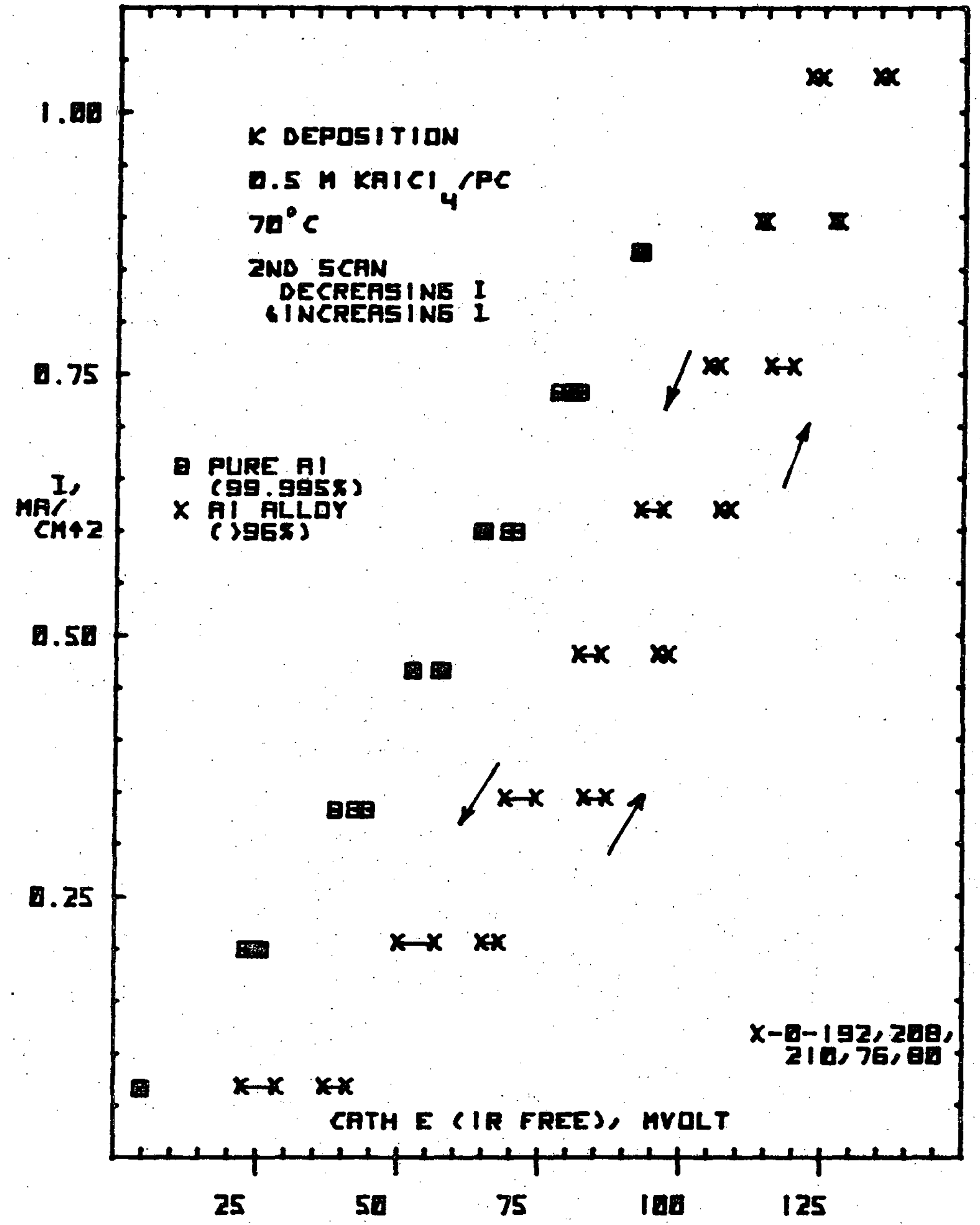

Figure 8-17. Overpotentials of potassium deposition on different electrode substrates, 70°C, 0.5 M $KAlCl_4$/PC, cell #8.

Table 8-2

Composition of Al alloy (6061T6)

| | |
|---|---|
| Al | >96.00% |
| Si | 0.4 |
| Fe | 0.7 |
| Cu | 0.15 - 0.4 |
| Mn | 0.8 - 1.2 |
| Cr | 0.04 - 0.35 |
| Zn | 0.25 |
| Ti | 0.15 |
| All other | 0.15 |

the overpotential of the deposition of potassium on pure aluminum and aluminum alloy from the second scan of the current. The overpotentials scatter widely for the Al alloy electrode. Since potassium is very electronegative, the Al alloy should not corrode and the metal elements in the alloy cannot contaminate the electrolyte. It is also unlikely for potassium to form an alloy.

In summary, the overpotential of the deposition of potassium has been measured by a steady state galvanostatic technique. Because of the passivating reaction on the surface, the transient (current pulse) and the steady state potentiostatic methods were not employed. Due to the large amount of charge passed to attain the steady state, the true exchange current density could not be obtained. Nevertheless, the apparent exchange current density does indicate the relative changes caused by changing the operating parameters. The overpotential is lower in 0.5 M $KAlCl_4$ electrolyte than in 0.1 or 1.0 M solution. The apparent exchange current density at 70°C is higher than that at 50°C, so the overpotential is lower at 70°C. Dupont Zonyl FSC fluorosurfactant was found to influence the overpotential data in a complicated manner; in the presence of the surfactant, the apparent $i_o$ is higher at 50°C while it is smaller at 70°C. The overpotentials were found to be higher on an Al alloy than on the pure metal.

The apparent exchange current density is in the range of $1 \times 10^{-4}$ to $5 \times 10^{-4}$ amp/cm$^2$, about a hundred times larger than the values reported by Jorne et al.[J4]. Even with the uncertainty of the surface area, two orders of magnitude difference between the values of $i_o$ is unreasonable. It is likely that the surface layer strongly affects the micropolarization measurements. Finally, the cathodic overpotentials, at least in the current density range investigated, are not excessively high in so far as the feasibility of commercial potassium winning or refining is concerned.

## 9. Conclusions

The foregoing study of the electrochemical behavior of potassium in propylene carbonate leads to the following conclusions:

(1) Reproducible results have been obtained only from high purity electrolytes because impurities strongly affect the behavior of potassium.

(2) Large amounts of good quality $KAlCl_4$/PC electrolyte (less than 1 ppm water) can be prepared in a straightforward manner: the solvent is purified by using alumina and molecular sieves or treated charcoal, and then by vacuum distillation; the electrolyte is prepared by dissolving $KAlCl_4$, instead of $AlCl_3$ and KCl separately, in PC.

(3) A surface layer is formed on a potassium electrode in $KAlCl_4$ solution; this layer affects the electrochemical behavior of potassium only slightly. The use of a potassium reference electrode is meaningful, provided high input impedance instruments are used.

(4) For all practical purposes potassium is stable in the electrolyte prepared. The reaction of the solvent with potassium proceeds at a rate less than that corresponding to 20 microampere/$cm^2$.

(5) The deposition of potassium proceeds with near 100% current efficiency. Aluminum is not co-deposited.

(6) The deposit morphology is strongly affected by temperature. Deposits obtained on different electrode substrates show no significant differences, ranging from loose powders at 25°C, fine needles at 50°C, and liquid globules at 70°C. Presence of a fluorinated surfactant yields large liquid globules at temperatures above the melting point of potassium.

(7) The steady state galvanostatic technique yielded kinetic parameters with reasonable reproducibility; $i_o$ was found to be in the range of $1 \times 10^{-4}$ to $5 \times 10^{-4}$ amp/cm$^2$. The current-pulse technique and the potentiostatic steady state method were found not ideally suited for the purpose of overpotential measurements.

(8) Cathodic overpotentials are influenced by the electrolyte concentration, temperature, concentration of cationic surfactant, and by the nature of the electrode substrate.

(9) Good deposits of potassium up to gram quantities have been obtained under practical conditions. When coupled with an appropriate anodic reaction, potassium could be electrowon or refined in PC electrolyte.

(10) Assuming aluminum dissolution as the anodic reaction, the energy requirement per kg of potassium in a plausible cell configuration is estimated at 2.4 kw-hr/kg

or at \$0.05/kw-hr, \$0.12/kg (Appendix III). Including the cost of Al at \$0.53/lb and KCl(99.9%) at \$40 per ton$^{C6}$ and not crediting the value of the side product $AlCl_3$, the total energy and material cost would amount to \$0.45/kg of potassium produced.

(11) The attractive energy and material cost, however, would be offset by the probable need for cumbersome reprocessing of the electrolyte, including removal of the product, $AlCl_3$. Nevertheless, the process of producing potassium electrolytically from sacrificial anodes in PC electrolyte has the potential of being economically feasible.

## 10. References

A1. Atanasoski, R., Henry Law, and Charles W. Tobias, to be published.

A2. Audrieth, L. F., and H. W. Nelson, Chem. Rev., vol. 8, p. 335, 1931.

A3. Audrieth, L. F., and Jacob Kleinberg, Non-Aqueous Solvents, John Wiley and Sons, New York, 1953.

A4. Atanasoski, R., Henry Law, and Charles W. Tobias, LBL-8505, 1978.

B1. Brenner, A., Advances in Electrochemistry and Electrochemical Engineering, P. Delahay and C. W. Tobias, eds., Interscience, New York, 1967, vol. 5.

B2. Burrows, B., and S. Kirkland, J. Electrochem. Soc., vol. 115, 1968, pp. 1164-1168.

B3. Badox-Lambling, Janine, and G. Cauquis, Analytical Aspects of Voltammetry in Non-aqueous solvents and melts, Electroanalytical Chemistry, ed. by H. W. Nurnberg, Wiley, 1974.

B4. Boden, D., H. Buhner, and V. Spera, Technical Report, ECOM-0385-F.

B5. Baud, E., Ann. Chim. phys., (8), vol. 1, pp. 8-72, 1904.

C1. Private communication, Callery Chemical Company, Pennsylvania, 1978.

C2. Chacon, Oscar A., M. S. Thesis, LBL 3542, University of California, Berkeley, 1974.

C3. Cogley, David R., James N. Butler, and Ernest Grunwald, J. Phys. Chem., vol. 75, 1971, pp. 1477-1486.

C4. Courtot-Coupez, J., and L'Her, Bull. Soc. Chim. France, 1970, 1631.

C5. Cedergren, A., Talanta, vol. 21, pp. 367-375, 1974.

C6. Potassium Chloride, chemical grade, 99.95% KCl, bulk, carlot, works, Chemical Marketing Reporter, Oct. 30, 1978, Schnell Publishing Co., Inc.

C7. Metallic Sodium, 12 lb bricks, dms., carlot works; Chemical Marketing Reporter, Oct. 30, 1978, Schnell Publishing Co., Inc.

C8. Cady, H. P., and R. Taft, J. Phys. Chem., vol. 29, 1057, 1925.

C9. Aluminum primary ingot, major U.S. producer, Metal Weeks, Nov. 4, quoted from Business Week, Nov. 20, 1978, McGraw-Hill.

D1. Jansta, J., F. P. Dousek, and J. Riha, Electroanal. Chem. and Interfacial Electrochem., vol. 38, pp. 445-450, 1972.

D2. Dousek, F. P., J. Riha, and J. Jansta, ibid., vol. 39, pp. 217-221, 1972.

D3. Jansta, J., F. P. Dousek, and J. Riha, ibid., vol. 44, pp. 263-273, 1973.

D4. Dousek, F. P., J. Jansta, and J. Riha, ibid., vol. 46, pp. 281-287, 1973.

D5. Dousek, F. P., and J. Jansta J. Electroanal. Chem., vol. 74, pp. 195-203, 1976.

D6. Dey, A. N., J. Electrochem. Soc., vol. 114, p. 823, 1967.

D7. Dey, A. N., and B. P. Sullivan, J. Electrochem. Soc., vol. 117, p. 222, 1970.

E1. Elliot, W., S. Hsu, and W. Towle, Proc. Annual Power Sources Conf., 18, p. 82, 1964.

E2. Eichinger, G., J. Electroanal. Chem., vol. 74, pp. 183-193, 1976.

F1. Fedot'ev, N. P., and R. N. Kinkul'skaya, Proceedings First All-Union Conf. Non-Aqueous Solutions, Kiev (USSR), 1935, p. 114, quoted from Brenner, reference B1.

G1. Gosse, B., and A. Denat, Electroanal. Chem. and Interfacial Electrochem., vol. 56, pp. 129-147, 1974.

G2. Gopal, Ram, and J. S. Jha, *Indian Journal of Chemistry*, vol. 15A, pp. 80-83, 1977.

H1. Harris, W., Ph. D. Thesis, University of California, Berkeley, UCRL 8381, 1958.

I1. Isabaev, V. D. Ponomarev, V. S. Mal'tsev, and R. U. Abisheva, S. M., *Izv. Vysshikh Uchebn. Zaved., Tsvetn. Met.*, vol. 9, no. 4, pp. 39-42, 1966 (Russian); *Chem. Abstracts*, vol. 66, col. 5010s, 1967

J1. Johnson, J. W., and M. A. Bredig, *J. Physical Chemistry*, vol. 62, pp. 604-7, 1958.

J2. Jackson, C. B., and R. C. Werner, *Advances in Chemistry Series*, vol. 19, A.C.S., 1957.

J3. Jorne, J., Ph. D. Thesis, LBL 1111, University of California, Berkeley, Calif., 1972.

J4. Jorne, J. and C. W. Tobias, *J. Electrochem. Soc.*, vol. 121, pp. 994-1000, 1974.

J5. Jorne, J. and C. W. Tobias, *J. Electrochem. Soc.*, vol. 122, pp. 624-632, 1975.

J6. Jorne, J. and C. W. Tobias, *J. Phys. Chem.*, vol. 78, p. 2576, 1974.

J7. Jorne, J., and C. W. Tobias, *J. Phys. Chem.*, vol. 78, p. 2521, 1974.

J8. Jorne, J. and C. W. Tobias, *J. Electrochem. Soc.*, vol. 122, pp. 1485-1487, 1975.

J9. Jorne, J. and C. W. Tobias, *J. Applied Electrochem.*, vol. 5, pp. 279-290, 1975.

J10. Jasinski, R., *Advances in Electrochemistry and Electrochemical Eng.*, vol. 8, ed. by P. Delahay and C. W. Tobias, Interscience, New York, 1971.

J11. Jasinski and S. Kirkland, *Anal. Chem.*, vol. 39, p. 1663, 1967.

J12. Jasinsksi, R. and S. Carroll, *J. Electrochem. Soc.*, vol. 117, p. 218, 1970.

K1. Kirk-Othmer, Encylopedia of Chemical Technology, vol. 16, pp. 361-368, 1968.

K2. Keller, R., J. N. Foster, D. C. Hansen, J. F. Hon and J. S. Muirhead, NASA-CR-1425, 1969.

K3. Kuta, Jaroslav and Ernest Yeager, Techniques of Electrochemistry, vol. 1, chapter 3, ed. by E. Yeager and A. Salkind, Wiley, 1972.

K4. Kendall, J., E. D. Crittenden and H. K. Miller, J. Am. Chem. Soc., vol. 45, pp. 963-996, 1923.

K5. van Krevelin, D. W., and H. A. G. Chermin, Chem. Eng. Sci., vol. 1, p.66, 1951; vol. 1, p. 238, 1952.

L1. Laszczynski, S. V., Z. Elektrochem., vol. 2, p. 55, 1895.

L2. Lasczcynski, S. V. and S. V. Gorski, Z. Elektrochem., vol. 4, p. 290, 1897.

L3. Levi, M. G. and M. Voghera, Gazz. Chim. Ital., vol. 35, p. 277, 1905.

M1. Mandell Jr., H. C., W. M. McNabb and J. F. Hazel, J. Electrochem. Soc., vol. 102, 263, 1955.

M3. Mezhennii, Ya. P., Zapiski Inst. Khim. Akad. Nauk Ukr. SSR, vol. 3, 361, 1936, quoted from Brenner, reference B1.

P1. Perugini, Giancarlo, Italian Patent 632,506, Jan. 29, 1962, Chemical Abstract, vol. 61, col. 2773f.

P2. Pompe, Robert, Electrochimica Acta, vol. 21, pp. 1111-1114, 1976.

P3. Putnam, G. L., and K. A. Kobe, Trans. Electro. Soc., vol. 74, p.609, 1938.

P4. Pospekhev, D. A., J. Appl. Chem. USSR, English Transl., vol. 27, p. 552, 1954.

S1. Sittig, Marshall, Chemical Engineering Progress, vol. 52, pp. 337-341, 1956.

S2. Silvester, L. F. and C. W. Tobias, LBL-2528, 1973.

T1. Tobias, C. W. and J. Jorne, U. S. Patent #3,791,945, 1974.

W1. Wu, Y. and H. Friedman, J. Amer. Chem. Soc., vol. 70, p. 2020, 1966.

## Appendix I. Thermodynamic Instability of Propylene Carbonate with Potassium

Although propylene carbonate is one of the more popular solvents investigated in recent years, its Gibbs free energy of formation has not been determined. In order to evaluate the thermodynamic instability between potassium and propylene carbonate, the free energy of

Table I-1

Estimation of Gibbs free energy of formation of PC by the group contribution method of van Krevelen and Chermin.[K5]

| | A | $B \times 10^2$ |
|---|---|---|
| $H_3C-$ | -10.943 | 2.215 |
| $>CH_2$ | -5.193 | 2.43 |
| $-\overset{\vert}{\underset{\vert}{C}}H$ | -0.705 | 2.910 |
| $>C=O$ | -28.08 | 0.91 |
| -O- | -15.79x2 | -0.85x2 |
| 5 mem. ring | 4.275 | -2.35 |
| | -72.23 | 4.42 |

At $300^{\circ}K$, $G = A + BT$

$= -59$ kcal/mole.

formation of PC was estimated by using the method of van Krevelan and Chermin.[K5] Table I-1 shows the calculation. The free energy of formation of PC was estimated to be -59 kcal/mole at 300°K. One likely reaction involving K and PC is

$$K(c) + PC \rightarrow K_2CO_3(c) + C_3H_6. \qquad (I\text{-}1)$$

Since the free energies of formation for $K_2CO_3$ and $C_3H_6$ are -255.5 and 14.99 kcal/mole respectively, the change of the free energy of reaction (I-1) is -181.5 kcal/mole. Therefore, it is safe to expect PC and K are thermodynamically unstable even if the method of estimating the free energy of formation of PC is not very accurate.

## Appendix II. Calculation of Kinetic Parameters

The apparent exchange current density and the cathodic transfer coefficient are calculated by performing the linear regression analysis on the cathodic overpotential data to yield a straight line $y = A + Bx$. From equation 8-4 with $y = \ln i/[\exp(nFE_s/RT) - 1]$ and $x = E_s$, the magnitude of the slope $|B|$ equals $a_c nF/RT$ and the y- intercept is $\ln i_o$. The overpotential $E_s$ is taken as the average value between the initial and steady values of the overpotential range obtained in the second scan.

The y-intercept of the least-squares line is

$$A = [\Sigma\, y \Sigma\, x^2 - \Sigma\, x\, \Sigma xy]/[n \Sigma\, x^2 - (\Sigma\, x)^2]$$

with n is the number of data points. The slope of the

Table II-1

Kinetic Parameters of the Potassium Deposition

| Temp, °C | Zonyl gm/l | $KAlCl_4$ M | $a_c$ | $i_o$ mA/cm$^2$ | r |
|---|---|---|---|---|---|
| 70 | 0.0 | 0.5 | 0.40 | 0.30 | 0.99 |
| 50 | 0.0 | 0.5 | 0.38 | 0.16 | 0.99 |
| 70 | 0.0 | 0.1 | 0.26 | 0.19 | 0.99 |
| 70 | 0.0 | 1.0 | 0.34 | 0.17 | 0.97 |
| 50 | 0.167 | 0.5 | 0.33 | 0.43 | 0.97 |
| 50 | 0.33 | 0.5 | 0.45 | 0.31 | 0.99 |
| 50 | 1.0 | 0.5 | 0.69 | 0.27 | 0.98 |

least-squares line is

$$B = [n \Sigma xy - \Sigma x \Sigma y]/[n \Sigma x^2 - (\Sigma x)^2]$$

To establish how well the data fit the linear regression, the linear correlation coefficient (r) is also calculated from the following equation.

$$r = \sqrt{\{[n \Sigma xy - \Sigma x \Sigma y]/[n(n-1) \Sigma x \Sigma y]\}^2}$$

The $a_c$ and the $i_o$ of the potassium deposition and the linear correlation coefficient are listed in Table II-1.

The fact that r is close to 1 (perfect fit) indicates that the use of equation 8-4 to present the data is valid, but it is not sufficient to prove that the kinetics of potassium deposition is governed by the Butler-Volmer equation.

## Appendix III. Preliminary estimation of the energy and material cost for potassium production.

A possible process for producing potassium near room temperature involves the use of KCl as the source of K, and Al metal as the sacrificial anode in $KAlCl_4$/PC electrolyte. The basic feasibility has been explored.[A4]

The proposed process is to dissolve aluminum anodically and to deposit potassium at the cathode while consuming potassium chloride and producing $AlCl_3$ or $KAlCl_4$. An apparent advantage is the low cost of raw materials. Potassium chloride is cheap, abundant and available with high purity (\$40 per ton, 99.9% pure[C6]). Aluminum metal is also relatively inexpensive (53 cents per lb[C9]).

Let's consider in detail the events occurring during potassium deposition from a solution of $KAlCl_4$/PC using an aluminum anode. Aluminum is dissolved anodically to form the trivalent aluminum ion,

$$Al \rightarrow Al^{3+} + 3\,e^- \qquad (1)$$

which would immediately solvate with the solvent according to Keller et al.[K2],

$$Al^{3+} + 6\ PC \rightarrow Al(PC)_6^{3+} \quad . \qquad (2)$$

The half-cell reaction (1) requires that three potassium atoms deposit on the cathode,

$$3\ K^+ + 3\ e^- \rightarrow 3\ K \quad . \qquad (3)$$

In the presence of chloride ions, the dominant aluminum species is $AlCl_4^-$:

$$4\ Al(PC)_6^{3+} + 12\ Cl^- \rightarrow Al(PC)_6^{3+} + 3\ AlCl_4^- \qquad (4)$$

The complexing ability of the aluminum ion makes possible the use of KCl in the propylene carbonate system. In spite of its low solubility, KCl will dissolve due to the complex formation to provide the potassium cations for deposition:

$$Al(PC)_6^{3+} + 4\ KCl \rightarrow 4\ K^+ + AlCl_4^- + PC \quad . \qquad (5)$$

In summary, the complete reaction for the process is

$$Al + 4\ KCl \rightarrow 3\ K + K^+ + AlCl_4^- \quad . \qquad (6)$$

For every three moles of potassium produced one mole of $KAlCl_4$ is formed. The $KAlCl_4$ may be removed by recrystallization if desired. Since aluminum chloride is a marketable chemical, it can be produced by further electrolysis in the absence of KCl to make concentrated aluminum chloride/PC solution. Aluminum chloride can then be recovered by conventional separation processes. The complete reaction hence is

$$Al + 3\,KCl \rightarrow 3\,K + AlCl_3 \quad . \qquad (7)$$

The proposed process for producing potassium appears economically attractive. The cost of raw materials, potassium chloride and aluminum, is low and the prices of the products, potassium metal and aluminum chloride, are high. Comparing with the current industrial potassium manufacturing method, the price of potassium produced by the proposed method can possibly be significantly reduced.

The energy requirement for the proposed electrolysis process can be estimated from the preliminary results reported.[A4] Aluminum dissolves anodically with 110% current efficiency. The aluminum complex, $AlCl_4^-$, is not reduced at the cathode and potassium chloride is depleted with 100% current efficiency. The rest potential of an active aluminum electrode with respect to potassium in $KAlCl_4$/PC solution is considered to be 2 volts. Operating at a current density of 10 $mA/cm^2$ with a total overpotential of 0.5 volt and assuming a cell gap of 5 mm and an electrolyte conductivity of 0.005 $ohm^{-1}$ $cm^{-1}$, it takes 2.40 kw-hr to produce one kg of potassium and to dissolve an equivalent amount of aluminum in a parallel plate cell. The cost of aluminum and potassium chloride would be $0.33/kg of potassium.

Further studies , however, are needed before one could securely evaluate the potential of the proposed scheme. The stability of PC electrolyte to the dissolution of aluminum and the deposition of potassium has to be established. How the impurities, such as water, influence the electrochemical reactions is not known as yet. Scale-up problems, such as the collection of potassium deposit and the recovery of aluminum chloride from the electrolyte, will have to be addressed. Parasitic reactions could make the process impractical. Nevertheless, the low energy and material cost and the market value of $AlCl_3$ could make this process economically attractive.

*TECHNICAL INFORMATION DEPARTMENT*
*LAWRENCE BERKELEY LABORATORY*
*UNIVERSITY OF CALIFORNIA*
*BERKELEY, CALIFORNIA 94720*